



International Agreement Report

Assessment of RELAP5/MOD2 Using Semiscale Large Break Loss-of-Coolant Experiment S-06-3

Prepared by
Kuo-Shing Liang, Lainsu Kao, Jeng-Lang Chiou,
Lii-Yih Liao, Song-Feng Wang, Yi-Bin Chen

Institute of Nuclear Energy Research
P.O. Box 3, Lung-Tan 32500
Taiwan, Republic of China

Office of Nuclear Regulatory Research
U.S. Nuclear Regulatory Commission
Washington, DC 20555

April 1992

Prepared as part of
The Agreement on Research Participation and Technical Exchange
under the International Thermal-Hydraulic Code Assessment
and Application Program (ICAP)

Published by
U.S. Nuclear Regulatory Commission

9206050049 920430
PDR NUREG
IA-0046 R PDR

NOTICE

This report was prepared under an international cooperative agreement for the exchange of technical information.* Neither the United States Government nor any agency thereof, or any of their employees, makes any warranty, expressed or implied, or assumes any legal liability or responsibility for any third party's use, or the results of such use, of any information, apparatus product or process disclosed in this report, or represents that its use by such third party would not infringe privately owned rights.

Available from:

Superintendent of Documents
U.S. Government Printing Office
P.O. Box 37082
Washington, D.C. 20013-7082

and

National Technical Information Service
Springfield, VA 22161



International Agreement Report

Assessment of RELAP5/MOD2 Using Semiscale Large Break Loss-of-Coolant Experiment S-06-3

Prepared by
Kuo-Shing Liang, Lainsu Kao, Jeng-Lan Chiou,
Lih-Yih Liao, Song-Feng Wang, Yi-Bin Chen

Institute of Nuclear Energy Research
P.O. Box 3, Lung-Tan 32500
Taiwan, Republic of China

Office of Nuclear Regulatory Research
U.S. Nuclear Regulatory Commission
Washington, DC 20555

April 1992

Prepared as part of
The Agreement on Research Participation and Technical Exchange
under the International Thermal-Hydraulic Code Assessment
and Application Program (ICAP)

Published by
U.S. Nuclear Regulatory Commission

NOTICE

This report documents work performed under the sponsorship of the Institute of Nuclear Energy Research of Taiwan. The information in this report has been provided to the USNRC under the terms of an information exchange agreement, Cooperative Program on Thermal-Hydraulic Code Assessment between the Coordination Council for North American Affairs (CCNAA) and the American Institute in Taiwan (AIT), March 22, 1986. Taiwan has consented to the publication of this report as a USNRC document in order that it may receive the widest possible circulation among the reactor safety community. Neither the United States Government nor Taiwan or any agency thereof, or any of their employees, makes any warranty, expressed or implied, or assumes any legal liability of responsibility for any third party's use, or the results of such use, or any information, apparatus, product or process disclosed in this report, or represents that its use by such third party would not infringe privately owned rights.

ABSTRACT

This report presents the results of the RELAP5/MOD2 posttest assessment utilizing a Semiscale large break loss-of-coolant experiment numbered S-06-3. Test S-06-3 is a 200% double ended cold leg break experiment performed in Semiscale Mod-1 facility in 1978 for the purpose of investigating the thermal and hydraulic phenomena accompanying a hypothetical large LOCA in a pressurized water reactor (PWR) system and providing a data base for a U.S. Nuclear Regulatory Commission standard problem. Through extensive comparisons between data and best-estimate RELAP5 calculations, the capabilities of RELAP5 to calculate the large LOCA accident were assessed. Emphasis was placed on the capability of the code to calculate break flow rates during system blowdown stage, emergency core cooling system (ECCS) injection bypass during refill stage, quenching during reflood stage, and the peak cladding temperature (PCT) behavior throughout the whole experiment. Besides, effects of several different modelings which include radial connections between core hot and average channels, maximum number of heat slab axial interval for 2-D refined calculation, number of nodes representing the core, cross-flow junctions on vessel entrances, reflood calculation etc., were all investigated.

SUMMARY

This paper includes the results and conclusions of assessment studies which involve comparisons between data from Semiscale test S-06-3 and RELAP5/MOD2 code calculation, and important sensitivity studies investigating features of several different modelings and options. Semiscale S-06-3 test simulated a large cold-leg break LOCA with continuous reactor coolant pump (RCP) operation. RELAP5/MOD2 is an advanced, one-dimensional, thermal-hydraulic computer code used to calculate reactor transient and accident response. The objective of this assessment study is to provide systematic assessment of the RELAP5/MOD2 code relative to code development, code improvement, and the enhancement of user guidelines.

Test S-06-3 was performed as part of the Semiscale Program conducted by EG&G Idaho, Inc., for the United States Government. This test was part of the LOFT counterpart test series (Test Series 6) performed to investigate the response of the Mod-1 system to specific variations in the peak power densities of the heater rods to assist the LOFT Program in the planning of the first LOFT nuclear test series. The test objective specific to Test S-06-3 was to determine the maximum cladding temperature associated with a high powered rod peak power density of 39.4 kW/m, or 75% of the maximum high powered rod peak power density of 52.5 kW/m. In addition, Test S-06-3 was designated as a Nuclear Regulatory Commission standard problem.

In our assessment, RELAP5 calculation correctly catches all important thermal-hydraulic phenomena except the counter-current flow limit (CCFL) which takes place in the blowdown and refill periods and makes the latter-on calculated consequence deviated. The calculated break flow rates from both ends matched the data very well especially for the break near the pump side. When accumulator injection began, owing to the lack of CCFL model in RELAP5, emergency core cooling (ECC) water bypass phenomenon was not simulated well, which in turn caused more ECC water entering the vessel. Thus, early refill and reflood were noted in the calculation. As for the prediction of cladding temperature responses, good agreement was achieved between the test and calculation except the timing of rewetting. In our calculation, earlier rewet was clearly shown as compared to the test data. Two likely reasons contributed to this; one was the early refill depicted above, and the other was the overprediction of entrained water pulled up by the up-going vapor after reflood began. Besides, superheated steam observed in the test was also simulated qualitatively well.

The effects of several different modelings or options were also investigated, which include pressurizer modeling, radial connections between core average and hot channels, the maximum number of axial heat slab axial interval for 2-D reflood calculation, number of hydraulic volumes representing the core, the cross-flow junctions on reactor vessel entrances, and reflood

calculation. Except the reflood calculation, effects of each individual modeling on the calculation of peak cladding temperature were quite negligible, but to some extent quench time calculations were affected. Generally speaking, modelings with in-core radial connection, larger number of heat slab axial interval for 2-D reflood calculation, larger number of axial hydraulic volumes representing the core, or cross-flow junctions on vessel entrances would postpone the fuel quench time. Besides, responses of cladding temperature on hot spot were heavily affected when defeating the reflood calculation, and it was identified that the usage of different heat transfer package majorly contributed to such difference instead of the two-dimensional conduction. Finally, the total CPU time used in the calculation with 22 axial volumes representing the core was about 3.4 times of that used in the base calculation in which 11 axial volumes were involved.

CONTENTS

	Page
ABSTRACT	iii
SUMMARY	v
ACKNOWLEDGMENTS	xvii
i. INTRODUCTION	1
2. TEST FACILITY AND TRANSIENT DESCRIPTION	3
2.1 Test Facility	3
2.2 Transient Description	5
3. MODELING DESCRIPTION	10
3.1 RELAP5 Modeling	10
3.2 Assumptions and Initial Conditions	12
4. RESULTS	15
4.1 Comparison with Measurement	15
4.1.1 Blowdown phase (0-35 seconds)	15
4.1.2 Refill phase (35-75 seconds)	18
4.1.3 Reflood phase (after 75 seconds)	37
4.2 Sensitivity Study	49
4.2.1 Pressurizer Modeling	65
4.2.2 Radial Connections Between Core Average and Hot Channels	65
4.2.3 Maximum Number of Heat Slab Axial Interval for 2-D Reflood Calculation	66
4.2.4 Number of Axial Hydraulic Volumes Repre- senting the Core	68
4.2.5 Cross-Flow Junctions on Reactor Vessel Entrances	69

4.2.6 Reflood Calculation	Page 70
5. RUN STATISTICS	108
6. CONCLUSIONS AND RECOMMENDATIONS	110
7. REFERENCES	115
8. APPENDIX	A-1

LIST OF FIGURES

	Page
Fig. 2-1. Semiscale Mod-1 System for Cold Leg Break Configuration-Isometric	7
Fig. 2-2. Electric Heater Rod Matrix for Mod-1 Core	8
Fig. 2-3. Semiscale Mod-1 Heated Core Plan View	9
Fig. 3-1. Semiscale Mod-1 System Noding Diagram	13
Fig. 4-1. Break Flow Rates near Pump Side	19
Fig. 4-2. Break Flow Rates near Vessel Side	20
Fig. 4-3. Pressurizer Pressures	21
Fig. 4-4. Pressurizer Outsurge Flow Rates	22
Fig. 4-5. Intact Loop Cold Leg Flow Rates	23
Fig. 4-6. Intact Loop Hot Leg Flow Rates	24
Fig. 4-7. Broken Loop Cold Leg Flow Rates	25
Fig. 4-8. Broken Loop Hot Leg Flow Rates	26
Fig. 4-9. Core Inlet Flow Rates	27
Fig. 4-10. Collapsed Water Levels across the Downcomer	28
Fig. 4-11. Collapsed Water Levels across the Lower Plenum	29
Fig. 4-12. Collapsed Water Levels across the Core	30
Fig. 4-13. High Power Rod Hot Spot Cladding Temperatures	31
Fig. 4-14. Low Power Rod Hot Spot Cladding Temperatures	32
Fig. 4-15. Lower Plenum Coolant Temperatures	33
Fig. 4-16. Upper Plenum Coolant Temperatures	34
Fig. 4-17. Broken Loop Cold Leg Coolant Densities	38
Fig. 4-18. Break Flow Rates near Vessel Side	39
Fig. 4-19. Core Barrel Wall Temperatures	40

	Page
Fig. 4-20. Collapsed Water Levels across the Downcomer	41
Fig. 4-21. Collapsed Water Levels across the Lower Plenum	42
Fig. 4-22. Low Power Rod Hot Spot Cladding Temperatures	43
Fig. 4-23. High Power Rod Hot Spot Cladding Temperatures	44
Fig. 4-24. Lower Plenum Coolant Temperatures	45
Fig. 4-25. Upper Plenum Coolant Temperatures	46
Fig. 4-26. Collapsed Water Levels across the Core	50
Fig. 4-27. Accumulator Flow Rates	51
Fig. 4-28. Broken Loop Cold Leg Coolant Densities	52
Fig. 4-29. Broken Loop Cold Leg Flow Rates	53
Fig. 4-30. Low Power Rod Hot Spot Cladding Temperatures	54
Fig. 4-31. High Power Rod Hot Spct Cladding Temperatures	55
Fig. 4-32. Curve Fitting of the Low Power Rod Peak Cladding Temperature versus Elevation	56
Fig. 4-33. Curve Fitting of the High Power Rod Peak adding Temperature versus Elevation	57
Fig. 4-34. Low Power Rod Peak Cladding Temperatures Versus Elevation	58
Fig. 4-35. High Power Rod Peak Ciadding Temperatures Versus Elevation	59
Fig. 4-36. Curve Fitting of the Low Power Rod Quench Time versus Elevation	60
Fig. 4-37. Curve Fitting of the High Power Rod Quench time versus Elevation	61
Fig. 4-38. Low Power Rod Quench Time versus Elevation	62
Fig. 4-39. High Power Rod Quench Time versus Elevation	63
Fig. 4-40. Pressurizer Outsurge Flow Rates	72

	Page
Fig. 4-41. Pressurizer Pressures	73
Fig. 4-42. Low Power Rod Peak Cladding Temperatures versus Elevation	74
Fig. 4-43. High Power Rod Peak Cladding Temperatures versus Elevation	75
Fig. 4-44. High Power Rod Bottom Section Cladding Temperatures	76
Fig. 4-45. High Power Rod Top Section Cladding Temperatures	77
Fig. 4-46. High Power Rod Quench Time versus Elevation	78
Fig. 4-47. Low Power Rod Quench Time versus Elevation	79
Fig. 4-48. Core Inlet Flow Rates	80
Fig. 4-49. Collapsed Water Levels across the Core	81
Fig. 4-50. Comparison of CPU Time	82
Fig. 4-51. High Power Rod Peak Cladding Temperatures versus Elevation	83
Fig. 4-52. Low Power Rod Peak Cladding Temperatures versus Elevation	84
Fig. 4-53. High Power Rod Quench Time versus Elevation	85
Fig. 4-54. Low Power Rod Quench Time versus Elevation	86
Fig. 4-55. High Power Rod Hot Spot Cladding Temperatures	87
Fig. 4-56. Low Power Rod Hot Spot Cladding Temperatures	88
Fig. 4-57. Comparison of CPU Time	89
Fig. 4-58. High Power Rod Peak Cladding Temperatures versus Elevation	90
Fig. 4-59. High power Rod Top Section Cladding Temperatures	91
Fig. 4-60. High Power Rod Quench Time versus Elevation	92
Fig. 4-61. High Power Rod Hot Spot Cladding Temperatures	93

	Page
Fig. 4-62. Collapsed Water Levels across the Core	94
Fig. 4-63. Comparison of CPU Time	
Fig. 4-64. Break Flow Rates near Pump Side	
Fig. 4-65. Break Flow Rate near Vessel Side	97
Fig. 4-66. Collapsed Water Levels across the Downcomer	98
Fig. 4-67. Collapsed Water Levels across the Lower Plenum	99
Fig. 4-68. Collapsed Water Levels across the Core	100
Fig. 4-69. High Power Rod Quench Time versus Elevation	101
Fig. 4-70. High Power Rod Peak Cladding Temperatures versus Elevation	102
Fig. 4-71. High Power Rod Hot Spot Cladding Temperatures	103
Fig. 4-72. Comparison of CPU Time	104
Fig. 4-73. Comparison of Peak Cladding Temperatures from with and without Reflood Calculations	105
Fig. 4-74. Comparison of Peak Cladding Temperatures from 1 Reflood Unit and 11 Reflood Unit in Series	106
Fig. 4-75. Comparison of CPU Time	107

LIST OF TABLES

	Page
Table 3-1. Comparison of Calculated and Measured Initial Conditions	14
Table 4-1. Sequences of Events	64
Table 5-1. Run Time Statistics for S-06-3 Simulations	109

ACKNOWLEDGMENTS

The authors wish to gratefully acknowledge the assistance provided by R.G. Hanson, G.E. Wilson, Y.S. Chen, and D. Bessette in the course of this work. The authors also want to thank Ms. Y.F. Ju for her enduring effort in typing this report.

1. INTRODUCTION

The assessment study documented in this report is expected to contribute to the overall code assessment effort, which is coordinated within the International Code Assessment and Applications Program (ICAP) sponsored by the U.S. Nuclear Regulatory Commission (NRC). The objective of the ICAP is to provide qualitative assessment of the major thermal-hydraulic computer codes relative to code development, code improvement, and the enhancement of user guidelines. In addition, the ICAP has the objective of providing the necessary data base for the qualitative characterization of computer code when applied in a best-estimate fashion to hypothetical accident scenarios.

This report includes the results and conclusions of assessment study involving comparisons between data from Semiscale Test S-06-3 [1] and RELAP5/MOD2 [2] code calculation. Test S-06-3 was performed as part of the Semiscale Mod-1 portion of the Semiscale Program conducted by EG&G Idaho, Inc., for the United States Government. This test was part of the LOFT counterpart test series (Test Series 6) performed to investigate the response of the Mod-1 system to specific variations in the peak power densities of the heater rods to assist the LOFT program in the planning of the first LOFT nuclear test series. The test objective specific to Test S-06-3 was to determine the maximum cladding temperature associated with a high powered rod peak power density of 39.4 kw/m, or 75% of the maximum high

powered rod peak power density of 52.5 kW/m. In addition, Test S-06-3 was designated as a Nuclear Regulatory Commission standard problem.

The assessment of RELAP5/MOD2 using Test S-06-3 specifically focused in the area of system blowdown, in-vessel water level variations and fuel rewet. Particularly, since steam binding was observed in the downcomer during the early phase of the test, the effect of counter-current flow limit (CCFL) was also investigated. Also examined were the sensitivities of several different modelings which included the radial connections between core hot and average channels, cross-flow junctions on the vessel entrances, maximum number of heat slab axial interval for 2-D reflood calculation, number of axial hydraulic volumes representing the core, reflood calculation, and nodes of pressurizer.

The following two sections of this report contain a description of the test and RELAP5/MOD2 modeling techniques employed in the calculation. The fourth section includes comparisons of calculated results to the test data and associated sensitivity studies. Before the final section of conclusions and recommendations is the run statistics statement.

2. TEST FACILITY AND TRANSIENT DESCRIPTION

2.1 Test Facility

The Semiscale Mod-1 system used for this test consisted of a pressure vessel with internals, including a 40-rod core with 36 electrically heated rods; an intact loop with steam generator, pump, and pressurizer; a broken loop with simulated steam generator, simulated pump, simulated reflood bypass lines, LOFT counterpart nozzles, and two rupture assemblies; a coolant injection accumulator for the intact loop; high and low pressure coolant injection pumps for the intact loop; and a pressure suppression system with a suppression tank, and heated steam supply system. Semiscale Mod-1 experimental system configuration information is provided in Reference 3. Figure 2-1 shows the system configuration for Test S-06-3.

For Test S-06-3, the 40-rod electrically heated core as shown in Figures 2-2 and 2-3, was operated at an axial peak power density which was 75% of the maximum peak power density (52.5 kW/m). Four rods (Rods D-4, D-5, E-4, and E-5) were operated at approximately 39.4 kW/m, 32 rods were operated at approximately 24.9 kW/m, and four rods (Rods C-4, D-6, E-3, and G-6) were unpowered to simulate LOFT passive rod locations. This configuration yielded a peaked power profile which simulates that of LOFT and provides a total core power of approximately 1.004 MW.

To achieve the desired objectives during the LOFT counterpart test series, it is necessary that the Mod-1

electrical heater rods behave in a manner that will produce the same results as those expected from the LOFT nuclear rod. To accomplish this, the Mod-1 core power must be controlled to compensate for differences between the electrical and nuclear rod thermal-physical properties. This control is based on analytical results obtained from the LOFT RELAP4/MOD5 "Hot Pin" model calculations [4]. From these results two parameters (heat transfer coefficient and fluid temperature) are used as boundary conditions for a one dimensional heat conduction model of a Mod-1 electrical rod. The Mod-1 core power is then iterated upon until a core power transient is found that will produce, within a certain accuracy, the same cladding temperature (and consequently surface heat flux) as that calculated by the LOFT "Hot Pin" model.

The Mod-1 system broken loop was subjected to simulating a double-ended cold leg break through two rupture assemblies and two LOFT counterpart nozzles, each having a break area of 0.000243 m^2 . In this broken loop, the pump and steam generator were simulated with due resistances. For example, the broken loop pump was simulated with an orifice having loss coefficient equal to 8.97.

The performance of the system during test was monitored by 224 detectors. The data obtained were recorded on both digital and analog data acquisition systems. Processing analysis has been performed only to the extent necessary to obtain appropriate

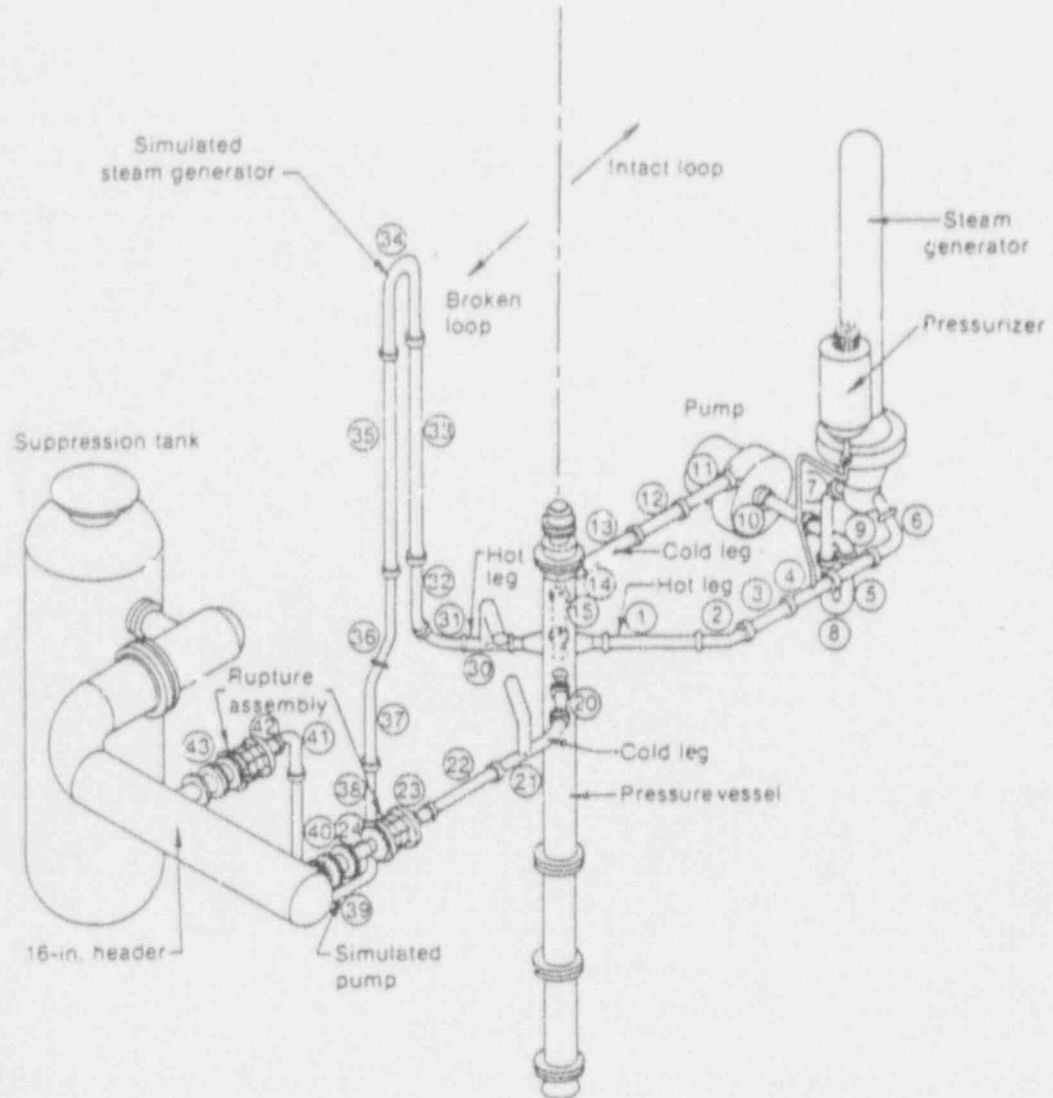
engineering units and to ensure that the data are reasonable and consistent. In all cases, in converting transducer output to engineering units, a homogeneous fluid was assumed. Further interpretation and analysis should consider that sudden decompression processes such as those occurring during blowdown may have subjected the measurement devices to nonhomogeneous fluid conditions.

2.2 Transient Description

Test S-06-3 was performed as part of the Semiscale Mod-1 portion of the Semiscale Program conducted by EG&G Idaho, Inc., for the United States Government. This test was part of the LOFT counterpart test series (Test Series 6) performed to investigate the response of the Mod-1 system to specific variations in the peak power densities of the heater rods to assist the LOFT program in the planning of the first LOFT nuclear test series. Hardware configuration and test parameters were selected to yield a system response that simulates the response of the LOFT nuclear facility during the first nuclear test series.

The test was conducted from initial conditions of 15769 kPa and 563 K (at the intact loop cold leg vessel inlet) with a simulated full size (200%) double-ended offset shear of the broken loop cold leg piping at an initial core power level of 1.004 MW, and an initial core inlet flow rate of 6.68 l/s. The instantaneous offset shear of the broken loop cold leg piping was simulated by simultaneous (within 10 ms) actuation of the rupture

assemblies. After initiation of blowdown, power to the heated core was reduced to simulate the predicted heat flux response of nuclear fuel rods during a loss-of-coolant accident. Blowdown was accompanied by simulated emergency core coolant injection into the cold leg piping of the intact loop. Coolant injection from the high pressure injection system pump began at blowdown and continued until test termination. Coolant injection from the accumulator started approximately 18.5 seconds after rupture at a system pressure of 4200 kPa and continued to depletion at 68 seconds after blowdown. Low pressure coolant injection began 25.5 seconds after rupture at a system pressure of 1900 kPa and continued until test termination. The core power was tripped off at 300 seconds after rupture and the test was terminated.



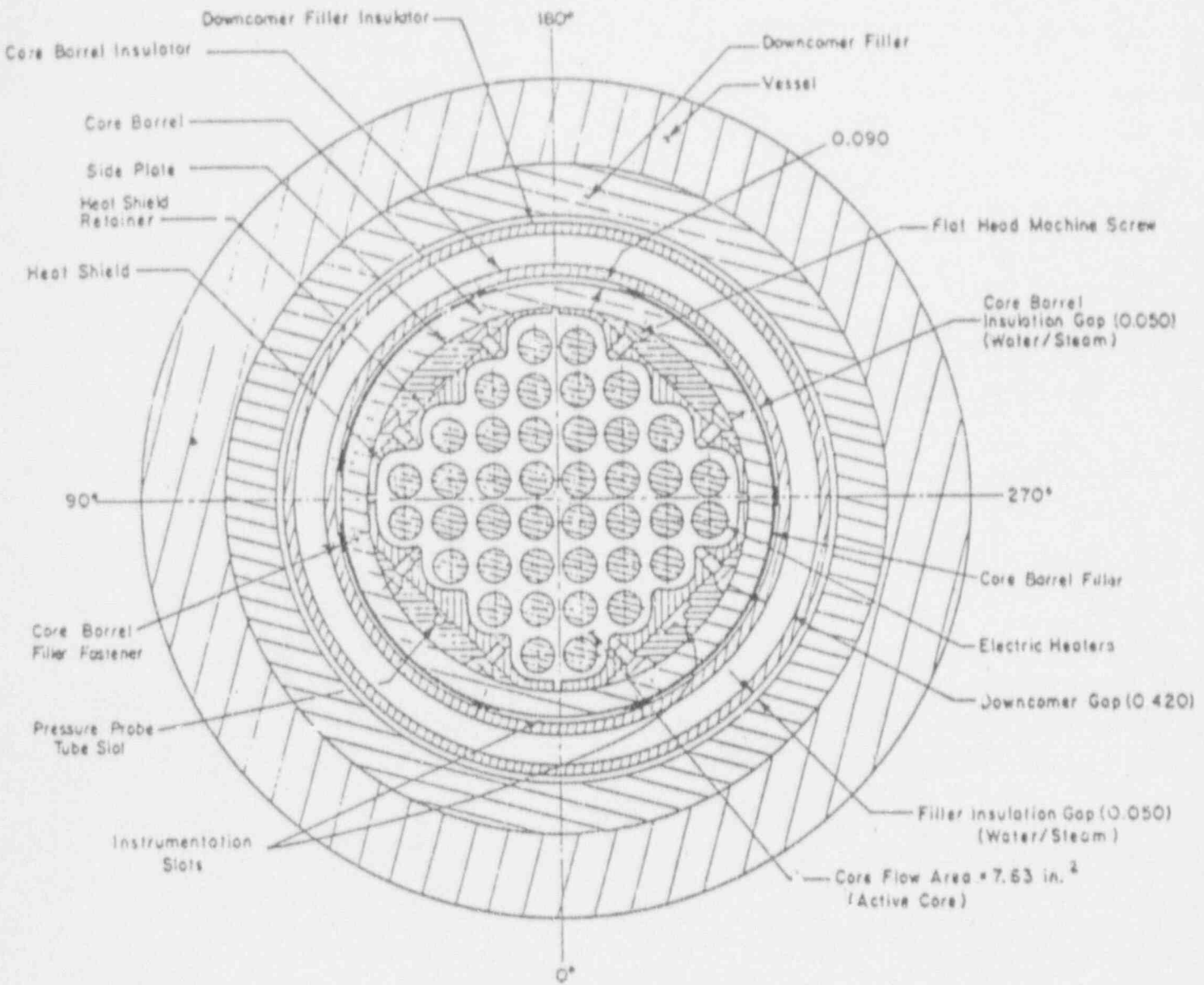


Fig. 2-2. Electric Heater Rod Matrix for Mod-1 Core

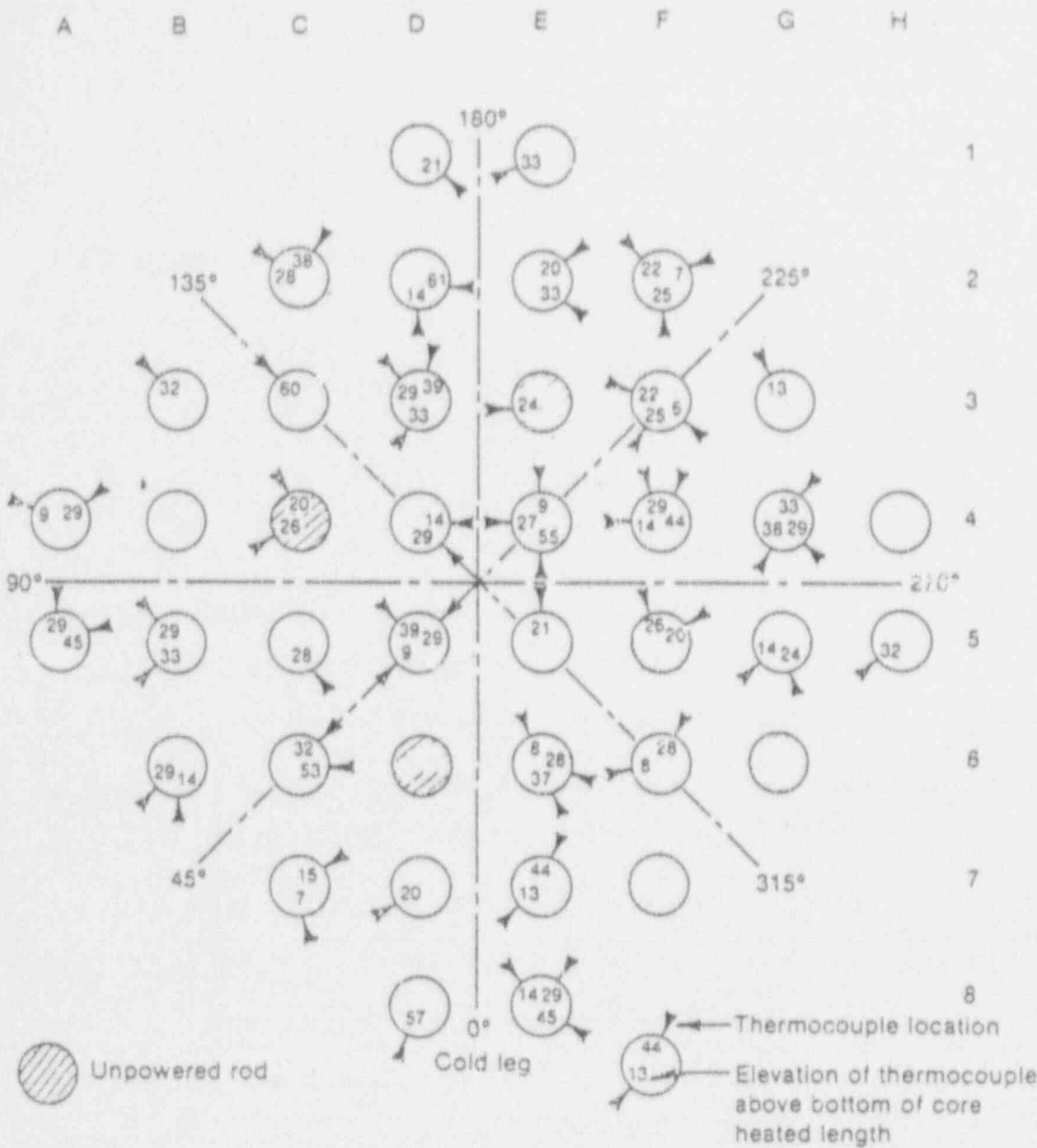


Fig. 2-3. Semiscale Mod-1 Heated Core Plan View

3. MODELING DESCRIPTION

3.1 RELAP5/MOD2 Modeling

RELAP5/MOD2 is an advanced one-dimensional system analysis computer code developed at the INEL for the U.S. Nuclear Regulatory Commission (NRC). The principal feature of the RELAP5 series is the use of a two-fluid, non-equilibrium non-homogeneous hydrodynamic model for transient and accident simulation of a two-phase system. Instead of only five equations used in the RELAP5/MOD1 version, RELAP5/MOD2 employs a full non-equilibrium, six-equation two-fluid model.

In this report, test data of Semiscale S-06-3 were used to assess version 36.04 of RELAP5/MOD2. In modeling of Semiscale Mod-1 system, a total of 95 hydraulic volumes, 107 junctions and 64 heat structures were used, as shown in Figure 3-1. In modeling of the reactor core, a total of 22 volumes were used to represent the core hydraulic space, which included both average and hot channels in parallel. Besides, 11 cross-flow junctions were also used to model radial connections between both average and hot channels. In modeling of both average power rods (32) and hot rods (4), a total of 22 heat structures were used with half set for each, in which the maximum number of axial interval for 2-D reflood calculation was set to 8 in the base model. In modeling of other parts of the pressure vessel, three volumes were used to model each lower and upper plena with attached heat slabs to simulate structure material, and annulus

components having 6 volumes were used to model vessel downcomer also with heat slabs attached.

In modeling of the pressurizer attached on the intact loop, 13 volumes were used to model the pressurizer vessel and 3 volumes were used to simulate surge line. In modeling of the steam generator on the intact loop, six volumes were used to represent the primary side with inlet and outlet plena included, and six volumes were used for the secondary side which included a downcomer and a separator. While in the modeling of the broken loop steam generator, only two volumes were used for the primary side with suitable resistances. In modeling of pumps, due pump component was used for the intact loop coolant pump. As for the broken loop pump modeling only a junction with adequate loss coefficient ($K=8.97$) was adopted.

In modeling of emergency core cooling system (ECCS), only three sets of time-dependent volumes and junctions were used to simulate each sub-system, which consisted of the high pressure injection system, the low pressure injection system and the accumulator.

In modeling of the double-ended cold leg breaks, two normal junctions with due area and chocking flag on were used to simulate both near pump and near vessel breaks. Two identical time-dependent volumes connected to each break junction were used to represent the pressure suppression tank.

In addition to the system modeling, adequate control variables were generated so that direct comparison with data could be made. Those reproduced parameters included the collapsed water levels, fuel temperatures and so on. All input data are listed in the Appendix.

3.2 Assumptions and Initial Conditions

In simulating the Semiscale S-06-3 test, following assumptions were made so that undesired calculation uncertainties could be avoided:

- (1) All ECCS injection flow rates including high pressure injection, low pressure injection and accumulator were provided as boundary,
- (2) Recorded pressure history in the pressure suppression tank was provided as boundary,
- (3) Measured power variance supplied to heater rods was provided,
- (4) Measured intact loop pump speed was also provided, and
- (5) Because the measured cladding temperature was actually obtained 0.076 cm below the surface of the cladding, associate² heater internal mesh temperature was used to compare instead of heater surface temperature.

Steady state was achieved by using some initialization techniques including pressurizer desired pressure and water level control, desired loop flow control and etc.. The resulting initial condition is listed in Table 3-1. The calculated and measured initial conditions [1] are matched quite well.

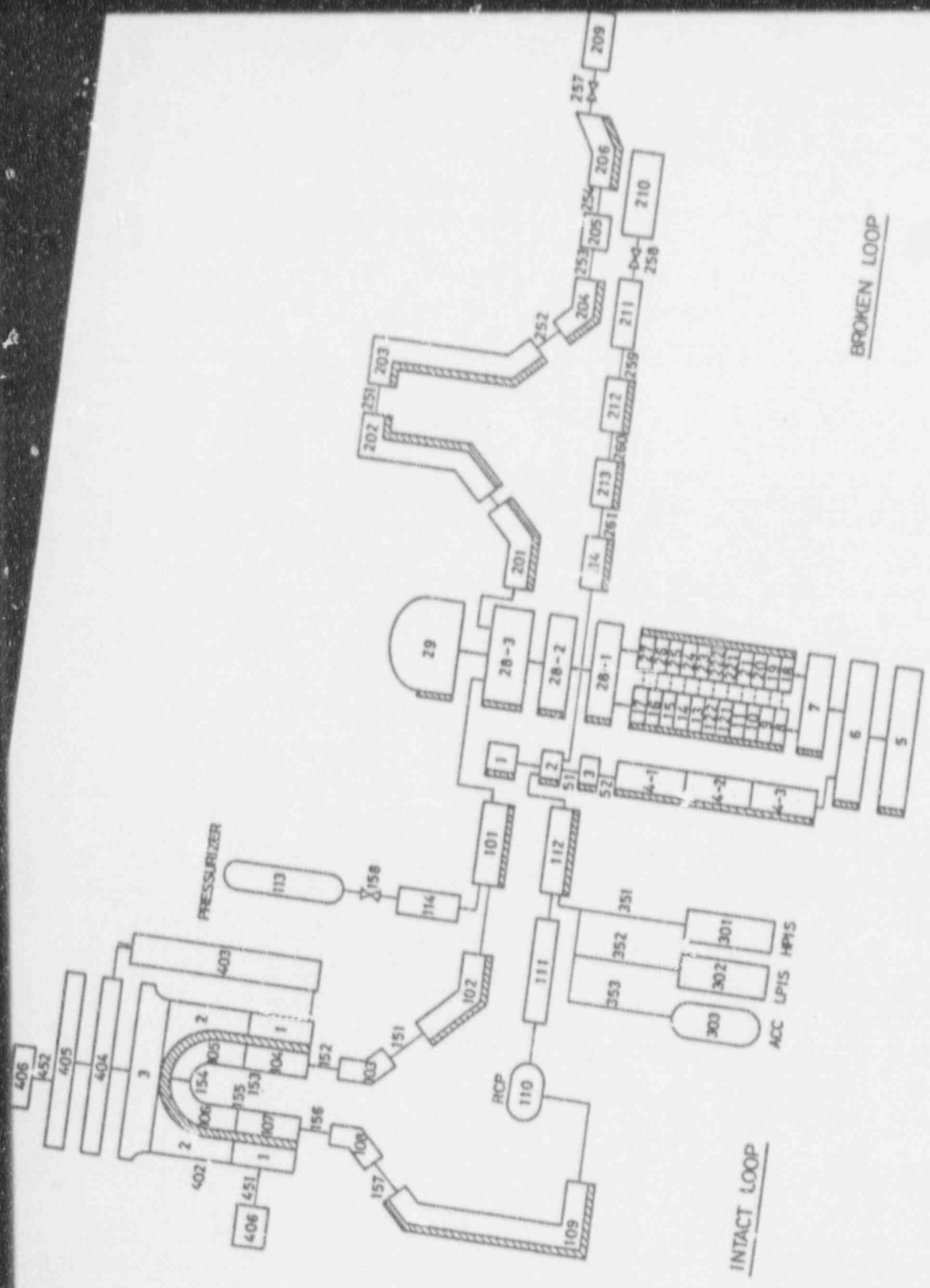


FIG. 3-1

Semiscale Mod-1 System Noding Diagram

Table 3-1 Comparison of Calculated and Measured
Initial Conditions

<u>Parameter</u>	<u>Measured</u>	<u>RELAPS</u>
Core power (MW)	1.004	1.004
Intact loop cold leg fluid temperature (K)	563.0	563.0
Intact loop hot leg fluid temperature (K)	598.0	598.0
Broken loop cold leg fluid temperature (K)	562.0	562.0
Broken loop hot leg fluid temperature (K)	591.0	
Intact loop cold leg flow (l/sec)	6.68	6.68
Pressurezer pressure (MPa)	15.769	15.766
Pressurizer liquid mass (kg)	9.09	9.09
S.G. Secondary side pressure (MPa)	6.55	6.53

* Uncertainties of each measurement are discussed in Reference 1

4. RESULTS

In this section, analytical results from the base modeling elaborated above are compared to the test data. Besides, effects of several different modelings are also independently investigated to ensure that results are within reliable domain.

4.1 Comparison with Measurement

Included in this subsection is comprehensive comparisons of the calculated results and measured data. The whole test can be classically divided into three different phases, namely blowdown, refill and reflood. In general, the blowdown phase is characterized by a fast system depressurization and finally the system is in equilibrium with the surroundings. During this phase large part of fuel rods will experience critical heat flux (CHF) due to rapid loss of reactor coolant. In the second refill phase, owing to the activation of injections ECCS, emergency coolant begins to accumulate in the reactor vessel. Once the lower plenum is filled up, this phase is terminated by definition. Because of continuous ECCS injections, vessel water level will keep on ascending up to the active core in the last reflood phase and finally all fuel rods will be rewetted again.

4.1.1 Blowdown Phase (0-35 seconds)

After the artificial rupture took place in the broken loop, the primary system began to blowdown. The resulting break flow rates at two ends from both simulation and measurement are shown

in Figures 4-1 and 4-2 respectively. Observing the break flow near the pump side, it can be found that the steam break flow rate seemed to be underpredicted a little. As for the break flow rate near the vessel side, they both matched quite well until the ECCS flow bypassed to the broken loop. When ECCS water bypassed to the broken loop cold leg, break flow rates from calculation and test began to oscillate. Nevertheless, oscillation magnitudes were little different.

The pressureizer pressure responses are compared in Figure 4-3. It can be observed that they also matched quite well except the timing of pressure inflection point. This inflection difference basically was caused by different pressurizer empty time. As well known, the pressurizer empty would cause an inflection of pressurizer pressure. To illustrate this feature, pressurizer outsurge flow rates are also compared, as shown in Figure 4-4. It is clear that the empty time exactly corresponded to each pressure inflection point. The late prediction of the pressurizer empty may come from several reasons. Among them are the modelling of heat transfer between liquid and vapor space, the stored heat of pressurizer vessel and the form loss of pressurizer surge line.

The intact loop cold leg and hot leg flow rates are shown in Figures 4-5 and 4-6 respectively. The calculated intact loop cold leg flow rate matched the data very well. As for the hot leg flow, the calculated one reversed a little late. Also

compared are broken loop flcw rates, as shown in Figures 4-7 and 4-8 for cold leg and hot leg respectively. Just the same as the intact loop, the calculated cold leg flow rate matched the data very well until the ECCS injection bypass occurred. With reference to the broken loop hot leg flow, they also matched well except in the early 3 seconds. Other than loop flow rates, the core inlet flow rates are also compared, as shown in Figure 4-9. As a result of ruptures, core flow was suddenly stagnated which was clearly elucidated in this figure.

As a result of system blowdown, water levels in the reactor vessel descended drastically. Collapsed water level responses ($\Delta P/\rho_f$) in the downcomer are shown in Figure 4-10. It can be seen that after the rupture began, water level declined steeply and at the end of blowdown there was almost no water existed in the downcomer. From the comparison, it can be found that the RELAP5 calculation agreed with what was measured. Concerning the water level in the lower plenum, since it is the lowest part of the system, water level in it varied less violently and at the end of blowdown it still detained about one-third of coolant in it, as shown in Figure 4-11. Again, reasonable agreement between calculation and measurement was also observed. Resulting core collapsed water level responses are shown in Figure 4-12. It can be seen that the calculated water level dropped below the active fuel within 5 seconds after ruptures began, which was about 10 seconds ahead of what was measured.

Peak cladding temperature responses of both high and low power rods are also compared. After ruptures began, system pressure would reduce sharply and core flow would quickly drop to zero due to stagnation as depicted above. As a result, fuel rods in the core experienced CHF quickly and consequently fuel cladding temperatures jumped to certain elevated values, as shown in Figures 4-13 and 4-14 for high and low power rods respectively. From the comparison, it can be found that calculated responses had a good agreement with what was measured, especially true for time to CHF.

As for the coolant temperature calculation, superheated steam was observed in the reactor vessel. Calculated coolant temperatures in both lower and upper plena are compared to associated measured temperatures, as shown in Figures 4-15 and 4-16 respectively. From comparisons, it can be found that superheated steam was calculated and reasonable agreement was achieved. In addition, owing to the reversed steam flow through the core the degree of steam superheating in the lower plenum ascended sharply and the resulting steam temperature was even higher than the initial heat slab temperature in this region. Basically, the reversed steam flow through the core was caused by the effect of condensation induced by the accumulator injection [5].

4.1.2 Refill Phase (35-75 seconds)

Before the end of blowdown, emergency cooling water provided

REACTOR EXCURSION AND LEAK ANALYSIS PROGRAM (RELAP5/MOD2/36.04)

SIMULATION OF SEMISCALE S-06-3 LARGE LOCA TEST

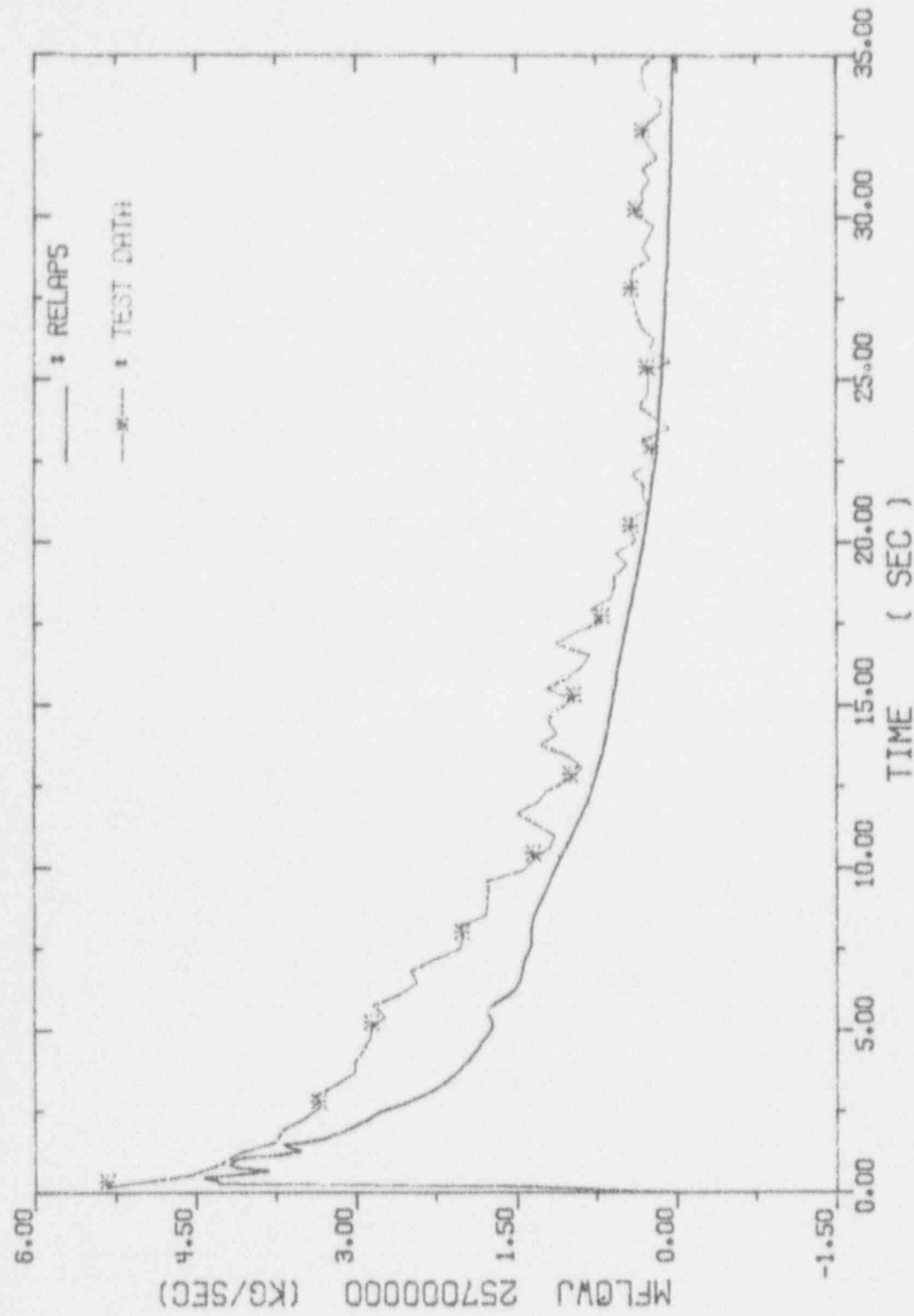


Fig. 4-1. Break Flow Rates near Pump Side

REACTOR EXCURSION AND LEAK ANALYSIS PROGRAM (RELAP5/MOD2/36.04)

SIMULATION OF SEMISCALE S-06-3 LARGE LOCA TEST

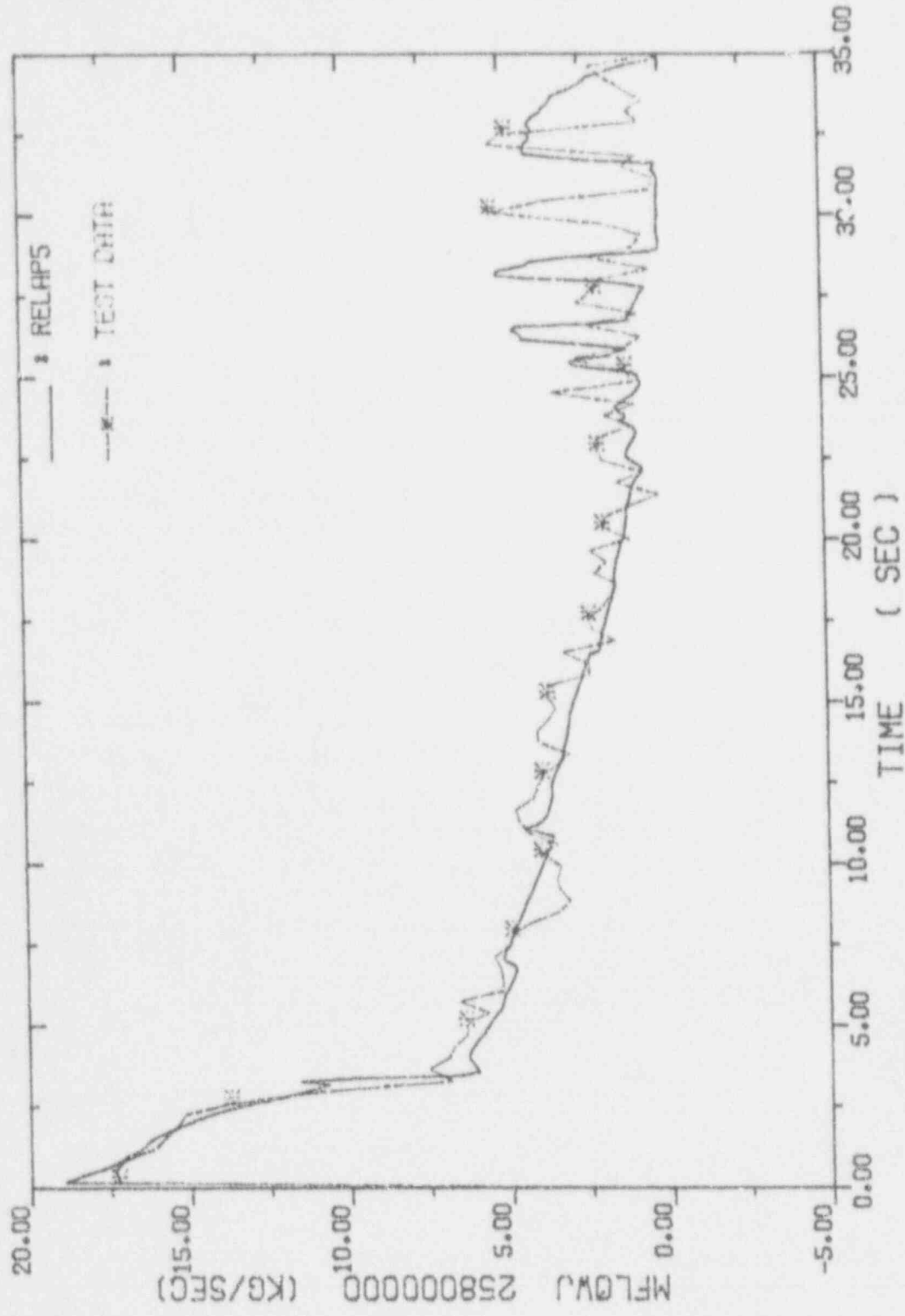


Fig. 4-2. Break Flow Rates near vessel Side

REACTOR EXCURSION AND LEAK ANALYSIS PROGRAM (RELAPS/MOD2/36.04)

SIMULATION OF SEMISCALE S-06-3 LARGE LOCA TEST

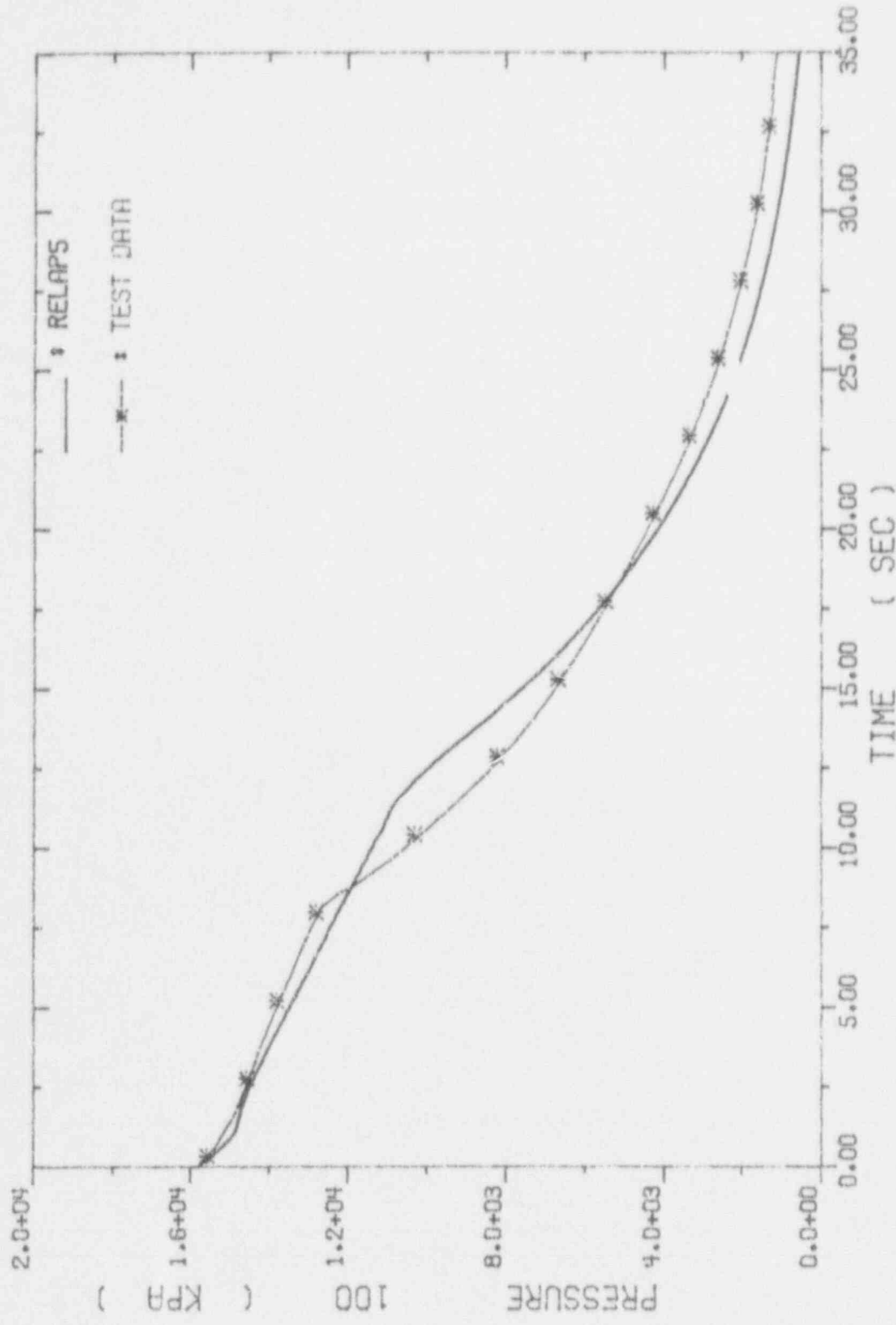


Fig. 4-3. Pressurizer pressures

REACTOR EXCURSION AND LEAK ANALYSIS PROGRAM(RELAPS/MOD2/36.04)

SIMULATION OF SEMISCALE S-06-3 LARGE LOCA TEST

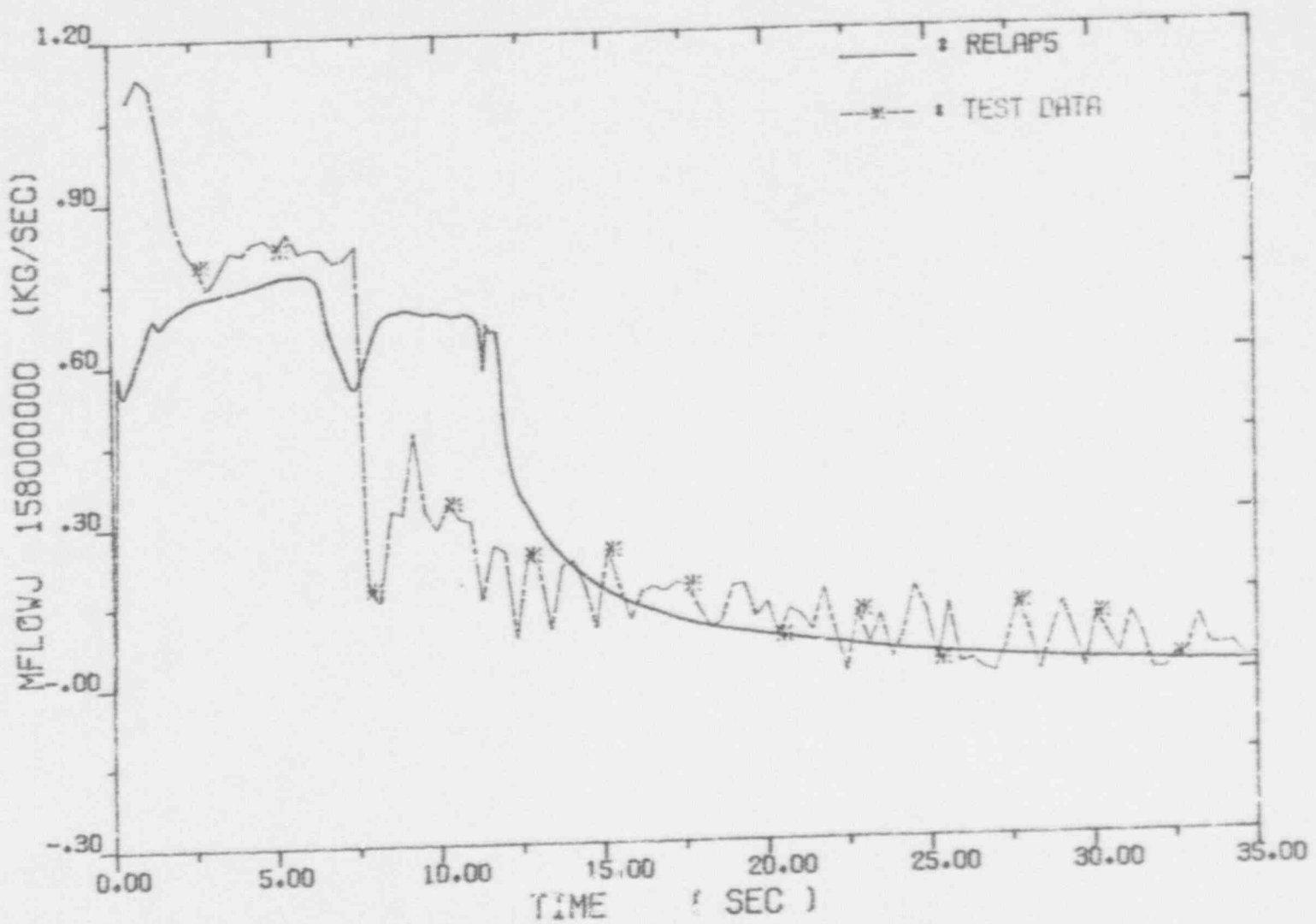


Fig. 4-4. Pressurizer Outsurge Flow Rates

REACTOR EXCLUSION AND LEAK ANALYSIS PROGRAM (RELAP5/MOD2/36.04)

SIMULATION OF SEMISCALE S-06-3 LARGE LOCA TEST

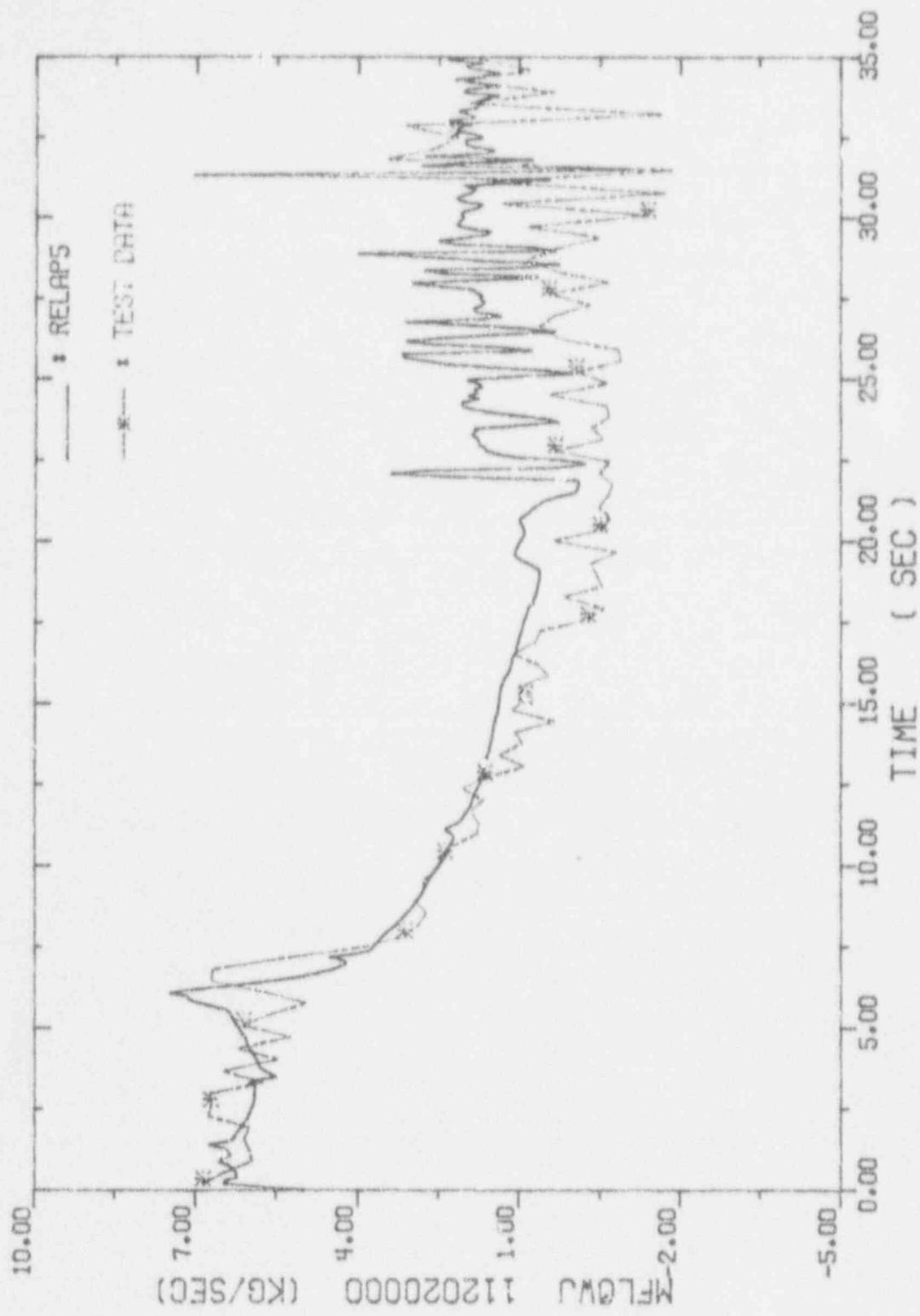


Fig. 4-5. Intact Loop Cold Leg Flow Rates

REACTOR EXCURSION AND LEAK ANALYSIS PROGRAM (RELAP5/MOD2/36.04)

SIMULATION OF SEMISCALE S-06-3 LARGE LOCA TEST

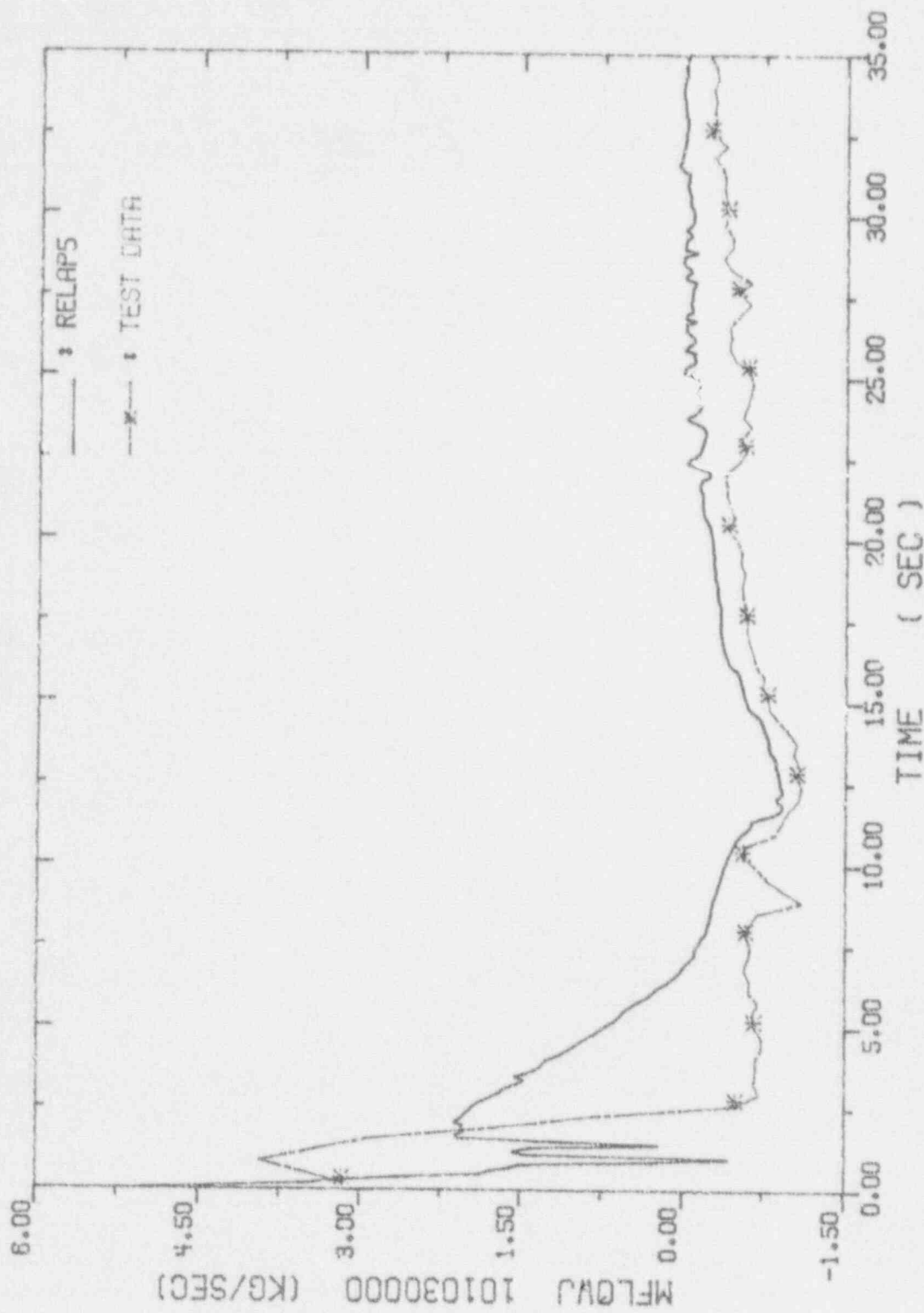


Fig. 4-6. Intact Loop Hot Leg Flow Rates

REACTOR EXCURSION AND LEAK ANALYSIS PROGRAM (RELAPS/MOD2/36.04)

SIMULATION OF SEMISCALE S-06-3 LARGE LOCA TEST

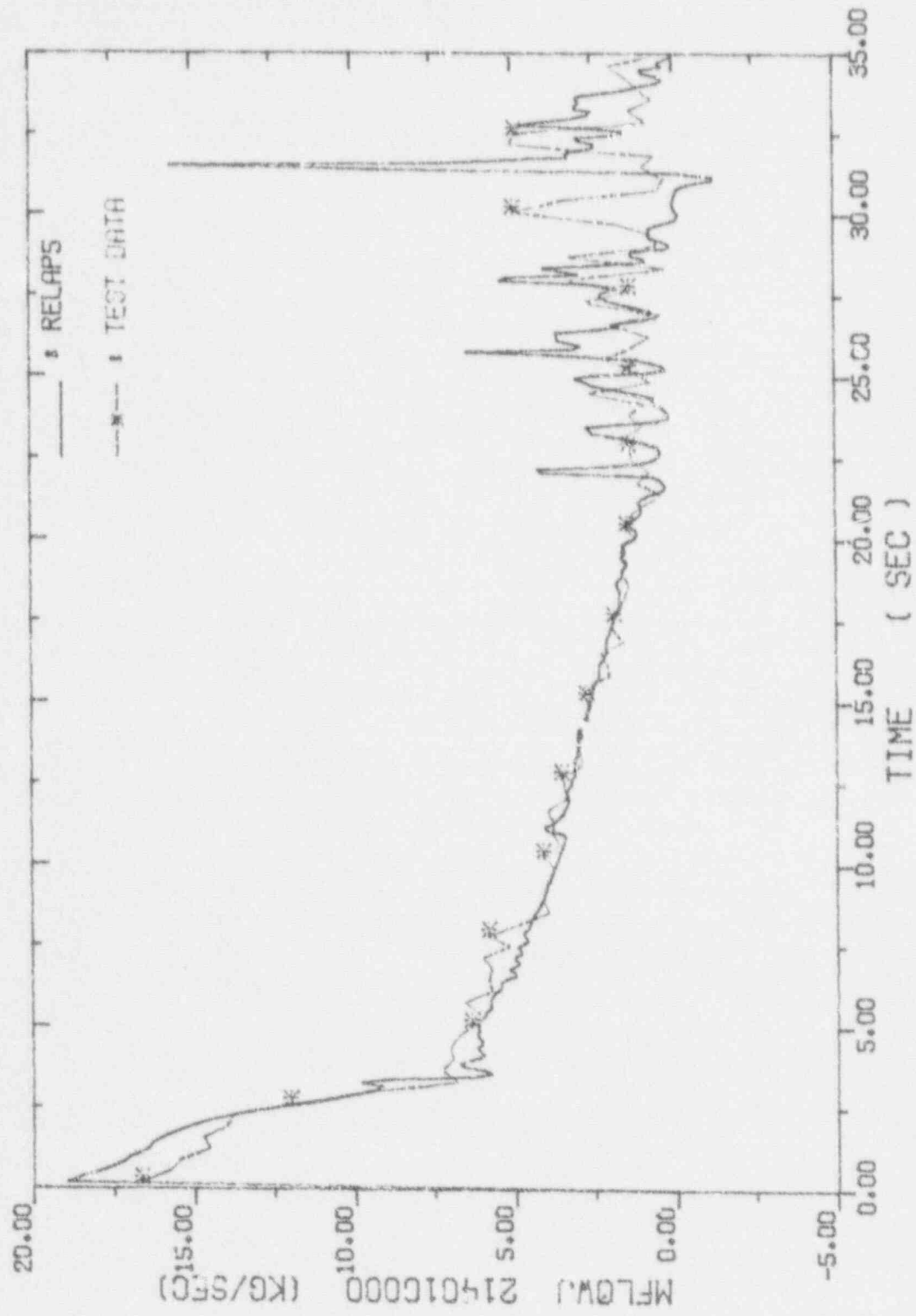


Fig. 4-7. Broken Loop Cold Leg Flow Rates

REACTOR EXCURSION AND LEAK F
SIMULATION OF SEMIS

PROGRAM(RELAP5/MOD2/36.04)

LARGE LOCA TEST

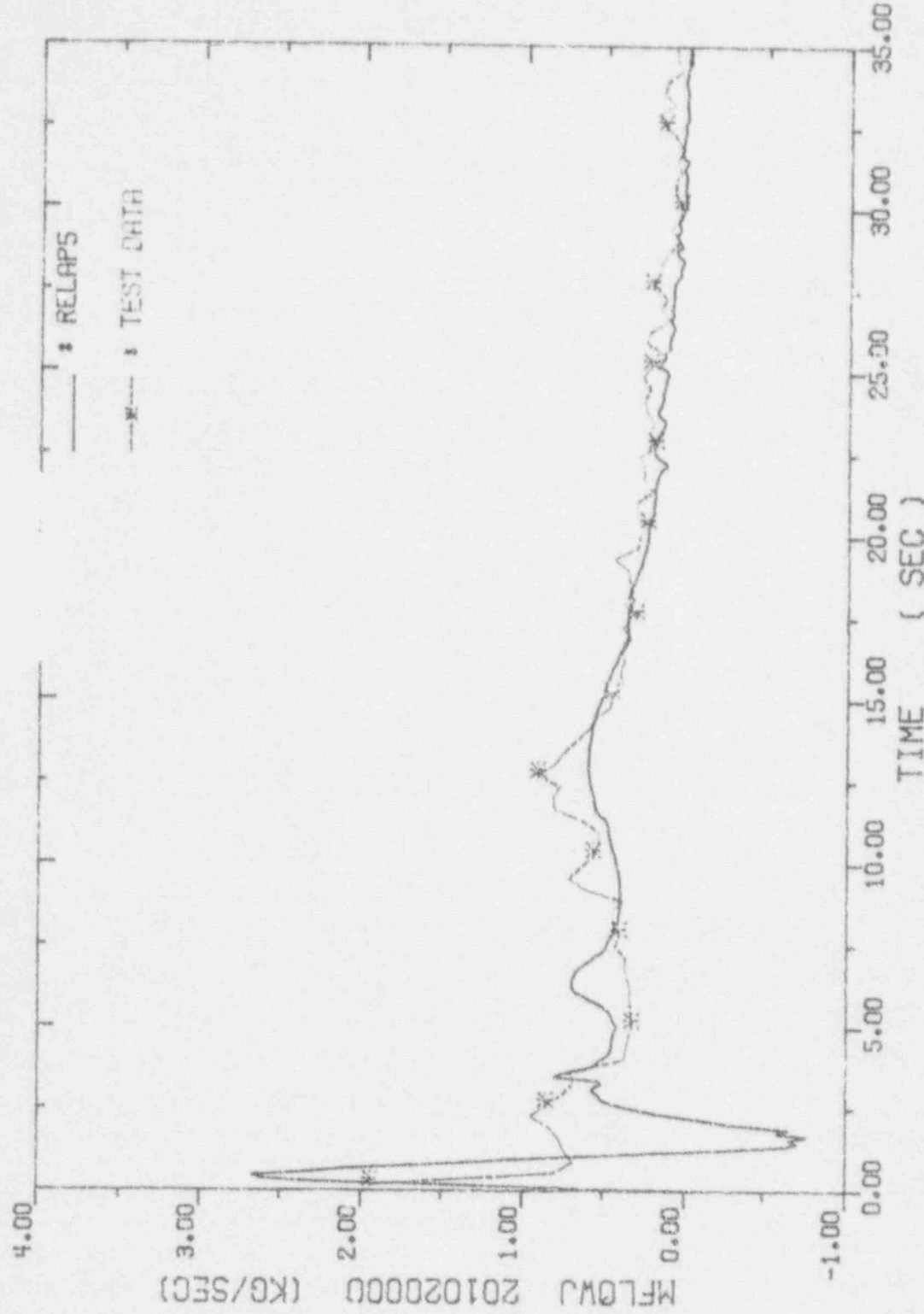


Fig. 4-8. Broken Loop Hot Leg Flow Rates

REACTOR EXCURSION AND LEAK ANALYSIS PROGRAM(RELAPS/MOD2/36.04)

SIMULATION OF SEMISCALE S-06-3 LARGE LOCA TEST

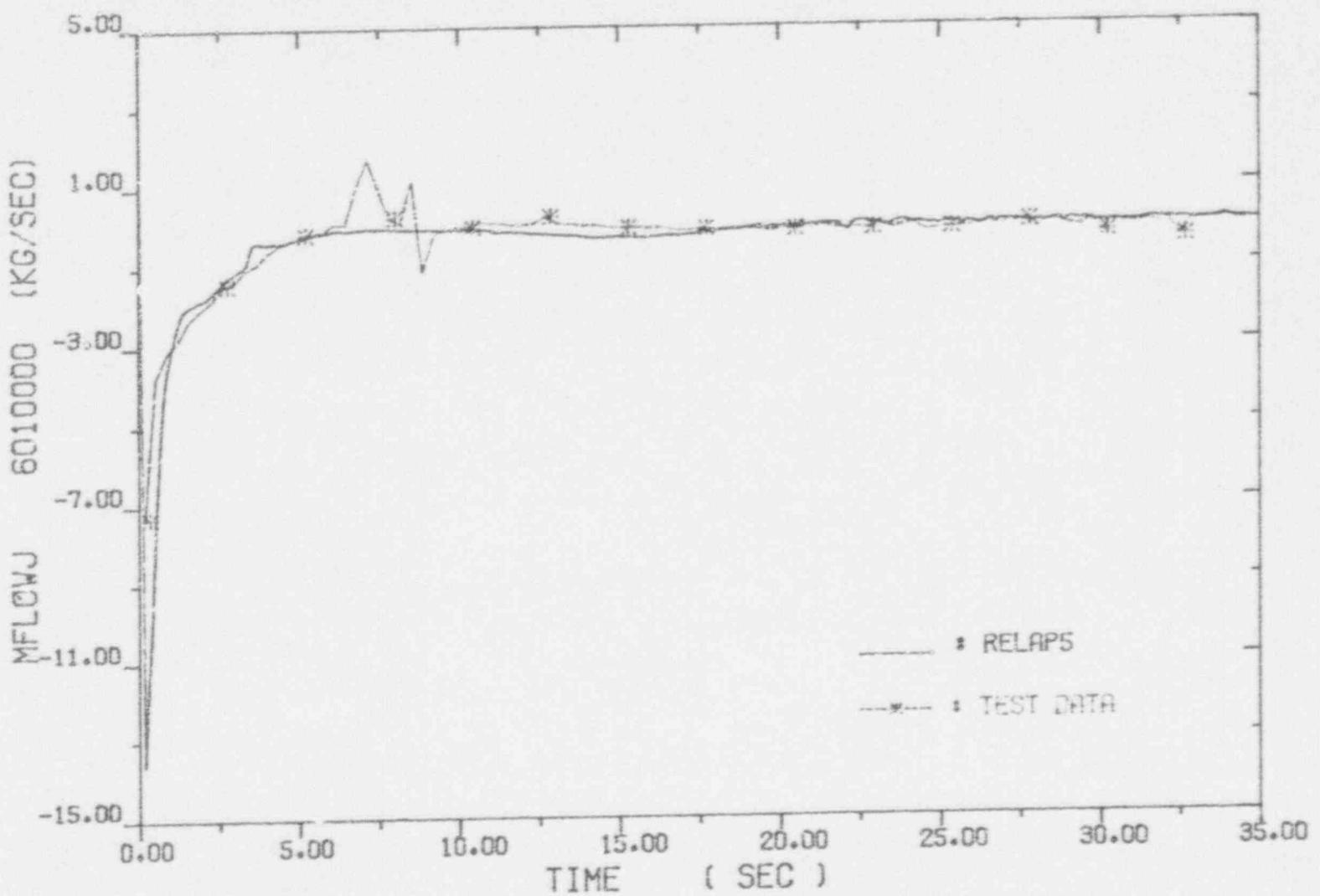


Fig. 4-9. Core Inlet Flow Rates

REACTOR EXCURSION AND LEAK ANALYSIS PROGRAM (RELAPS/MOD2/36.04)

SIMULATION OF SEMISCALE S-06-3 LARGE LOCA TEST

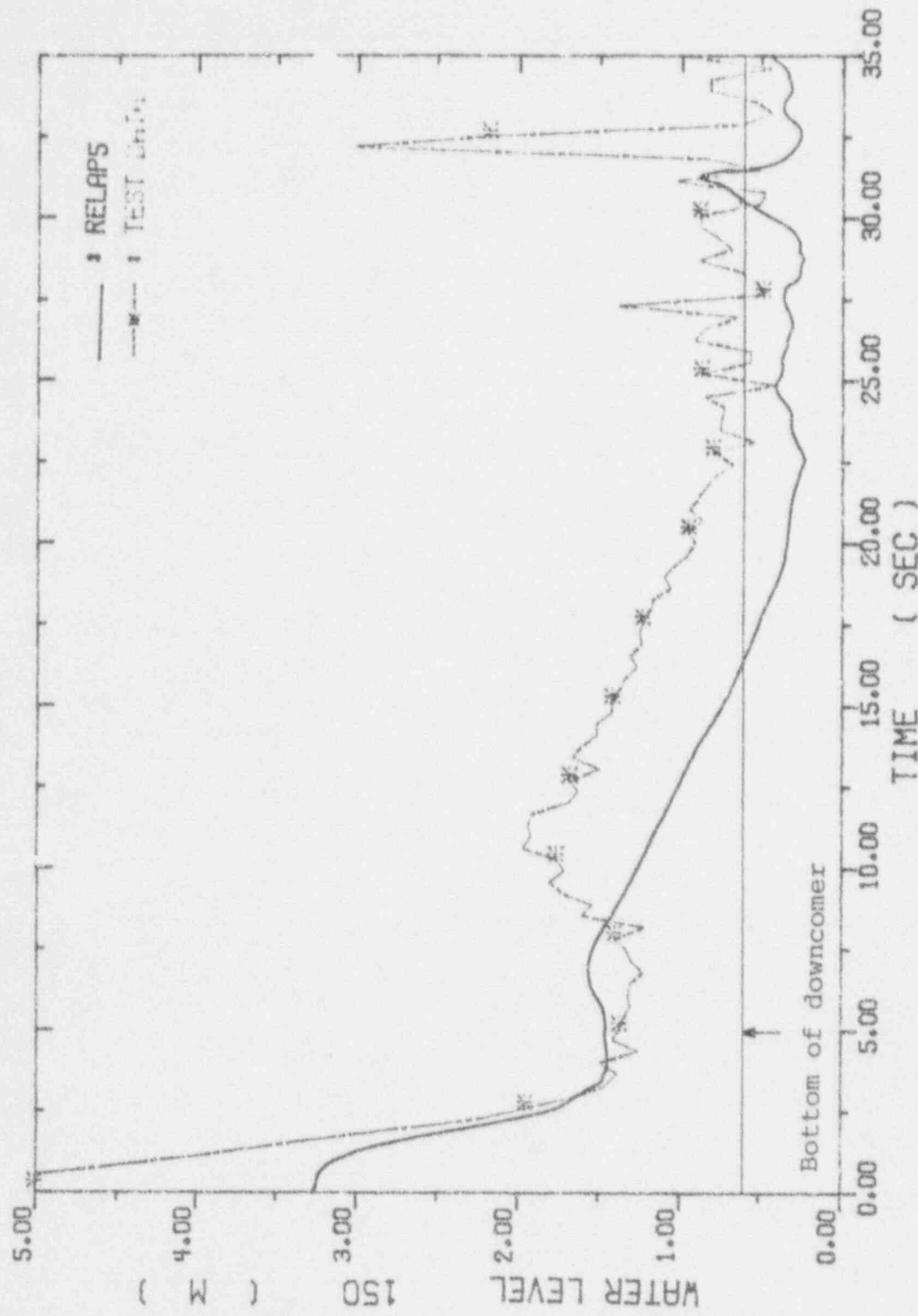


Fig. 4-10. Collapsed Water Levels across The Downcomer

REACTOR EXCURSION AND LEAK ANALYSIS PROGRAM(RELAP5/MOD2/36+04)

SIMULATION OF SEMISCALE S-06-3 LARGE LOCA TEST

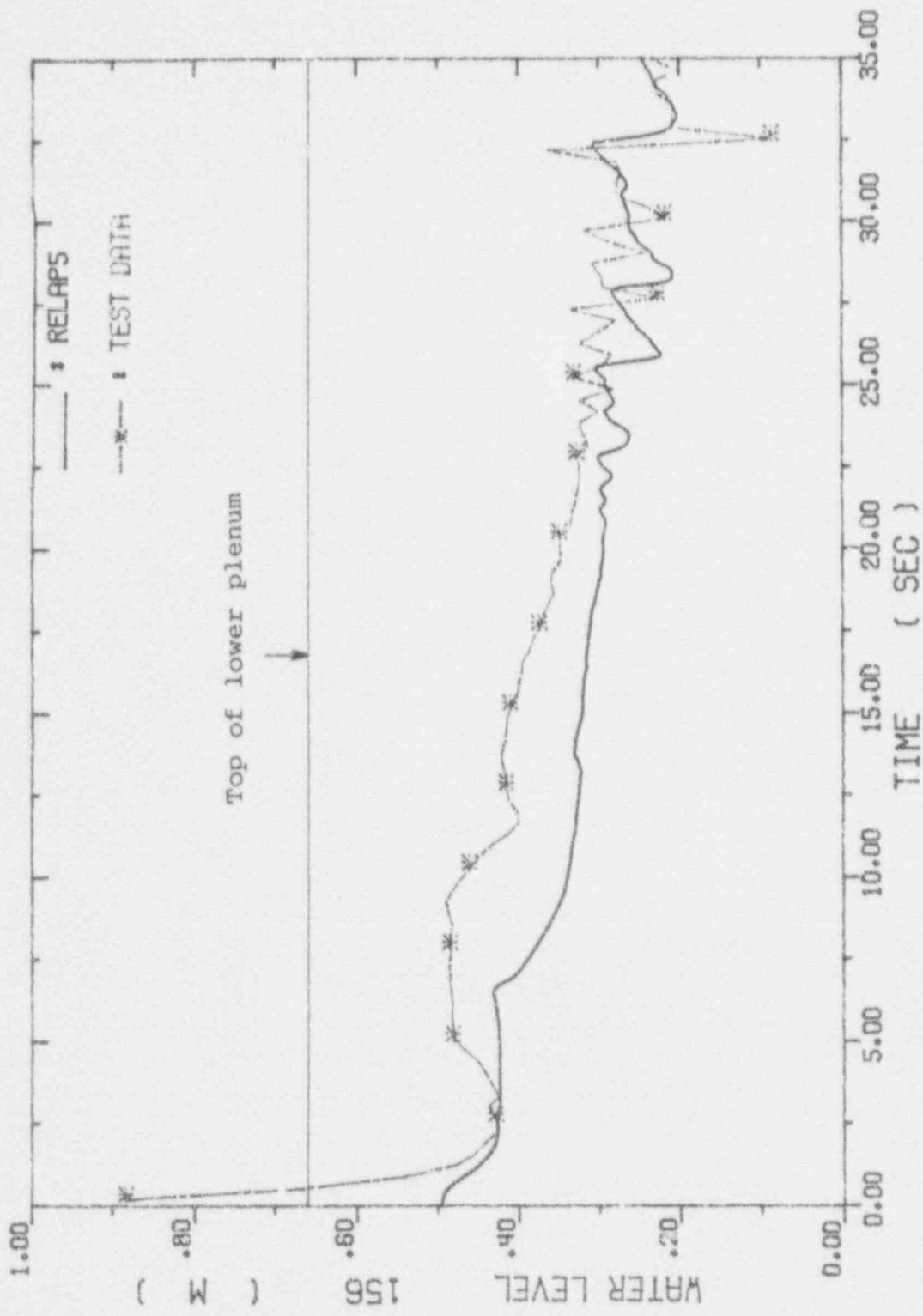


Fig. 4-11. Collapsed Water Levels across The Lower Plenum

REACTOR EXCURSION AND LEAK ANALYSIS PROGRAM(RELAPS/MOD2/36.04)

SIMULATION OF SEMISCALE S-06-3 LARGE LOCA TEST

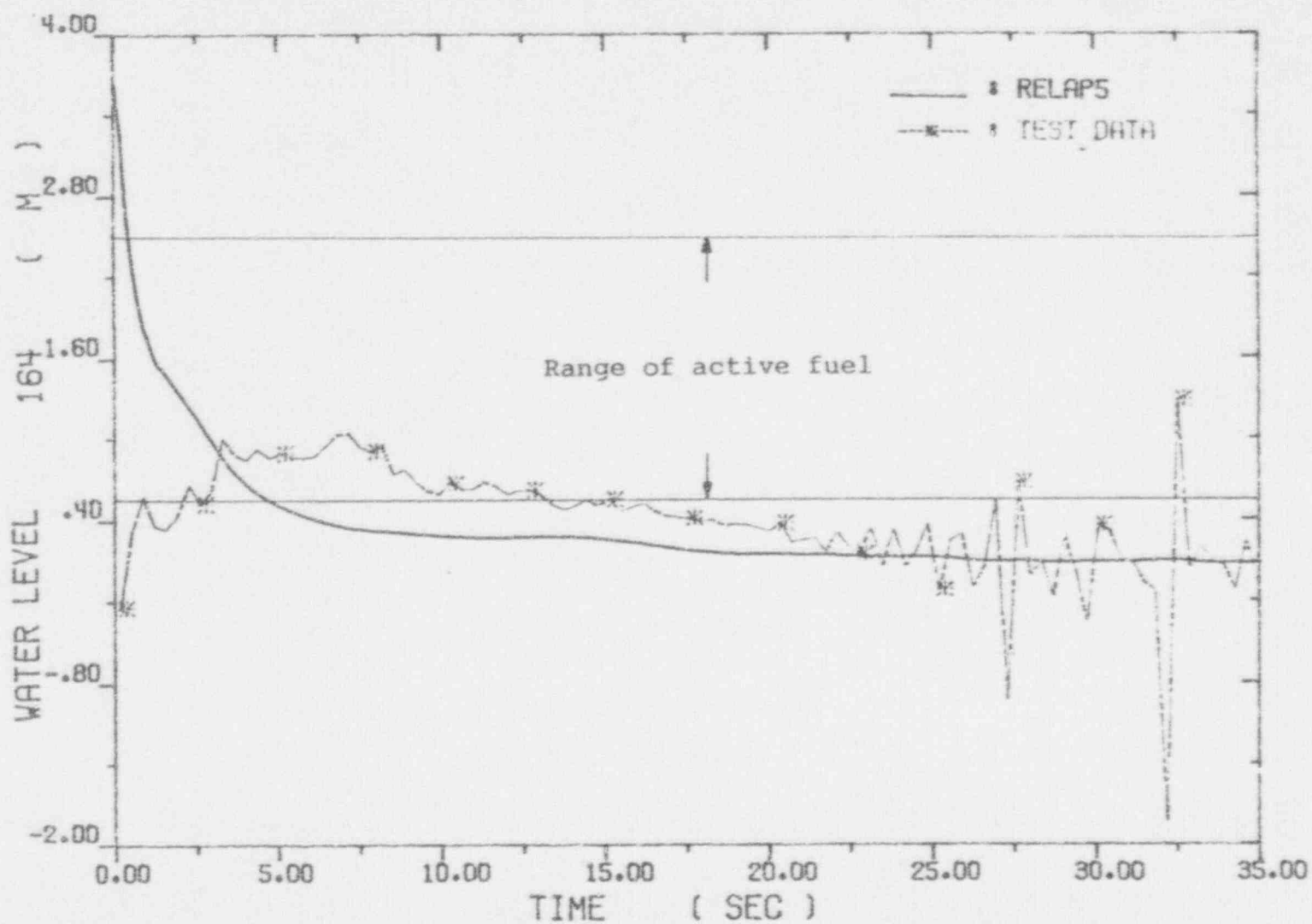


Fig. 4-12. Collapsed Water Levels across The Core

REACTOR EXCURSION AND LEAK ANALYSIS PROGRAM(RELAPS/MGDD2/36.04)

SIMULATION OF SEMISCALE S-06-3 LARGE LOCA TEST

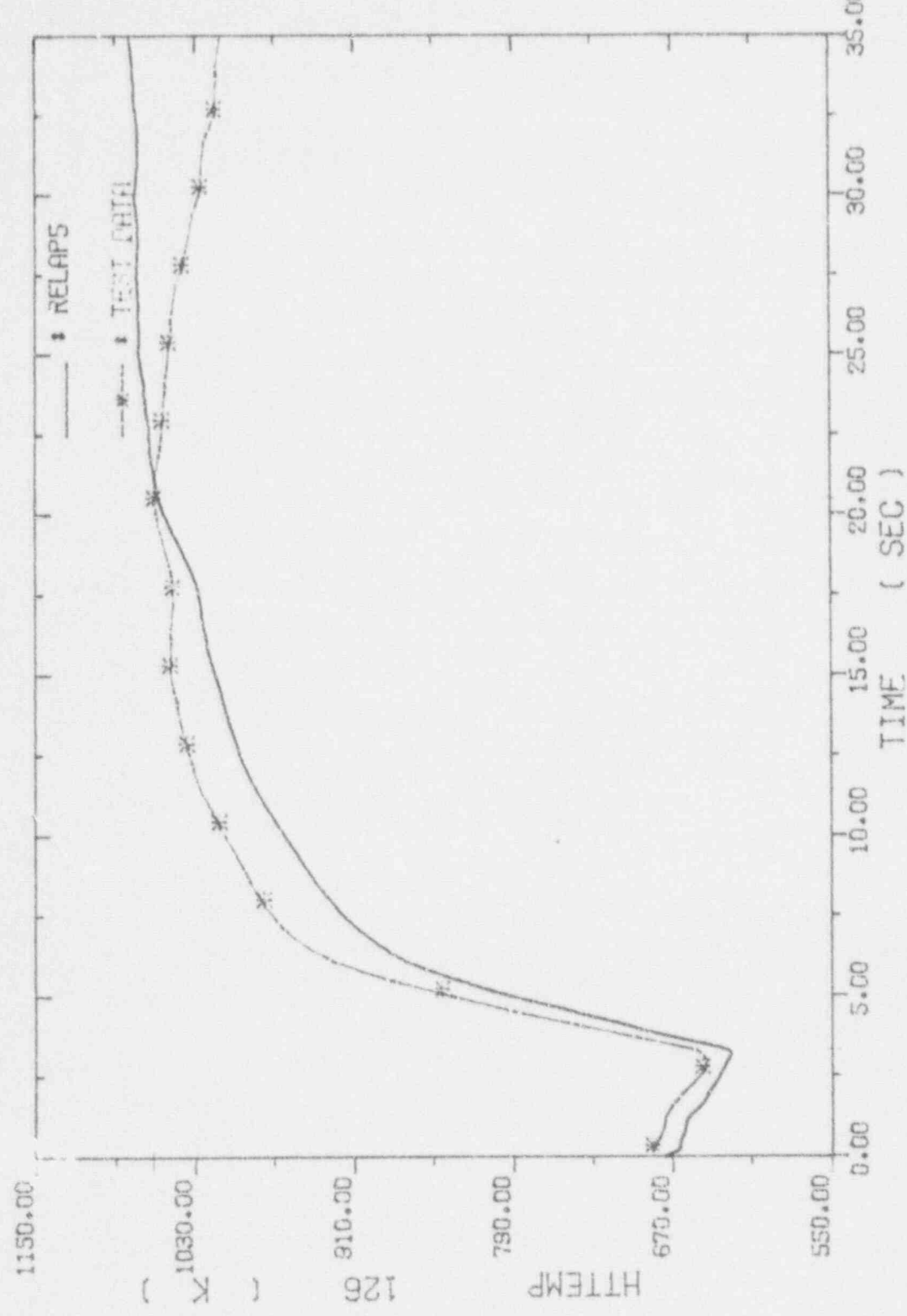


Fig. 4-13. High Power Rod Hot Spot Cladding Temperatures

REACTOR EXCUSION AND LEAK ANALYSIS PROGRAM(RELAPS/MOD2/36.04)

SIMULATION OF SEMISCALE S-06-3 LARGE LOCA TEST

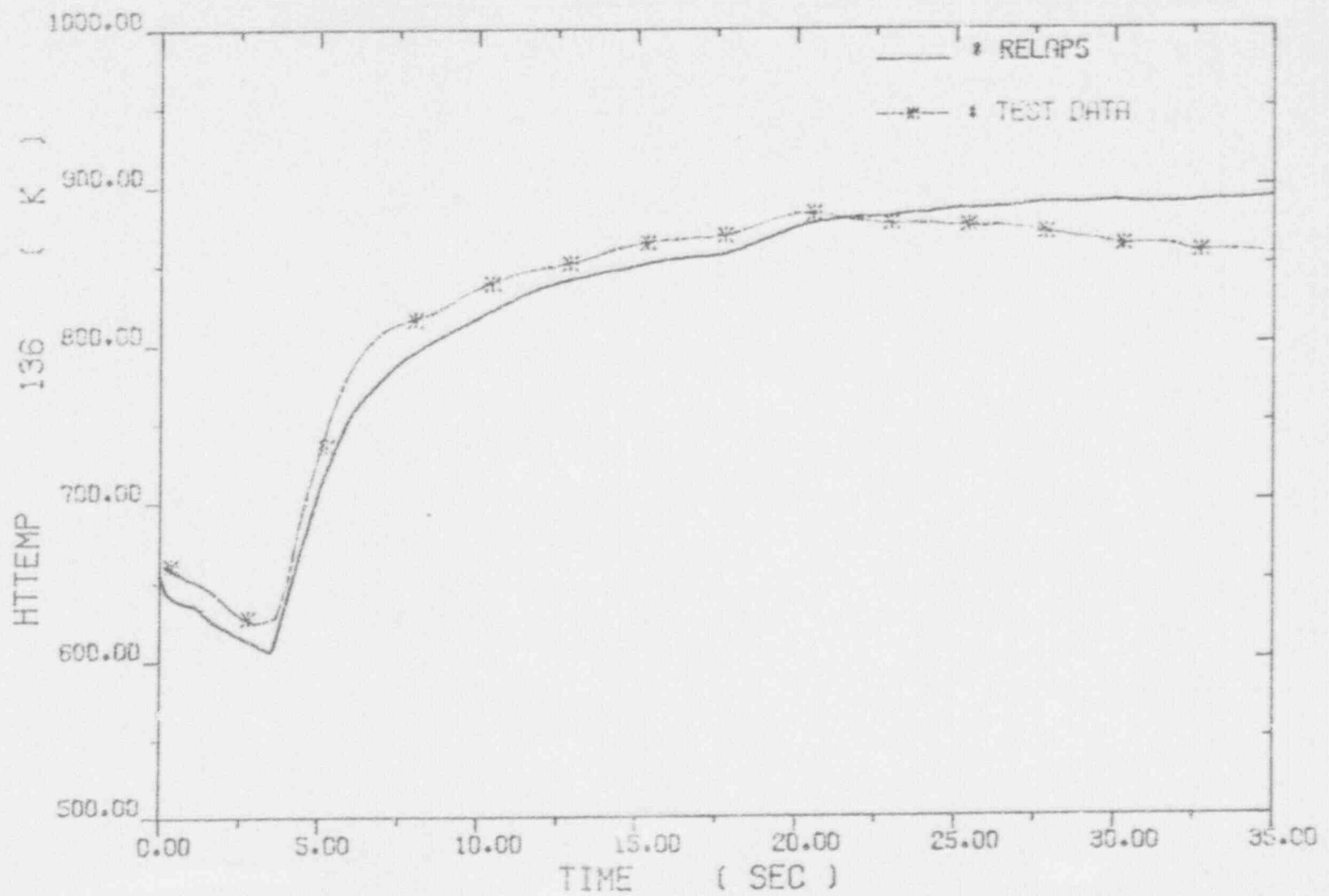


Fig. 4-14. Low Power Rod Hot Spot Cladding Temperatures

REACTOR EXCURSION AND LEAK ANALYSIS PROGRAM(RELAP5/MOD2/36.04)

SIMULATION OF SEMISCALE S-06-3 LARGE LOCA TEST

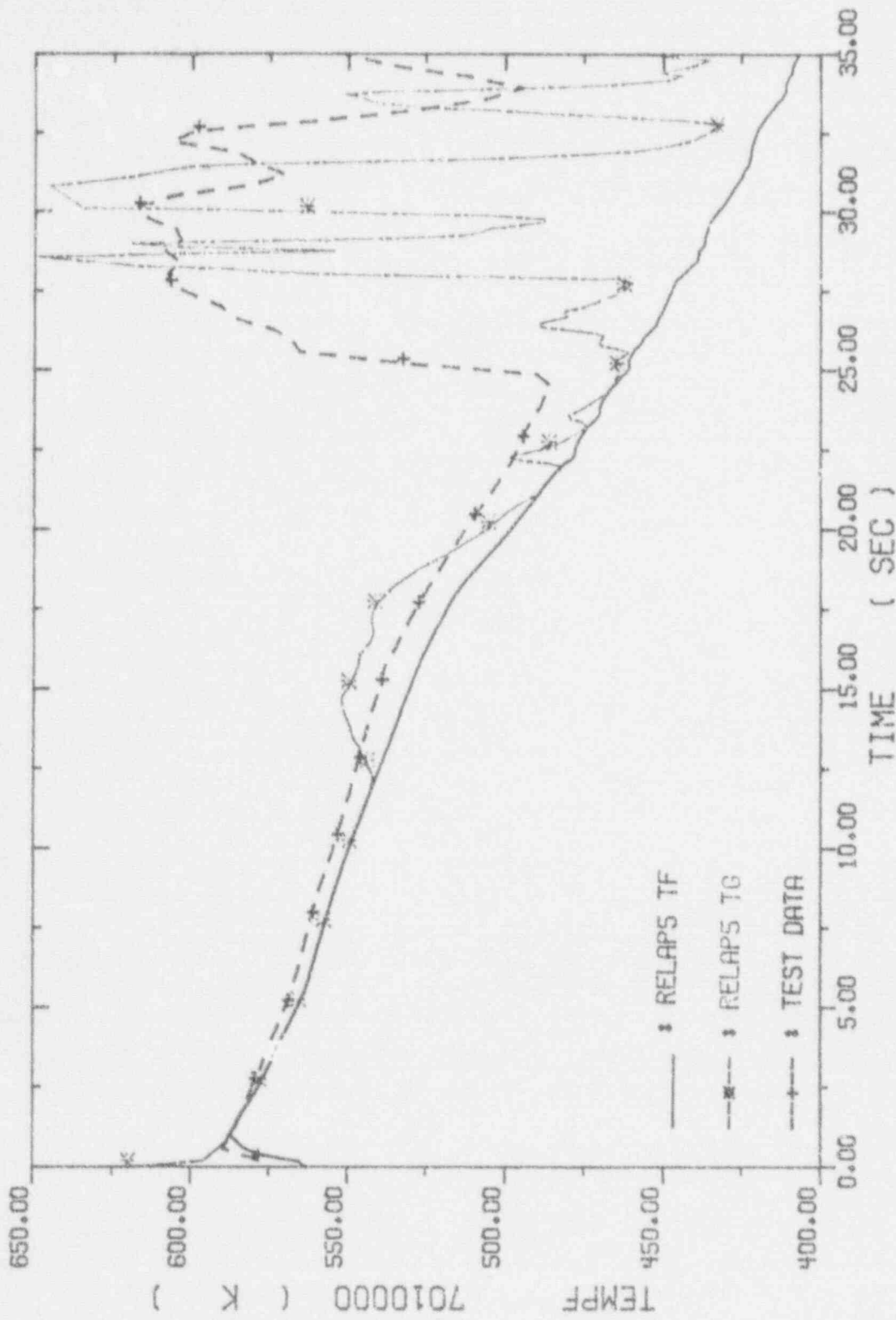


Fig. 4-15. Lower Plenum Coolant Temperatures

REACTOR EXCURSION AND LEAK ANALYSIS PROGRAM (RELAP5/MOD2/36.04)

SIMULATION OF SEMISCALE S-06-3 LARGE LOCA TEST

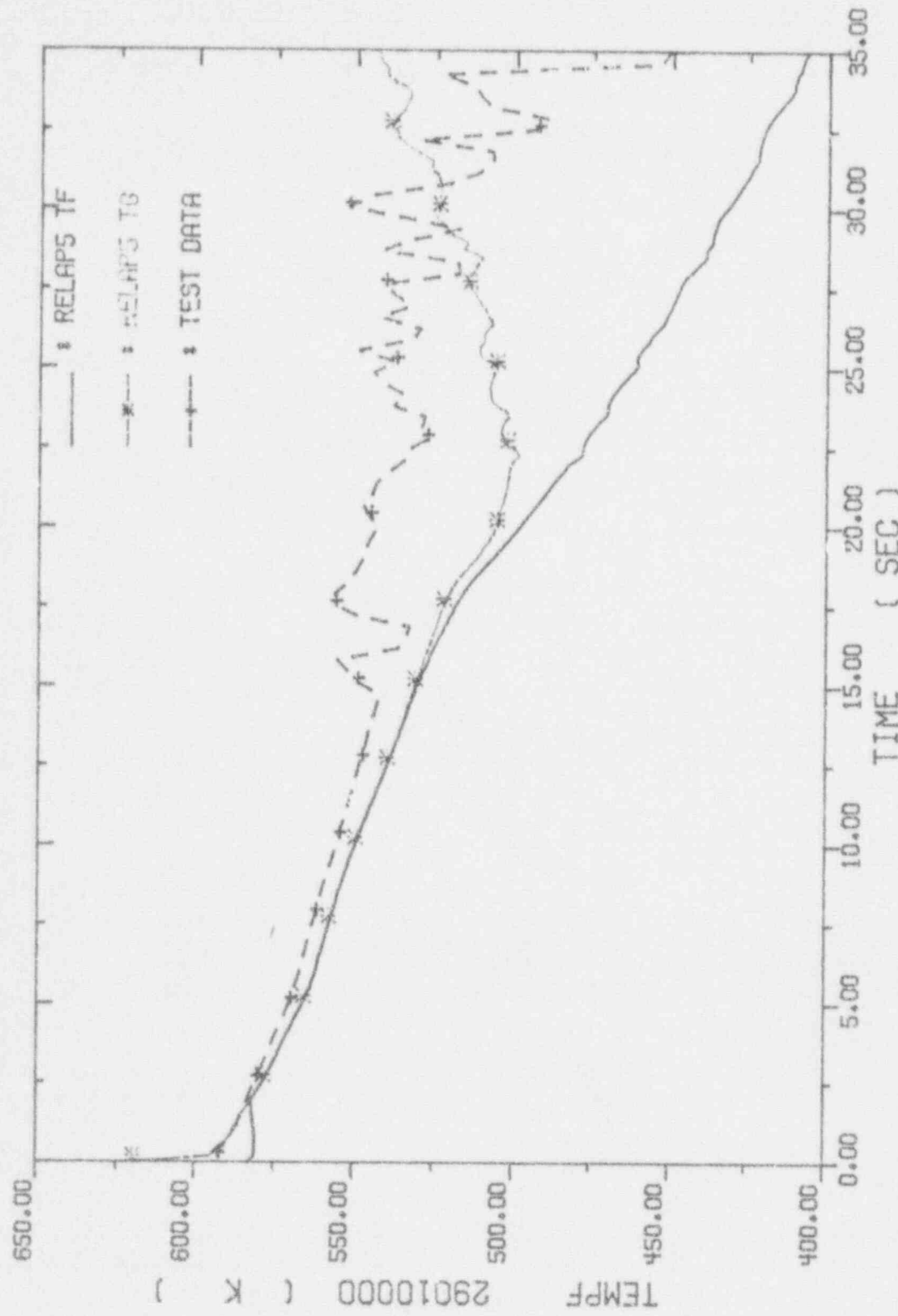


Fig. 4-16. Upper Plenum Coolant Temperatures

by the ECCS would enter the system when system pressure was low enough. In our calculation ECCS injections were provided as a given boundary condition to exclude unnecessary uncertainties.

When accumulator injection began at about 20 seconds, apparent ECC bypass was observed in the test. While in the calculation, due to lack of counter-current flow limit (CCFL) model this phenomenon could not be caught well. In the test, two ECC bypass delay periods were identified [6]; a blowdown-force ECC bypass period supported by counter-current flow-flooding phenomenon in the downcomer annulus; a "hot wall" delay period due to steam generation as cold ECC water comes in contact with the vessel hot walls. As an evidence of this phenomena, broken loop cold leg densities and break flow near vessel side from both experiment and calculation are compared and shown in Figures 4-17 and 4-18 correspondingly. From the comparison, it can be seen that the cold leg density in the test obviously increased after accumulator injection began, while in the calculation the density change was very small only after the downcomer was filled up with water, which will be described later. As for the break flows near the vessel side, it can be also observed that after accumulator injection began, measured break flow rate was obviously higher than what was calculated until about 60 seconds. After 60 seconds, the downcomer was filled up with water in the calculation and therefore following ECC water directly flowed to the broken loop cold leg, which caused the break flow near the

vessel side rose again just as appeared in the associated figure. Serving as another evidence was the core barrel temperature response. Comparison of core barrel temperatures is shown in Figure 4-19. It can be seen that after accumulation injection, core barrel temperature in the calculation began to decrease with another slope, while in the test this temperature behaved just on the contrary until ECC water penetrated the downcomer at the time of 42 seconds.

As a result of inability to properly simulate ECC bypass, the calculated water level in the downcomer rose much earlier than what was measured, as shown in Figure 4-20. Same as in the downcomer, the lower plenum was also filled up earlier in the calculation, as shown in Figure 4-21. As a result, the low plenum was filled up with water at 52 seconds in the calculation, while it was 71 seconds in the test.

During the refill period, there is no water entering the active core except a little droplets entrained by the up-going vapor [7]. As a result, the fuel cladding temperature would remain elevated, as shown in Figure 4-22 and 4-23 for low and high power rods respectively. Owing to the entering of ECC water during this period, superheated steam existed in the lower plenum began to be suppressed, as shown in Figure 4-24. Since the ECC water entered earlier in the simulation, calculated superheated steam in this region was suppressed sooner as expected. As for the coolant temperature response in the upper

plenum shown in Figure 4-25, due to the overpredicted interfacial drag when flow was vertically stratified [8], once ECC water entered the lower plenum droplets would entrain into the active core, and some of them even could penetrate the core then entering the upper plenum. As a result, the calculated superheated steam in this region was suppressed sooner in this phase.

4.1.3 Reflood Phase (after 75 seconds)

During this phase, water began to flow into the active core and consequently fuel rods were rewetted again. Water levels across the core (from lower to upper plenum) are shown in Figure 4-26. Same as in the lower plenum, the calculated core water level ascended earlier than what was measured. From the comparison, it also can be observed that the calculated water level oscillated with larger magnitudes, especially after the termination of accumulator injection. The accumulator injection flow rates were shown in Figure 4-27. It can be seen that the injection was terminated at about 90 seconds which exactly corresponded to the oscillations of the core water level. As direct results of the injection termination, the calculated broken loop cold leg density and flow began to oscillate, as shown in Figure 4-28 and 4-29 respectively, which in turn would cause core water level to oscillate. As for the reason why the calculated cold leg density and flow began to oscillate right after the termination of accumulator injection, the different status of the broken loop cold leg may be the explanation. From

REACTOR EXCURSION AND LEAK ANALYSIS PROGRAM(RELAPS/MOD2/36.04)

SIMULATION OF SEMISCALE S-06-3 LARGE LOCA TEST

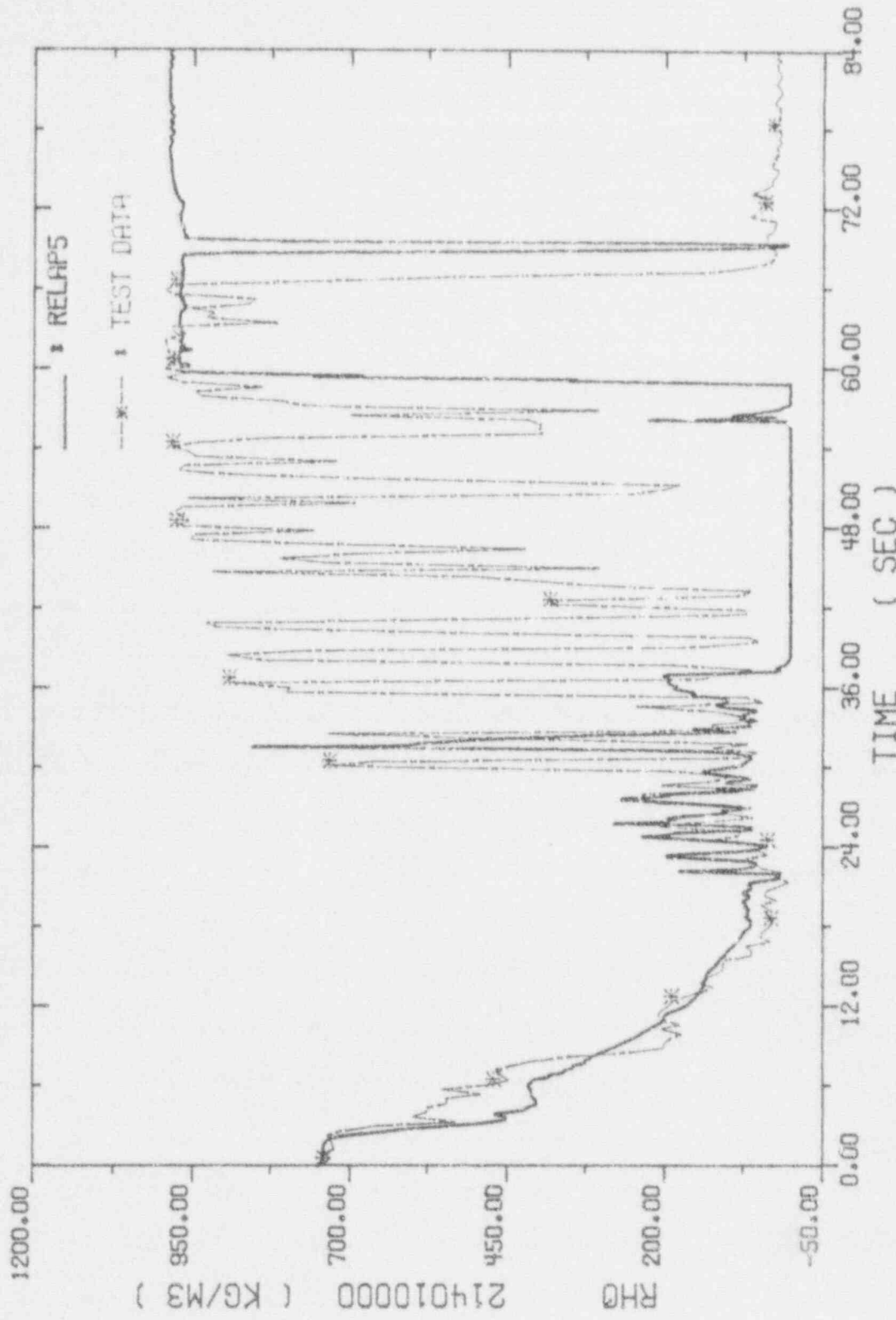


Fig. 4-17. Broken Loop Cold Leg Coolant Densities

REACTOR EXCURSION AND LEAK ANALYSIS PROGRAM (RELAPS/MOD2/36.04)

SIMULATION OF SEMISCALE S-06-3 LARGE LOCA TEST

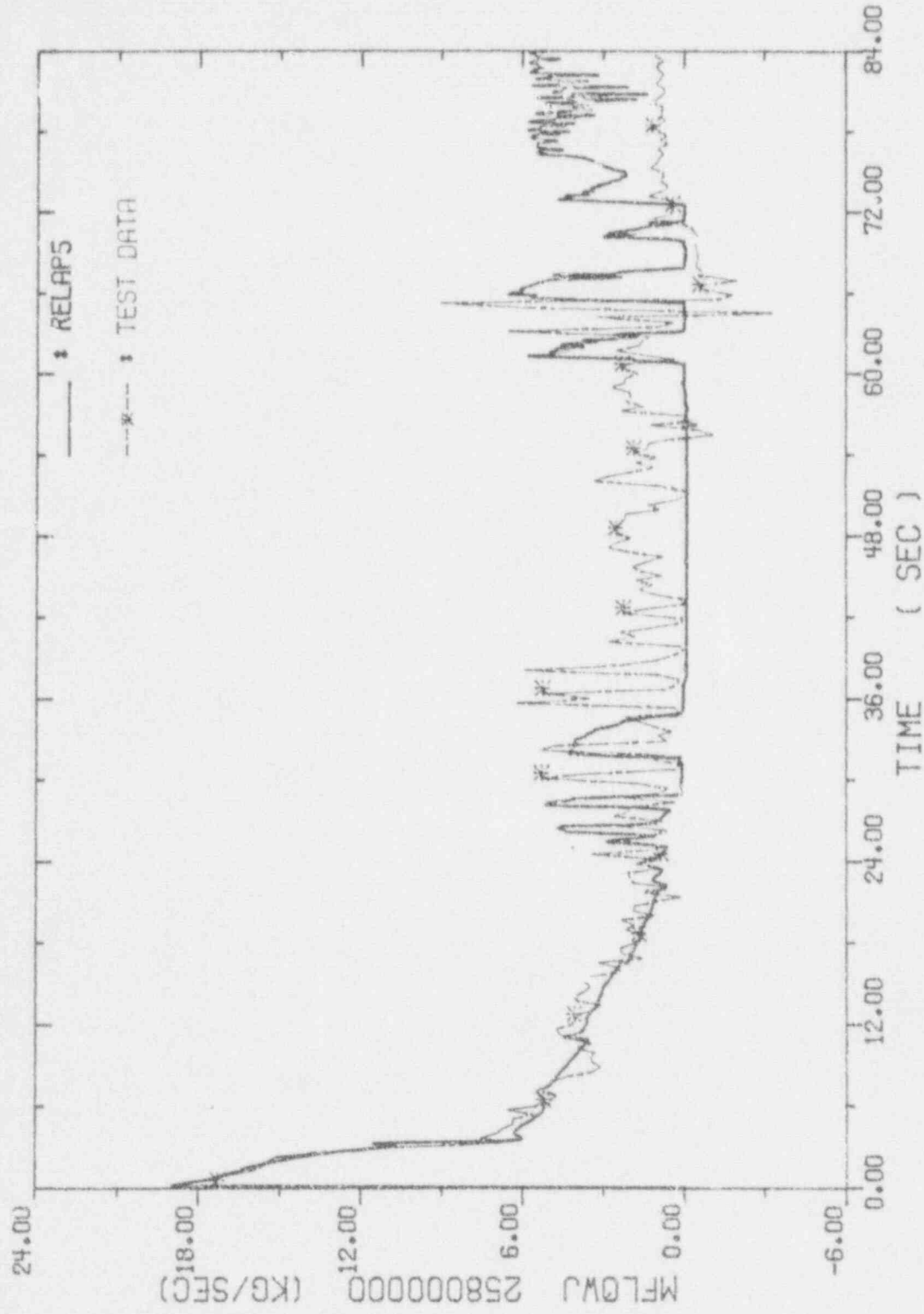


Fig. 4-18. Break Flow Rates near vessel side

REACTOR EXCURSION AND LEAK ANALYSIS PROGRAM(RELAPS/MOD2/36.04)

SIMULATION OF SEMISCALE S-06-3 LARGE LOCA TEST

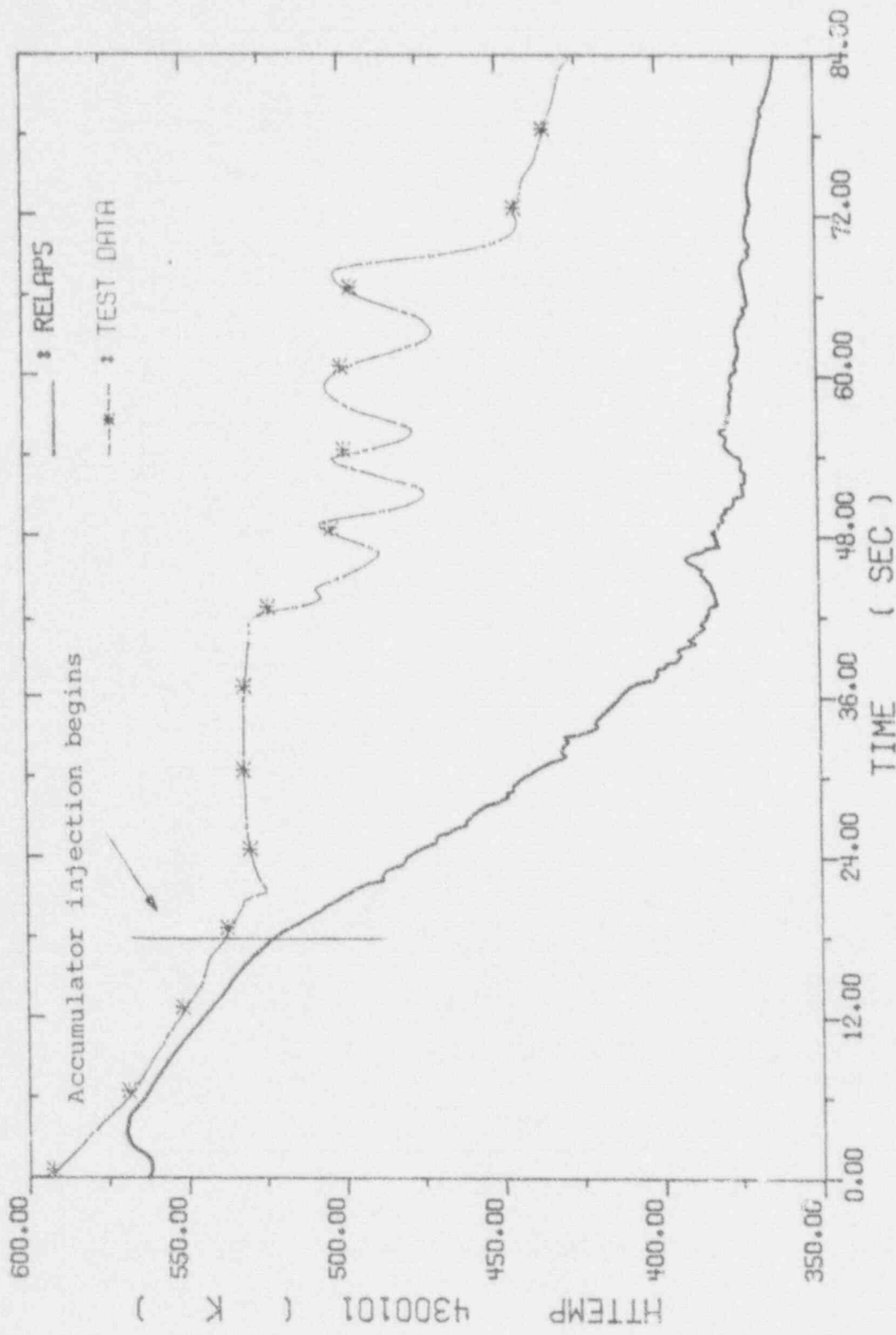


Fig. 4-19. Core Barrel Wall Temperatures

REACTOR EXCURSION AND LEAK ANALYSIS PROGRAM (RELAPS/MOD2/36.04)

SIMULATION OF SEMISCALE S-06-3 LARGE LOCA TEST

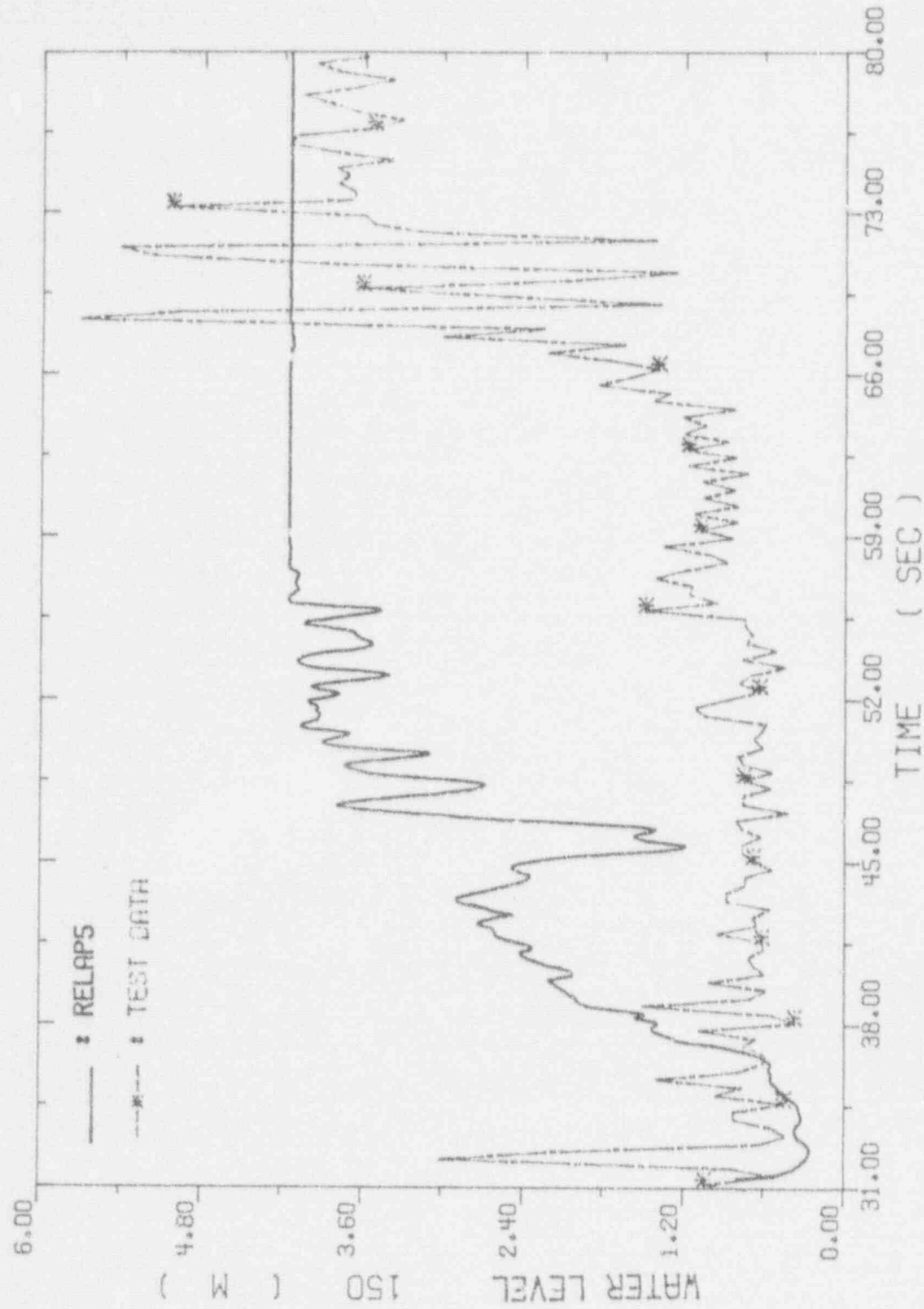


Fig. 4-20. Collapsed Water Levels across The Downcomer

REACTOR EXCURSION AND LEAK ANALYSIS PROGRAM (RELAPS/MOD2/36.04)

SIMULATION OF SEMISCALE S-06-3 LARGE LOCA TEST

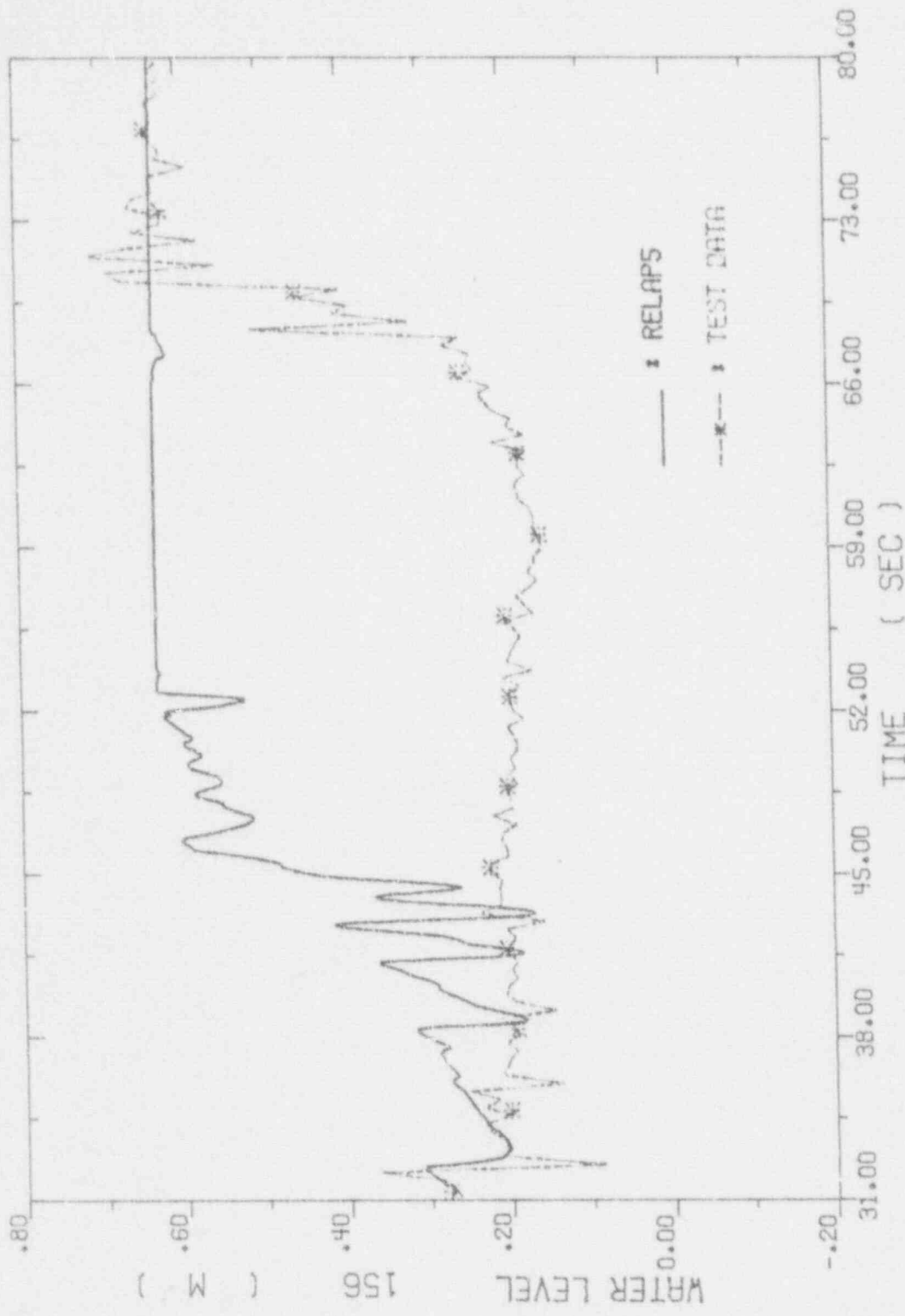


Fig. 4-21. Collapsed Water Levels across the Lower Plenum

REACTOR EXCURSION AND LEAK ANALYSIS PROGRAM (RELAP5/MOD2/36.04)
SIMULATION OF SEMISCALE S-06-3 LARGE LOCA TEST

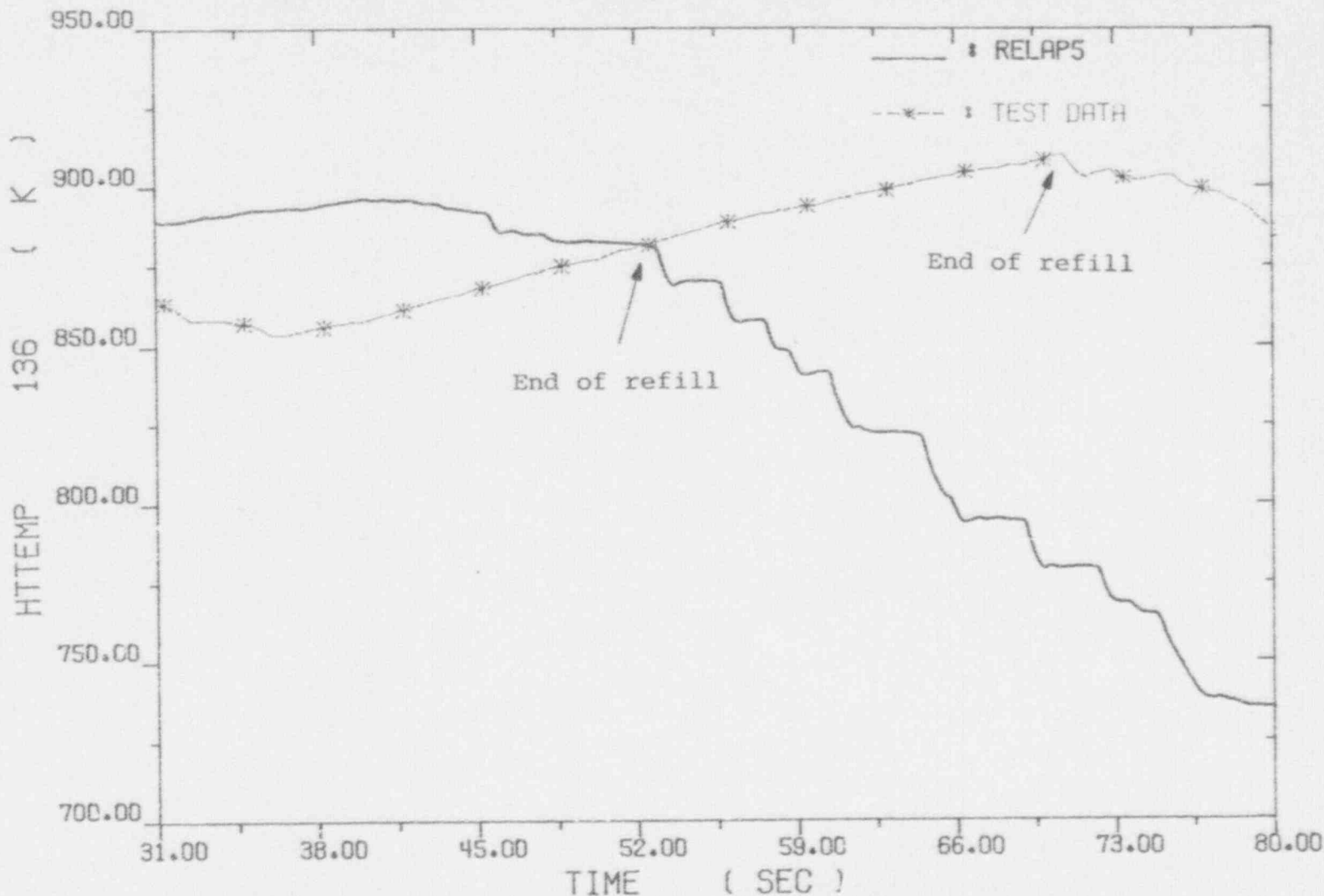


Fig. 4-22. Low Power Rod Hot Spot Cladding Temperatures

REACTOR EXCURSION AND LEAK ANALYSIS PROGRAM (RELAPS/MOD2/36.04)

SIMULATION OF SEMISCALE S-06-3 LARGE LOCA TEST

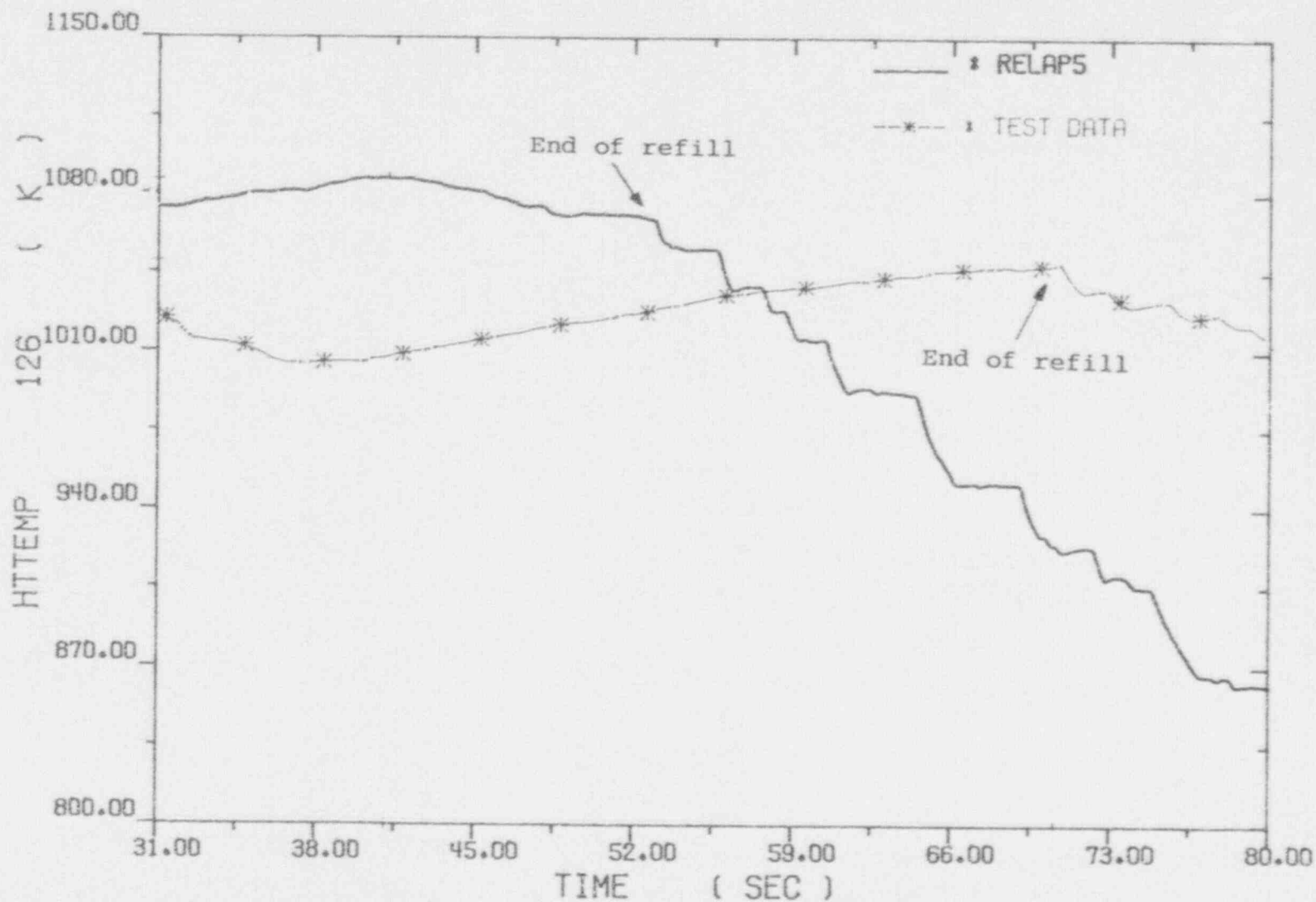


Fig. 4-23. High Power Rod Hot Spot Cladding Temperatures

REACTOR EXCURSION AND LEAK ANALYSIS PROGRAM(RELAPS/MOD2/36.04)

SIMULATION OF SEMISCALE S-06-3 LARGE LOCA TEST

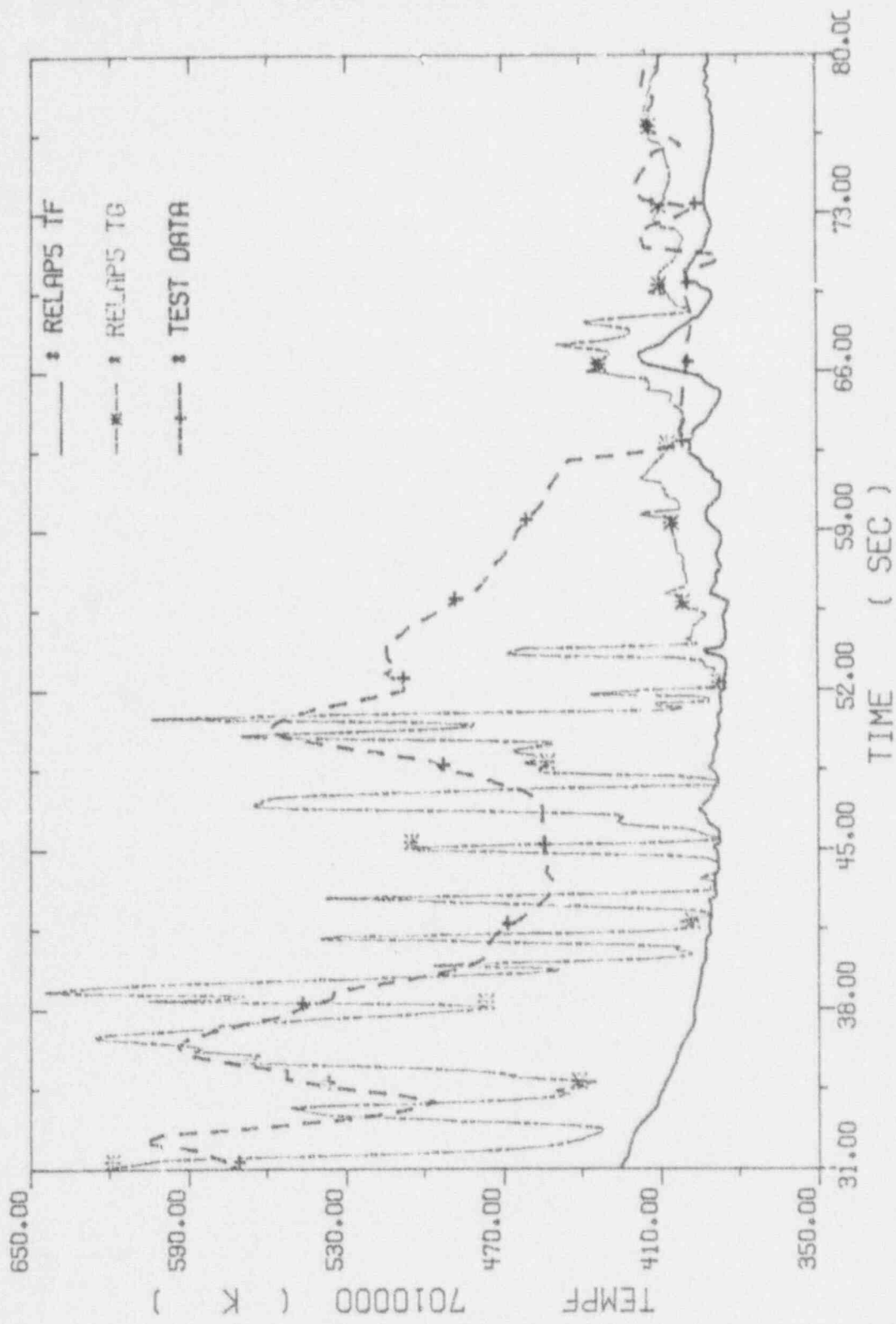


Fig. 4-24. Lower Plenum Coolant Temperatures

REACTOR EXCURSION AND LEAK ANALYSIS PROGRAM(RELAPS/MOD2/36.04)

SIMULATION OF SEMISCALE S-06-3 LARGE LOCA TEST

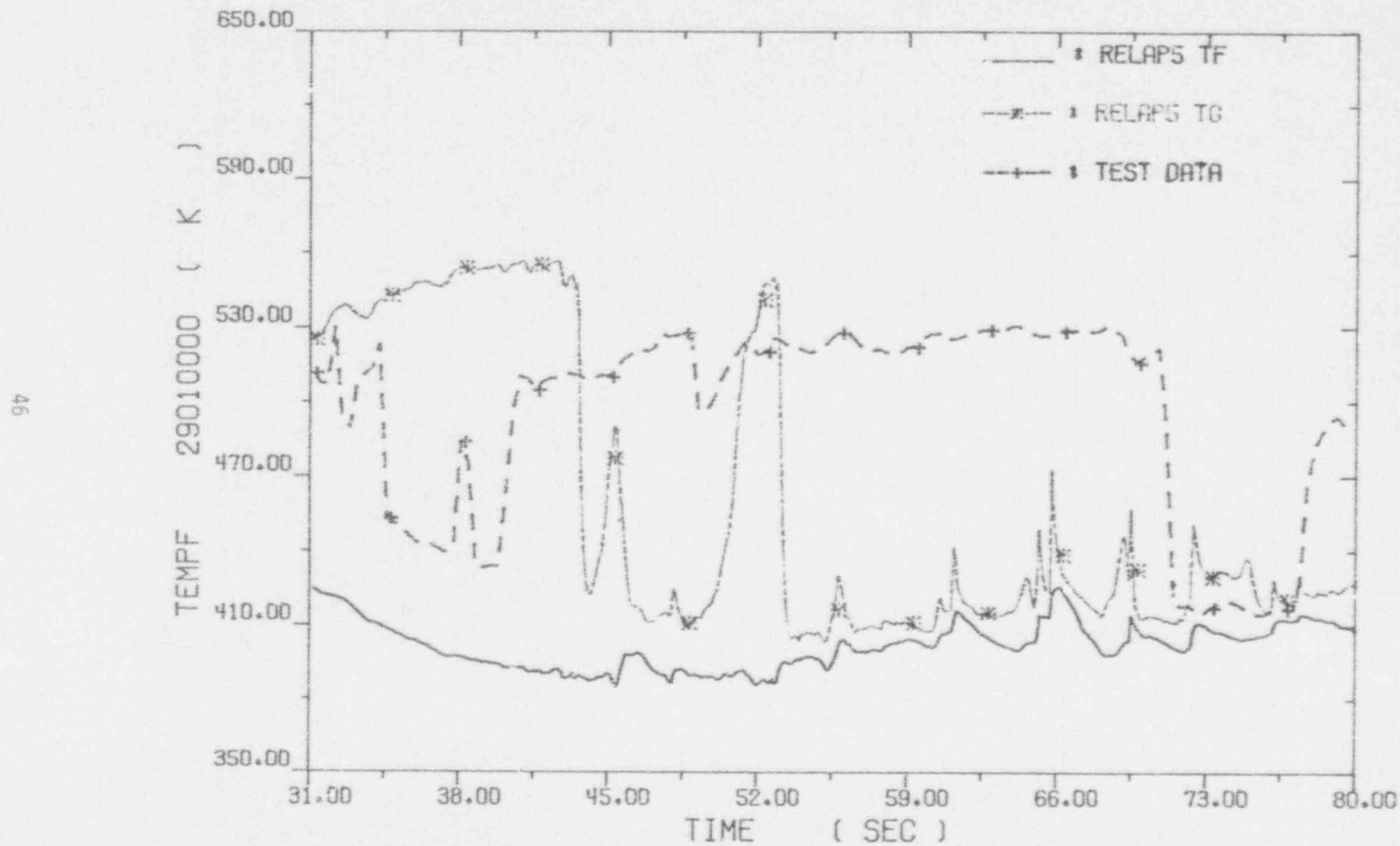


Fig. 4-25. Upper Plenum Coolant Temperatures

the comparison of cold leg density (Figure 4-28), it can be observed that prior to the injection termination, the calculated broken loop cold leg was filled with liquid provided by the accumulator bypass. In the calculation, the accumulator bypass revealed in Figure 4-29 began right after the occupation of downcomer at about 60 seconds shown in Figure 4-20. After the termination of accumulator injection, part of water remained in the broken loop cold leg flowed back to the vessel, which also can be seen in Figure 4-29.

Comparisons of peak cladding temperature responses are shown in Figures 4-30 and 4-31 for low and high power rods respectively. From the comparisons, it can be observed that prior to the rewetting of the hot spots, substantial heat transfer took place. This cooling was attributed to the interaction between entrained water and rods above the quench front and was named precursor cooling [7]. As illustrated, the calculated precursor cooling seemed to be more effective. This difference probably was resulted from the overprediction of liquid entrainment under low flow reflood condition at low pressure [8] and the use of Dougall-Rohsenow correlation for film boiling heat transfer [9]. Other than this, it also can be easily found that the calculated rewetting occurred much earlier than in the test. This discrepancy basically was caused by the earlier refill in the calculation. Furthermore, it also can be found that the calculated rewet temperature was a little lower. The highest

cladding temperatures along fuel rods were also compared. In the test, there were 4 high power rods and 32 low power rods, among which about 70 fuel temperature sensors were distributed. While in our simulations, all fuel rods were modelled only with two heat structures, one representing low power rods and the other representing high power rods. To make comparisons more representative, two curves were used to fit those distributed measurements of cladding temperatures, one for lower power rod as shown in Figure 4-32 and the other for high power rods as shown in Figure 4-33; the method used for curve fitting is Least Squares [10]. In the following discussions, one should bear in mind that the representative curves represent a generalized concept of the maximum cladding temperature response and the real data are always scattered around these curves. Comparisons of representative curves with calculated results are shown in Figures 4-34 and 4-35 for low and high power rods respectively. It can be found from the comparison that the calculated highest cladding temperatures along low power rods matched the data very well, while for the high power rods there was a little shifting of the calculated one. As a result, the calculated position of the highest cladding temperature of the high power rods was 17 cm higher than measured. Besides, the calculated peak value was lower about 30K. Concerning the quench time, same as the fitting of peak cladding temperatures two curves were used to fit the quench time distribution, as shown in Figures 4-36 and 4-

37 for low and high power rods correspondingly. Comparisons of fitting curves to calculated quench time are shown in Figures 4-38 and 4-39 for low and high power rods respectively. As observed, recorded top quenching phenomena was caught in calculation for both low and high power rods. As is well known, this phenomena occurs from cooling provided by the two-phase flow moving upward through the core and the fallback of water which is deentrained at the top of the core or in the upper plenum. The net effect of this is to quench the uppermost part of the fuel rods sooner than would occur from the propagation of the bottom quench front. Top-down cooling generally does not extend to the hot spot [7], which also can be easily observed in these figures. However, all rods in calculation were obviously rewetted earlier, especially for the high power sections. Besides, the latest quenching positions in the calculation for both low and high power rods seemed to be a little lower than what was observed in the test. Basically the calculated earlier rewet can be attributed to the earlier refill and more liquid entrained upward by the up-going vapor during reflood period.

As a summary, important sequence of events is listed in Table 4-1 and compared to what were recorded in the test.

4.2 Sensitivity Study

To ensure that analytical results are within reliable domains and to investigate effects of several different modelings and options, the following sensitivity studies are

REACTOR EXCURSION AND LEAK ANALYSIS PROGRAM (RELAP5/MOD2/36.04)

SIMULATION OF SEMISCALE S-06-3 LARGE LOCA TEST

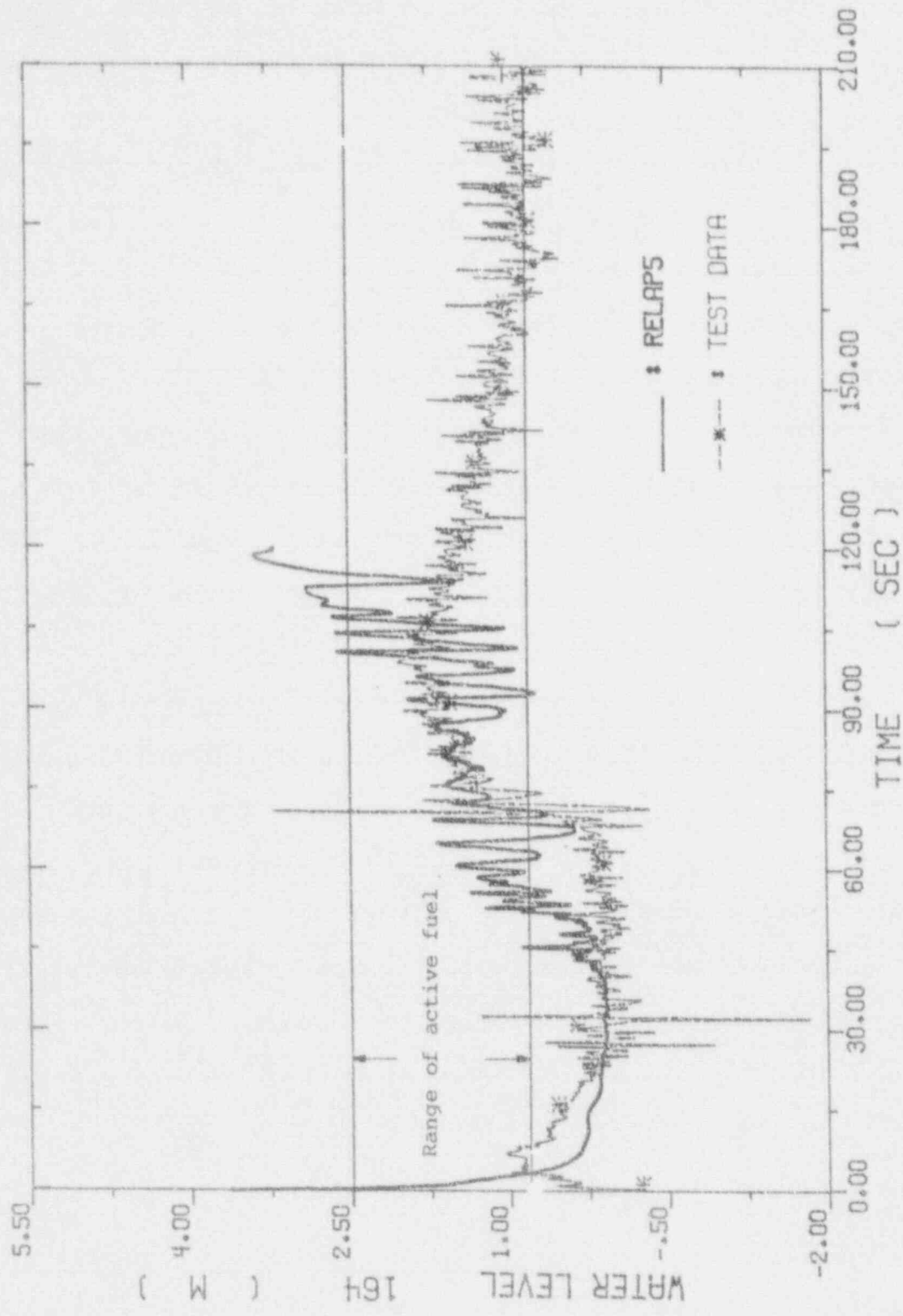


Fig. 4-26. Collapsed Water Levels across the Core

REACTOR EXCURSION AND LEAK ANALYSIS PROGRAM(RELAP5/MOD2/36.04)

SIMULATION OF SEMISCALE S-06-3 LARGE LOCA TEST

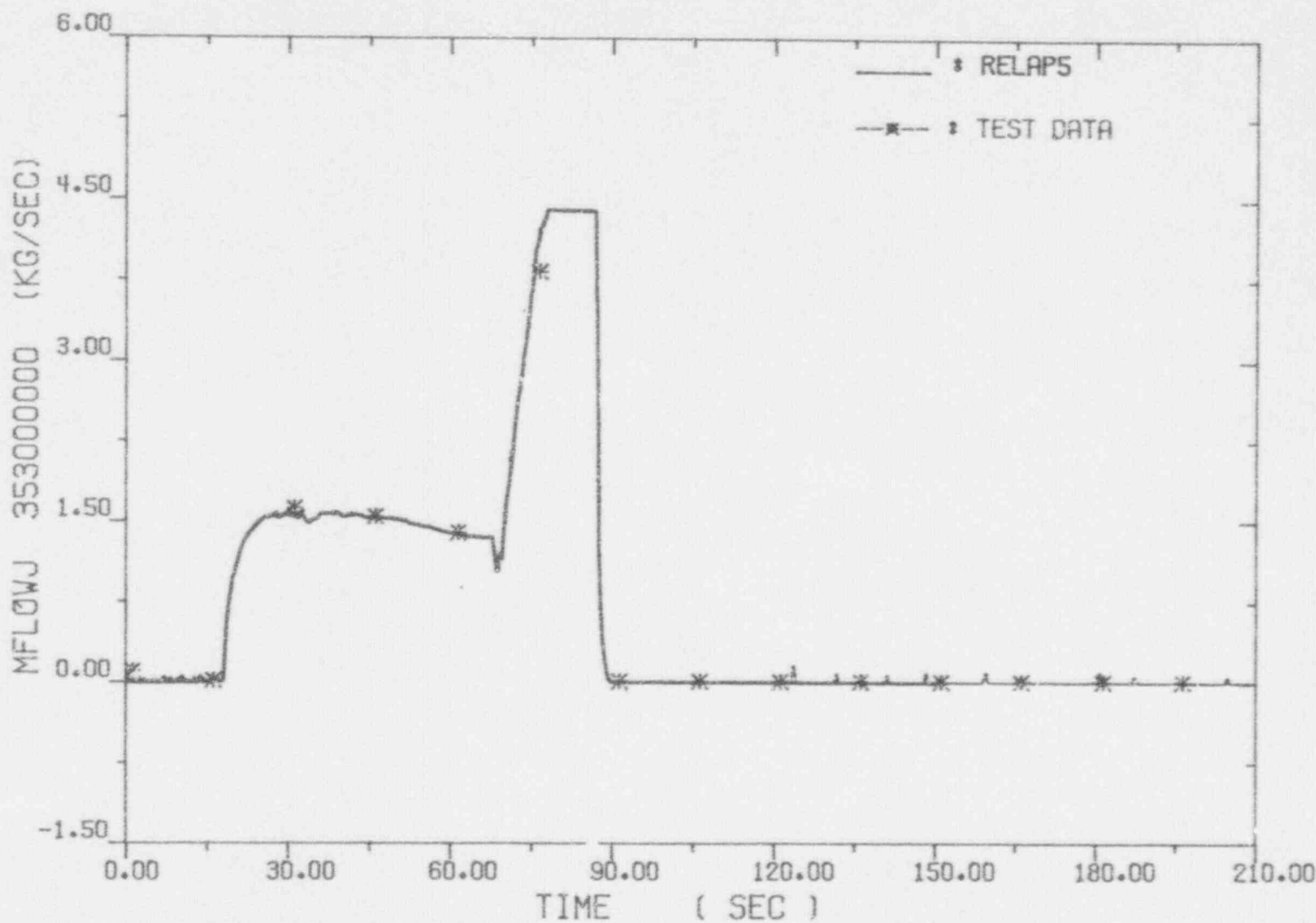


Fig. 4-27. Accumulator Flow Rates

REACTOR EXCURSION AND LEAK ANALYSIS PROGRAM (RELAPS/MOD2/36.04)

SIMULATION OF SEMISCALE S-06-3 LARGE LOCA TEST

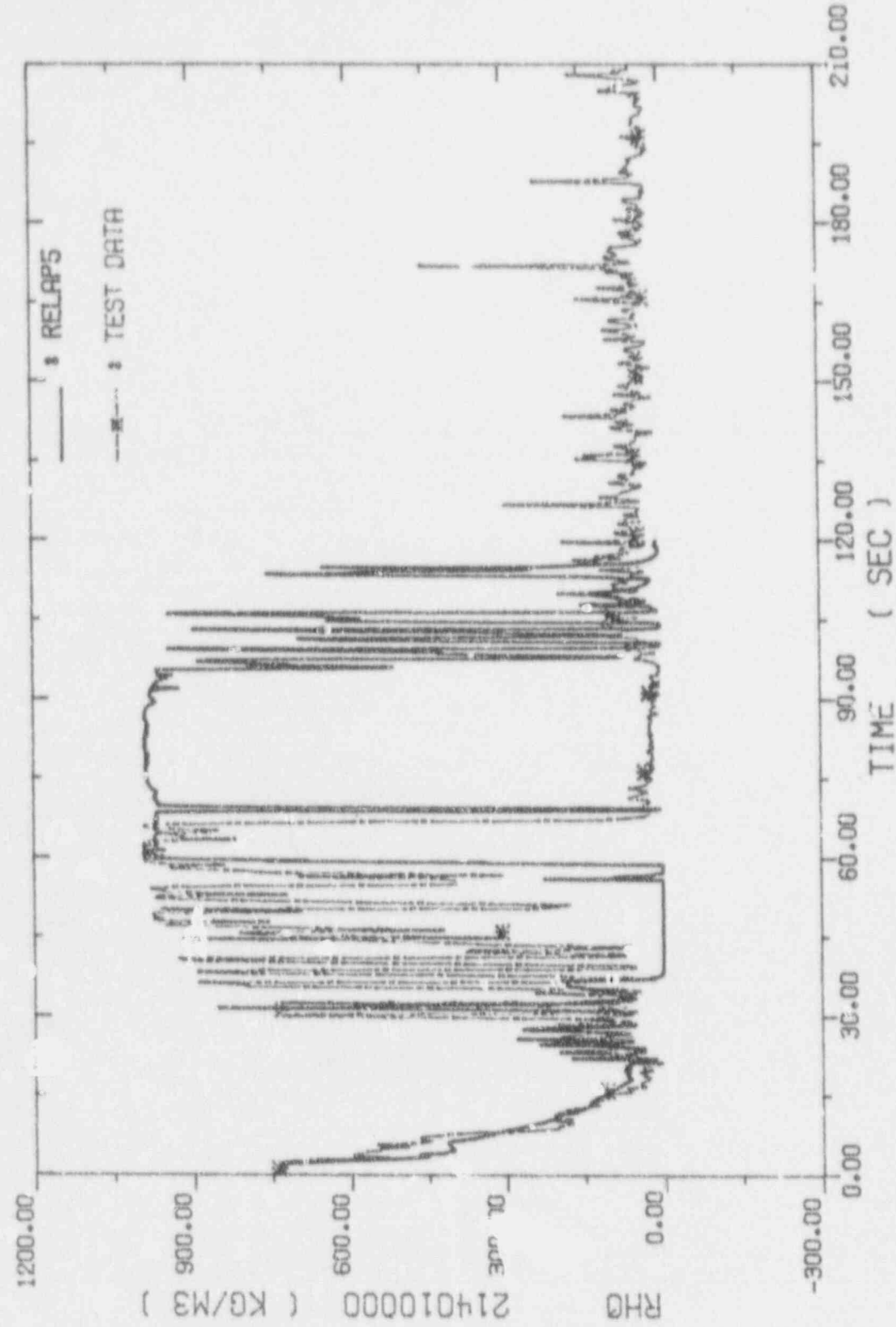


Fig. 4-28. Broken Loop Cold Leg Coolant Densities

REACTOR EXCURSION AND LEAK ANALYSIS PROGRAM (RELAPS / MOD2 / 36.04)

SIMULATION OF SEMISCALE S-06-3 LARGE LOCA TEST

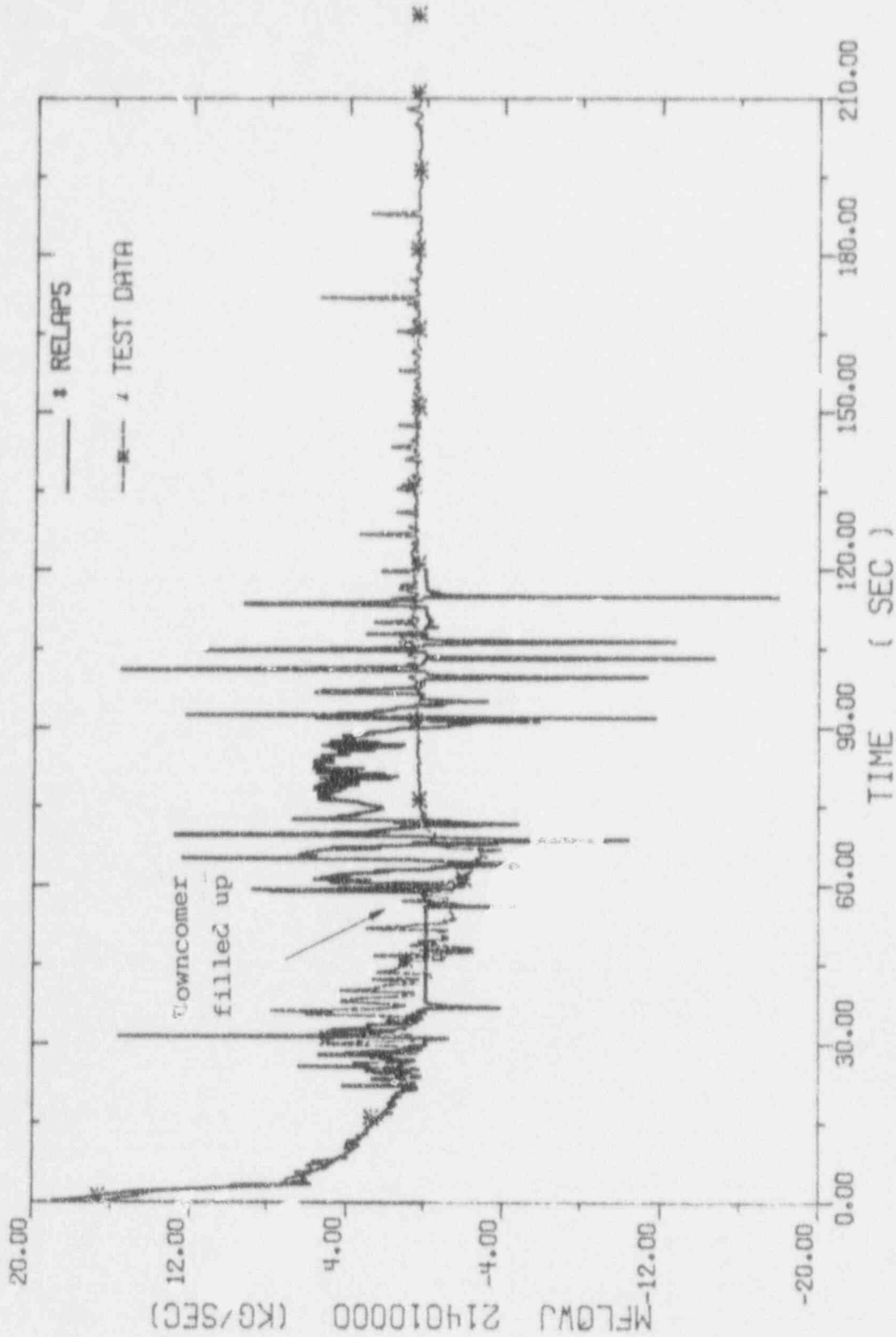


Fig. 4-29. Broken Loop Cold Leg Flow Rates

REACTOR EXCURSION AND LEAK ANALYSIS PROGRAM (RELAPS/MOD2/3E.04)

SIMULATION OF SEMISCALE S-06-3 LARGE LOCA TEST

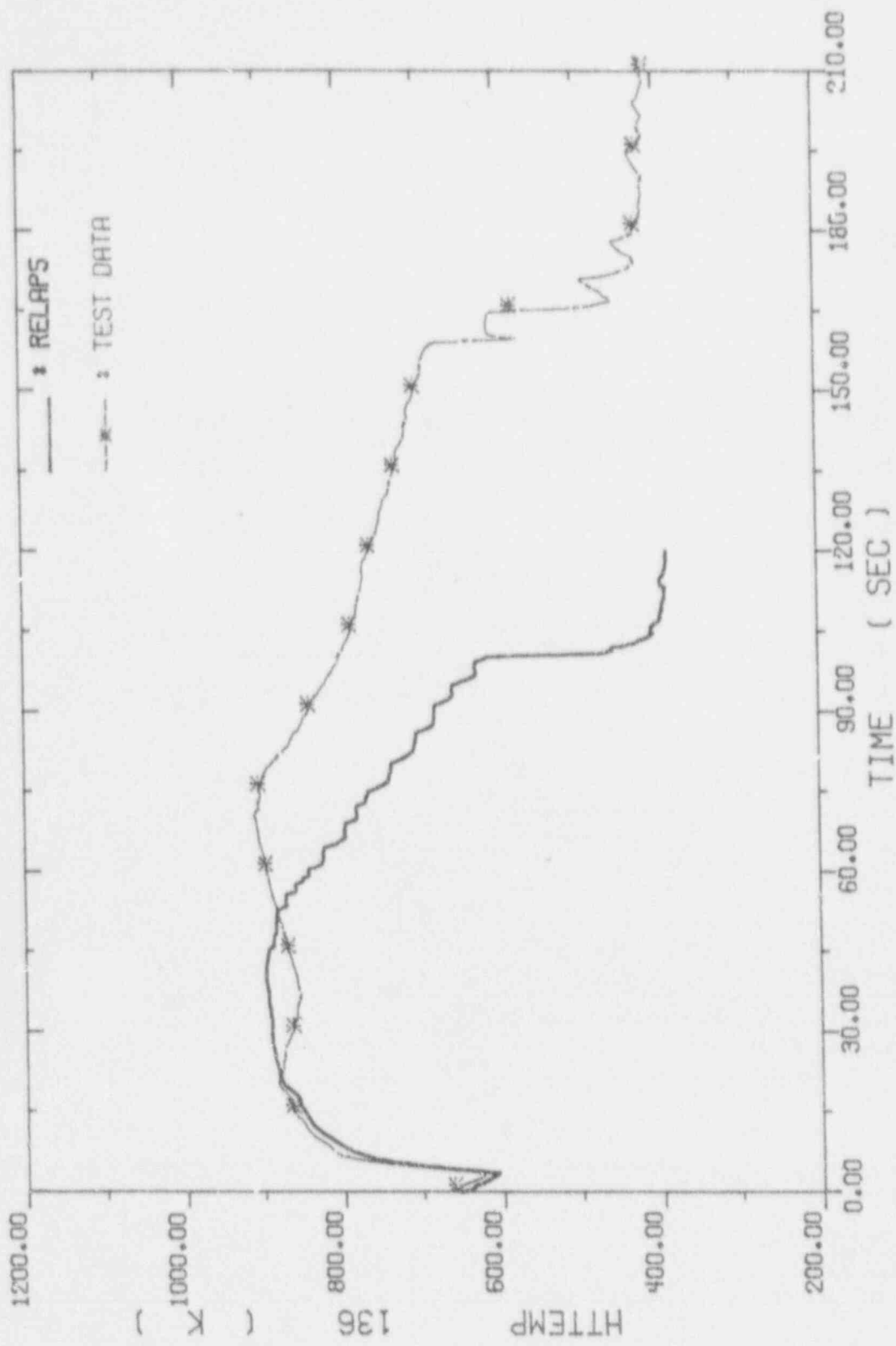


Fig. 4-30. Low Power Rod Hot Spot Cladding Temperatures

REACTOR EXCURSION AND LEAK ANALYSIS PROGRAM(RELAPS/MOD2/36.04)

SIMULATION OF SEMISCALE S-06-3 LARGE LOCA TEST

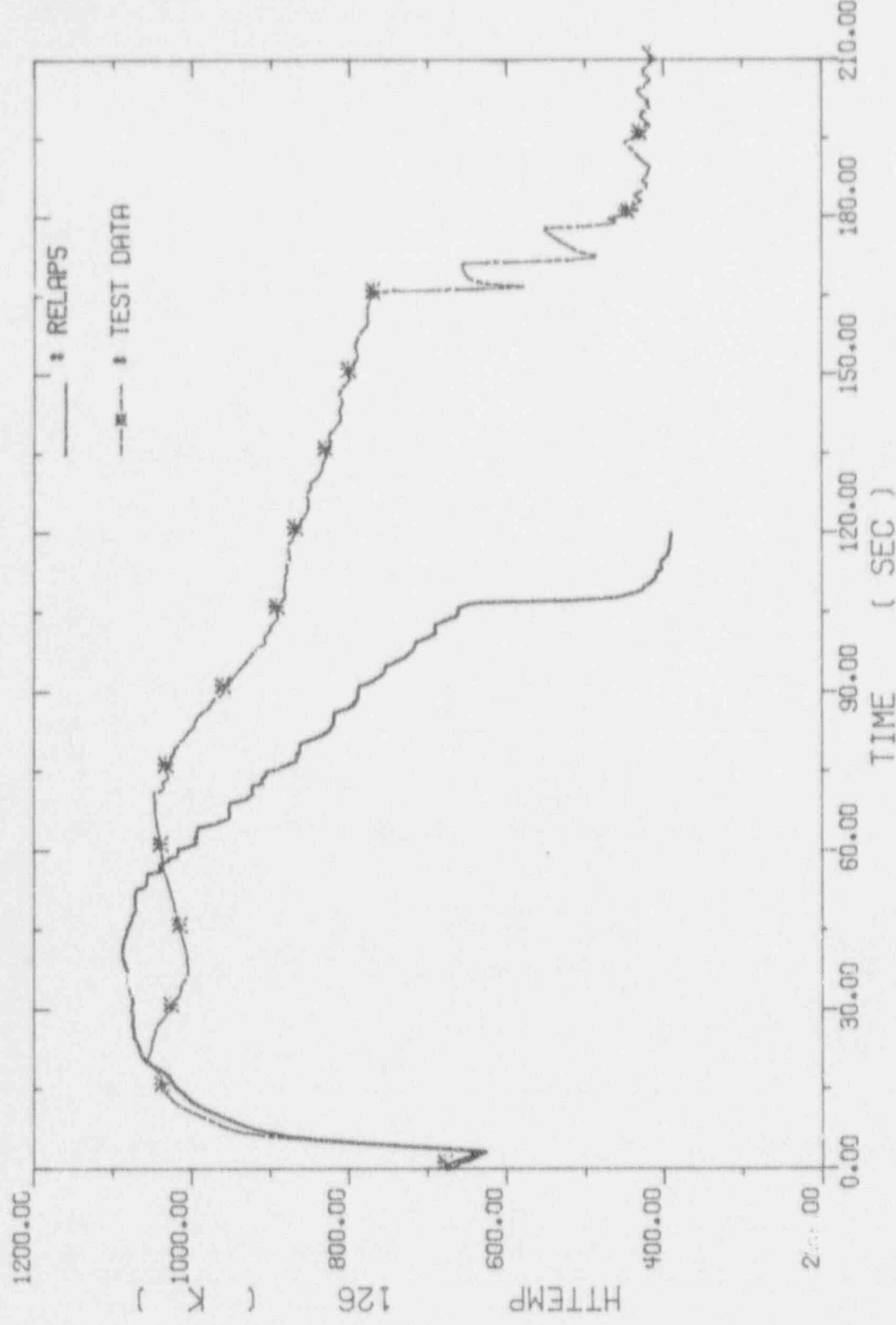


Fig. 4-31. High Power Rod Hot Spot Cladding Temperatures

REACTOR EXCURSION AND LEAK ANALYSIS PROGRAM(RELAPS/MOD2/36.04)

SIMULATION OF SEMISCALE S-06-3 LARGE LOCA TEST

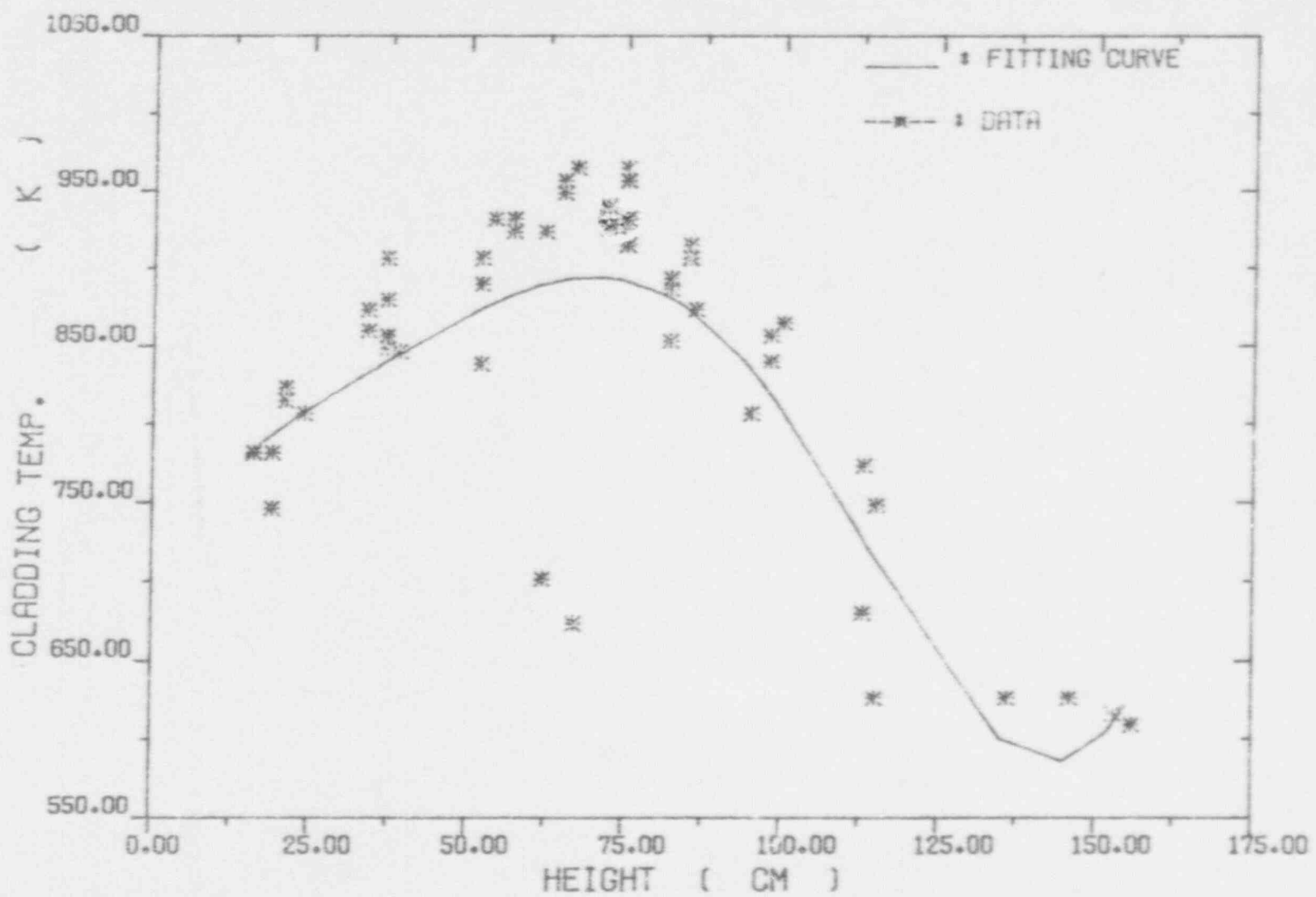


Fig. 4-32. Curve Fitting of The Low Power Rod Peak
Cladding Temperature versus Elevation

REACTOR EXCURSION AND LEAK ANALYSIS PROGRAM(RELAP5/MOD2/36.04)

SIMULATION OF SEMISCALE S-06-3 LARGE LOCA TEST

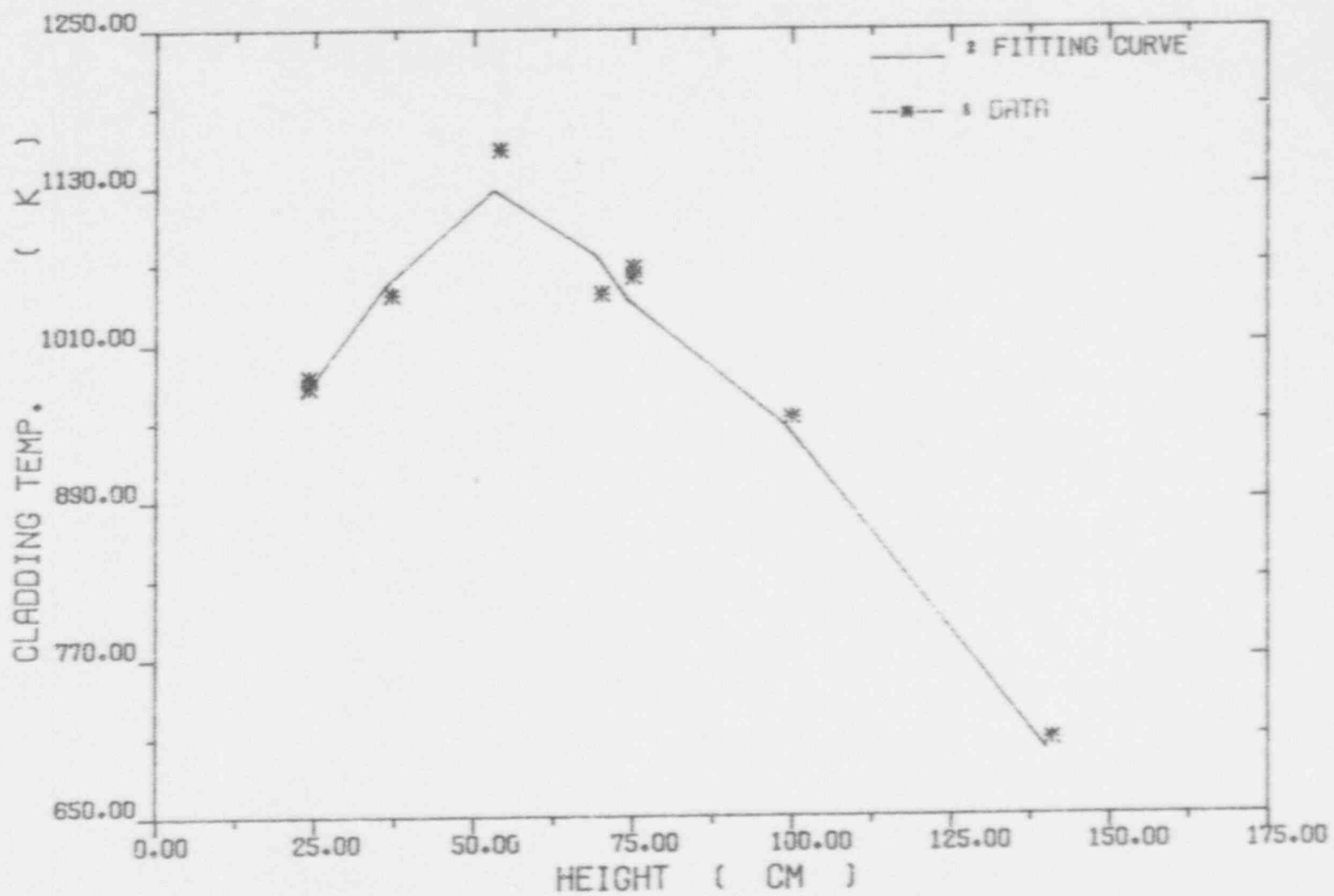


Fig. 4-33. Curve Fitting of The High Power Rod Peak
Cladding Temperature versus Elevation

REACTOR EXCURSION AND LEAK ANALYSIS PROGRAM: RELAPS/MOD2/36.04)

SIMULATION OF SEMISCALE S-06-3 LARGE LOCA TEST

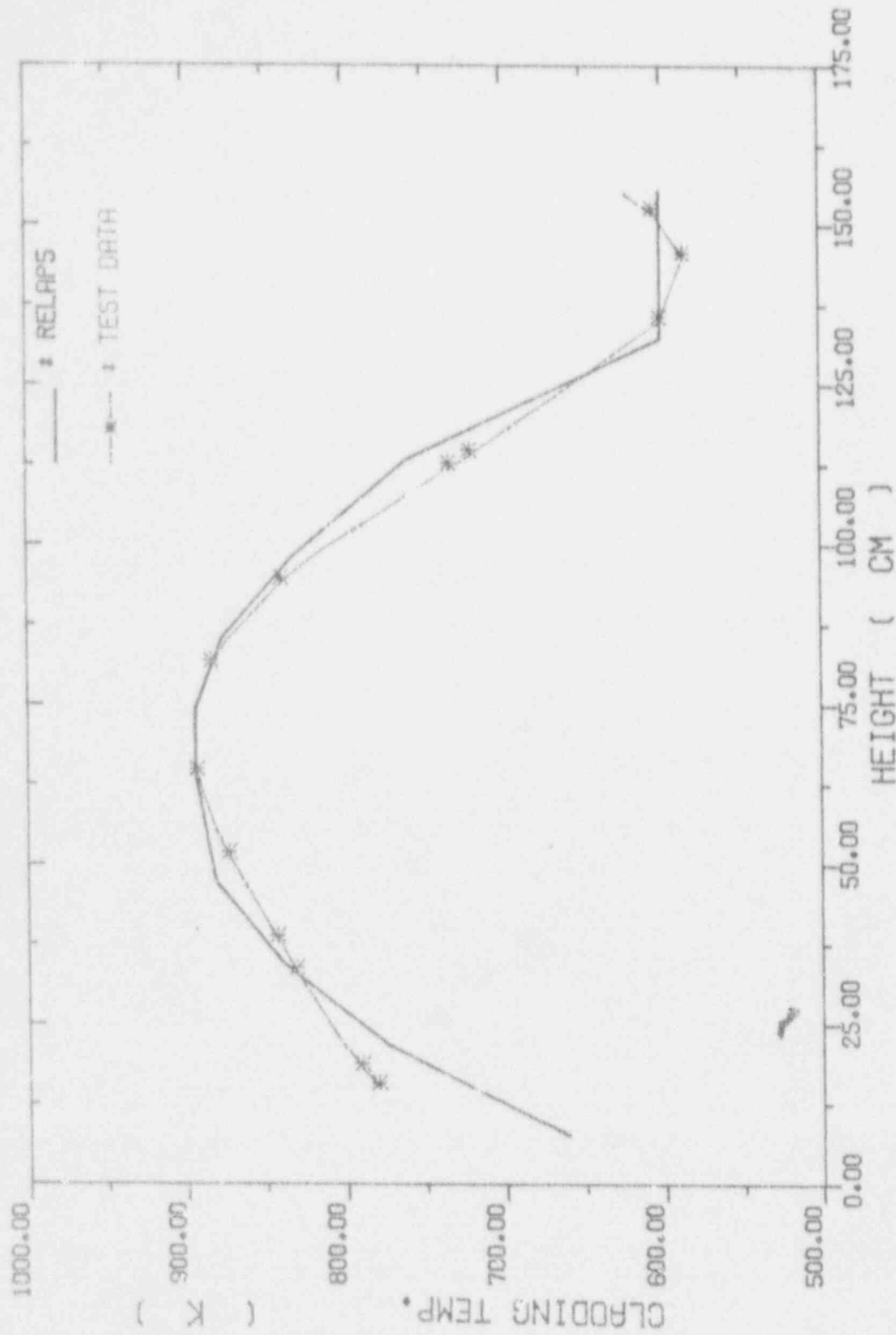


Fig. 4-34. Low Power Rod Peak Cladding Temperatures
versus Elevation

REACTOR EXCURSION AND LEAK ANALYSIS PROGRAM (RELAPS/MOD2/36.04)

SIMULATION OF SEMISCALE S-06-3 LARGE LOCA TEST

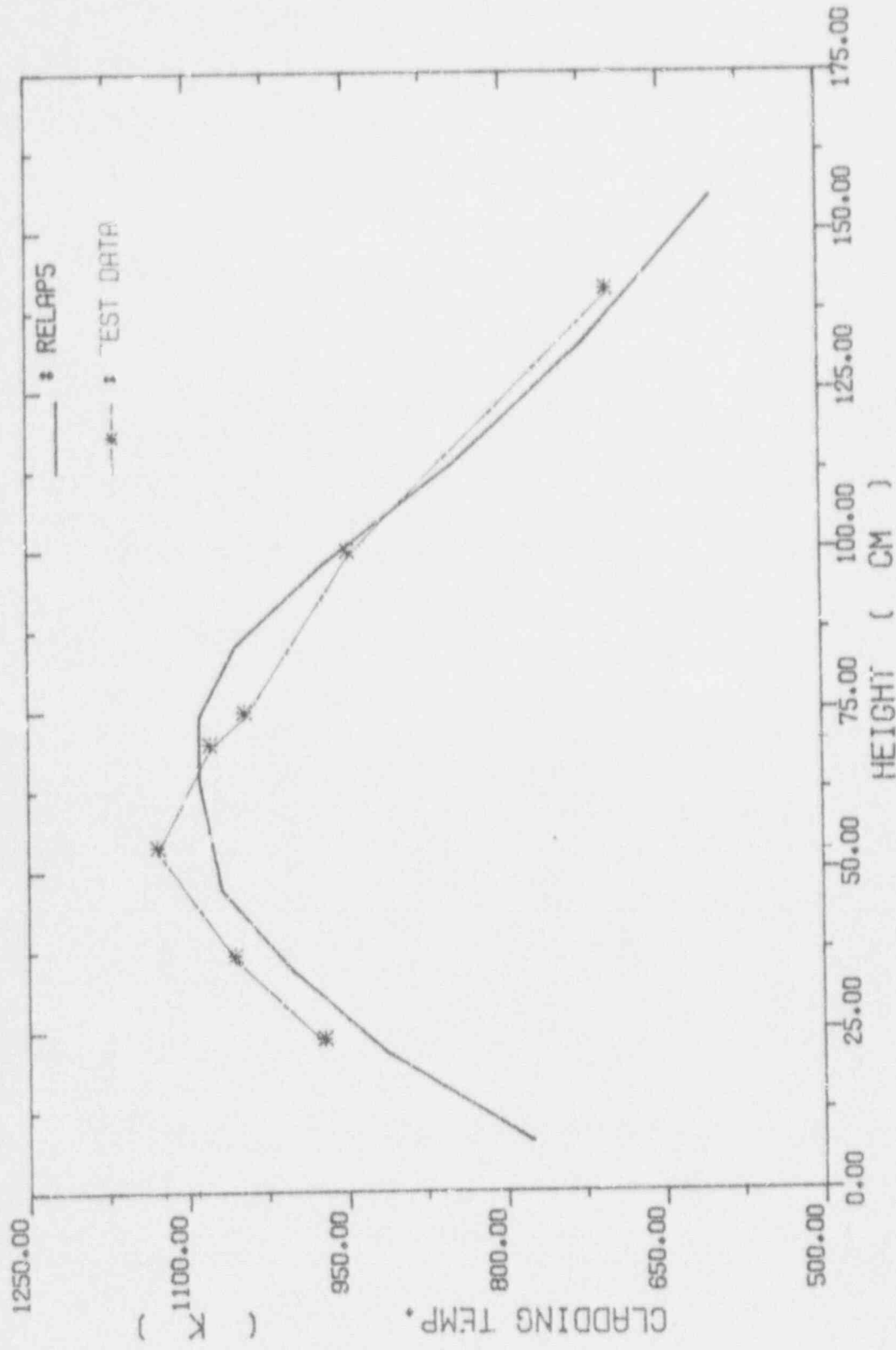


Fig. 4-35. High Power Rod Peak Cladding Temperatures Versus Elevation

REACTOR EXCURSION AND LEAK ANALYSIS PROGRAM (RELAP5/MOD2/36.04)

SIMULATION OF SEMISCALE S-06-3 LARGE LOCA TEST

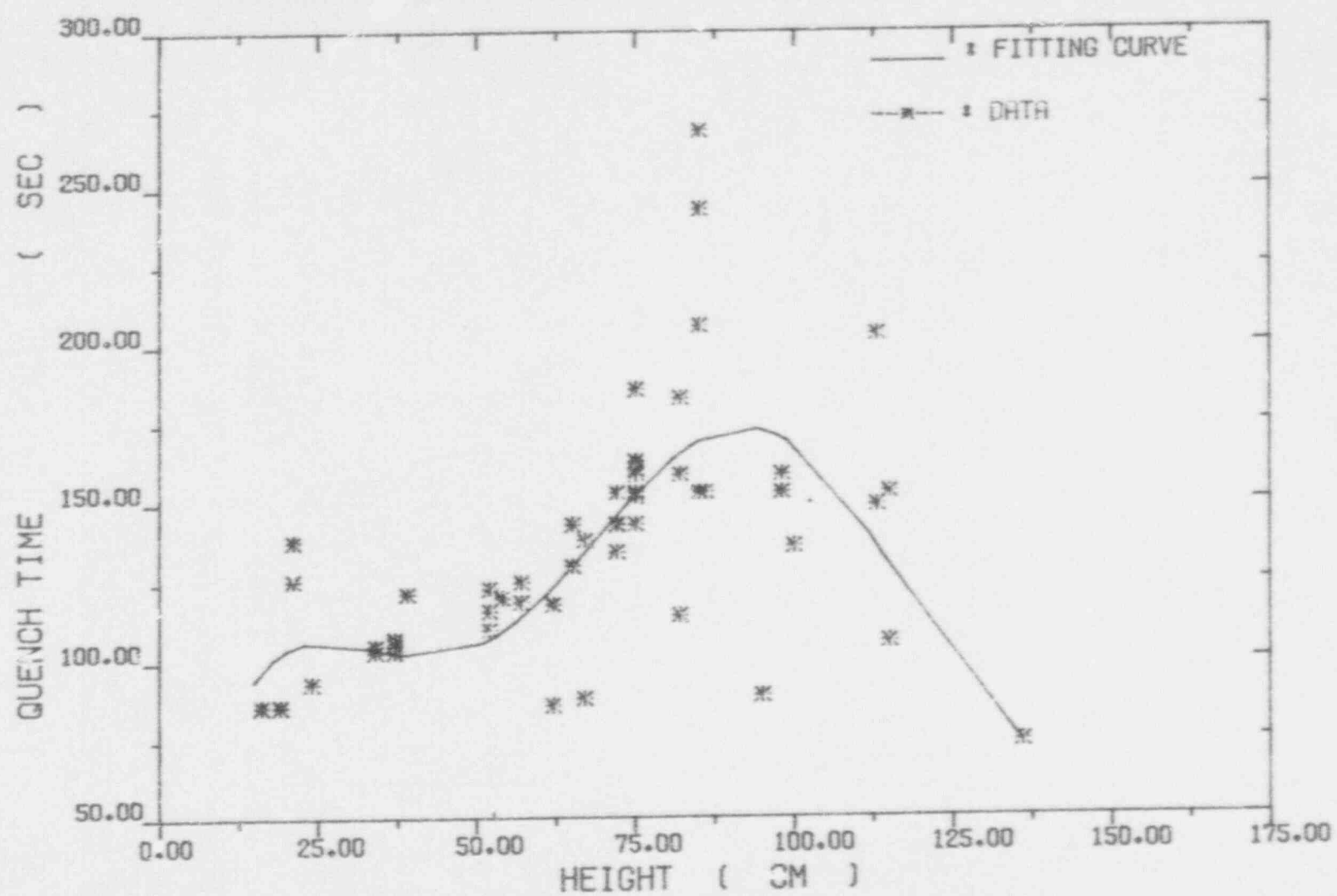


Fig. 4-36. Curve Fitting of The Low Power Rod Quench Time versus Elevation

REACTOR EXCURSION AND LEAK ANALYSIS PROGRAM(RELAP5/MOD2/36.04)

SIMULATION OF SEMISCALE S-06-3 LAGE LOCA TEST

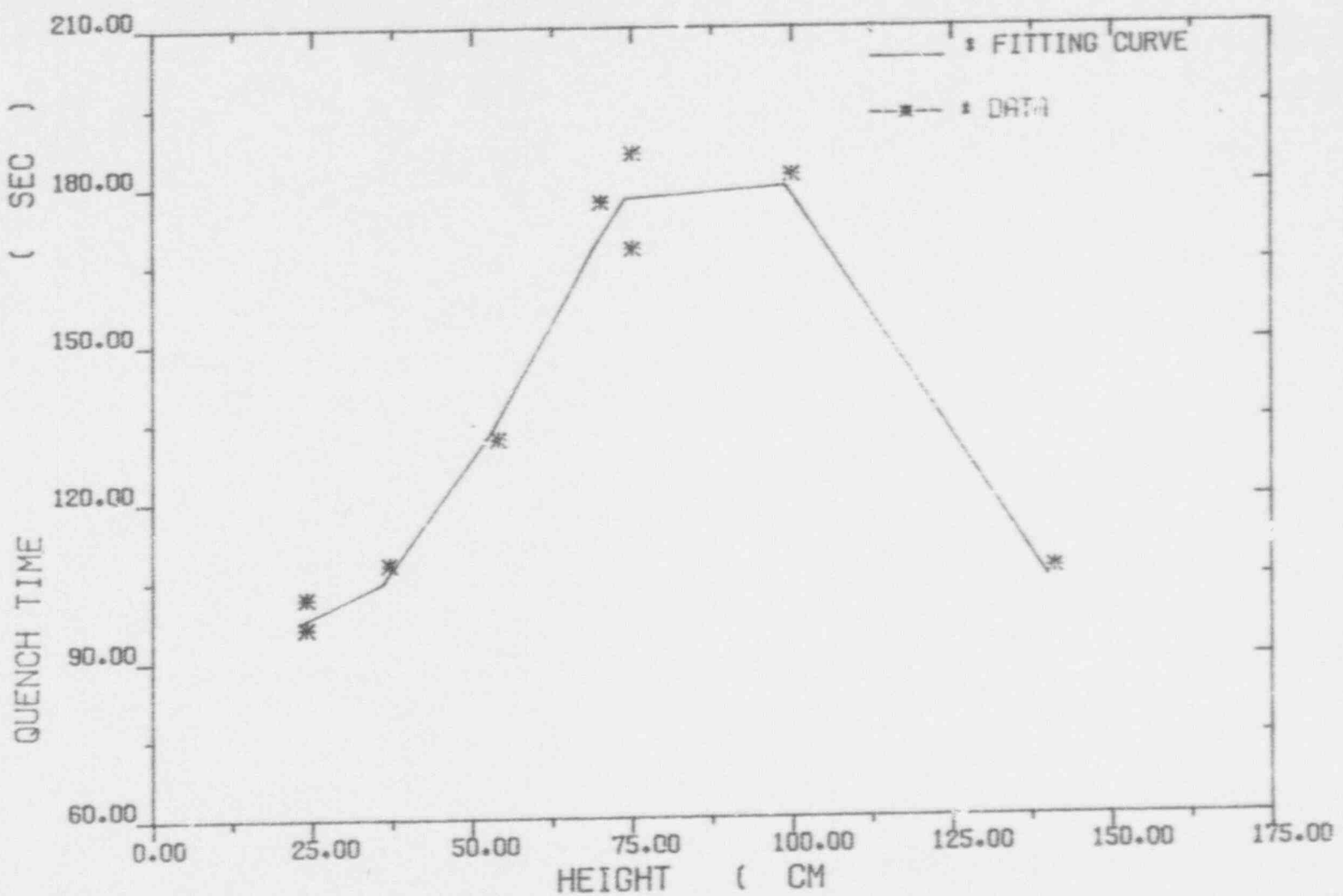


Fig. 4-37. Curve Fitting of The High Power Rod Quench
Time versus Elevation

REACTOR EXCURSION AND LEAK ANALYSIS PROGRAM (RELAPS/MOD2/36.04)

SIMULATION OF SEMISCALE S-06-3 LARGE LOCA TEST

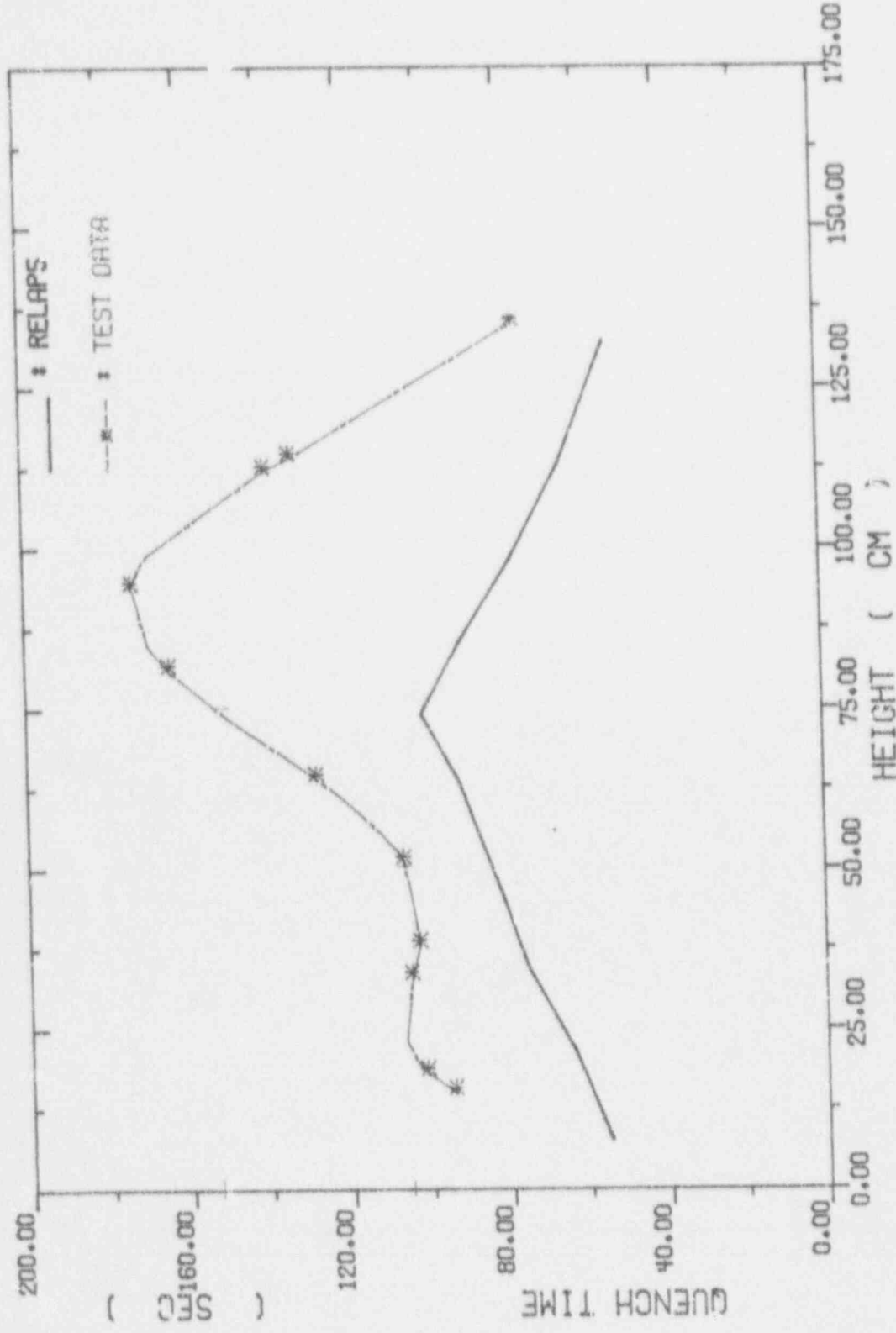


Fig. 4-38. Low Power Rod Quench Time versus Elevation

REACTOR EXCURSION AND LEAK ANALYSIS PROGRAM(RELAPS/MOD2/36.04)

SIMULATION OF SEMISCALE S-06-3 LARGE LOCA TEST

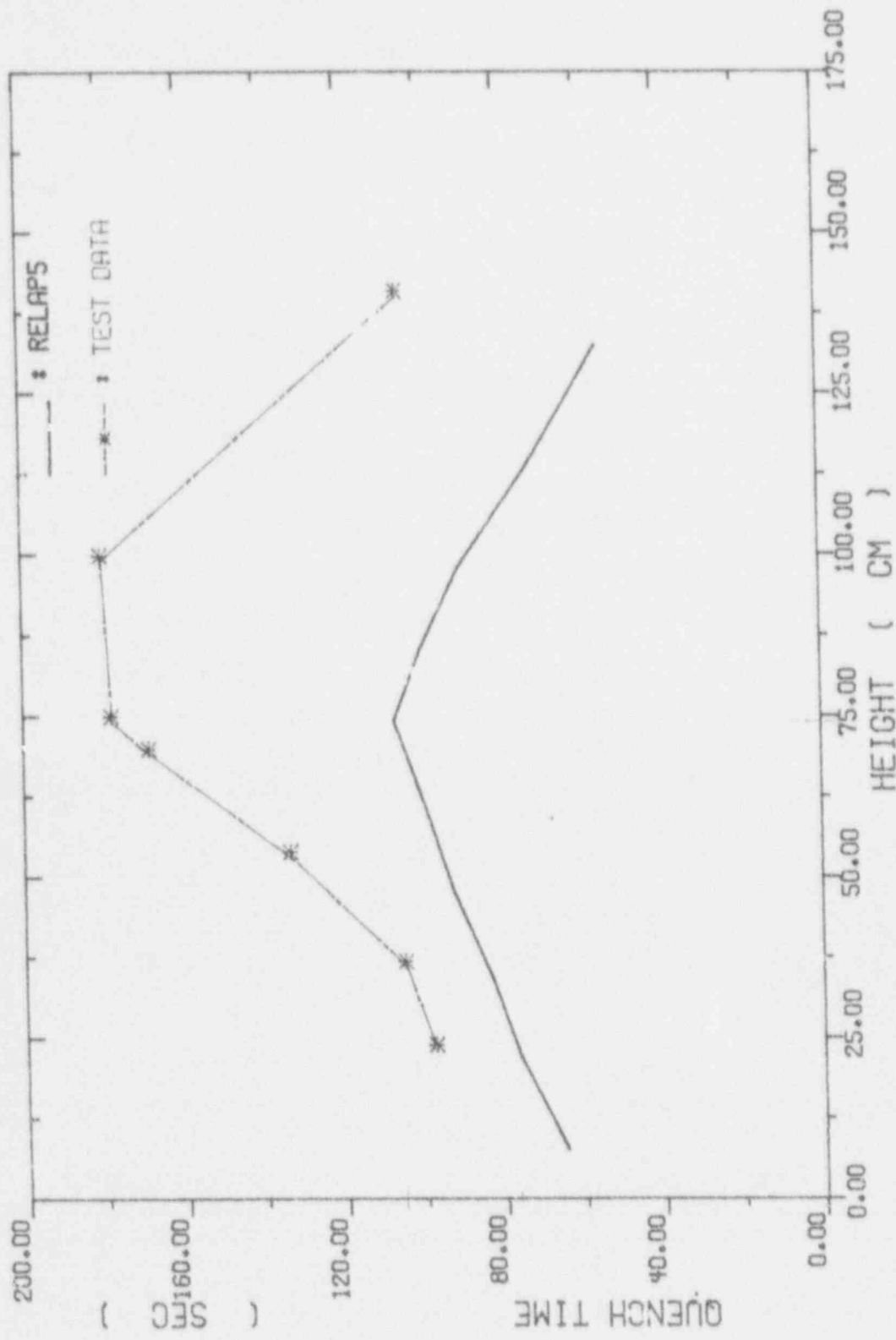


Fig. 4-39. High Power Rod Quench Time versus Elevation

Table 4-1 Sequence of Events

<u>Event</u>	<u>Measured</u>	<u>Time (s)</u> <u>RELAP5</u>
Blowdown initiated	0.0	0.0
High pressure injection started	0.0	0.0
Core power decay transient started	1.27	1.27
Fuel hot spot temperature excursion began	2.94	3.33
Pressurizer emptied	7.5	12.5
Accumulator injection started	18.5	18.5
PCT reached	20.5	41.0
Downcomer penetration	42.0	*
Lower plenum water level began to increase	60.0	32.5
Lower plenum filled up	71.0	52.0
Downcomer filled up	73.0	58.0
Accumulator injection stopped	90.0	90
Fuel hot spot rewetted	165.0	105

* Fail to simulate

performed. Each different modeling or option is isolated and results are compared to what were obtained from the base modeling described in the previous section.

4.2.1 Pressurizer Modeling

In the base model pressurizer was represented by 13 volumes, while in this study noding was reduced to 5. Pressurizer surge flow and pressure responses during blowdown period from both models are compared and shown in Figures 4-40 and 4-41. It can be seen that the slope change of surge flow corresponding to the pressurizer empty was better simulated in the base model, and two-slope pressure response resulted from pressurizer empty was also more obvious in the base calculation.

4.2.2 Radial Connections Between Core Average and Hot Channels

As depicted in the previous section, radial connections between core average and hot channels were modelled in the base case using cross-flow junctions. In this study, such radial links are disconnected. The resulting peak cladding temperatures of both low and high power rods along the fuel elevations are shown in Figures 4-42 and 4-43 respectively. For the low power rods, the peak temperatures along the fuel were almost identical in both cases. However, for the high power rods the peak temperatures located on the bottom and top sections of the fuel were a little different. Such discrepancies actually were caused by different cladding temperature responses on both sections.

The cladding temperature responses on both end sections are shown in Figures 4-44 and 4-45 correspondingly. As revealed from the comparisons, it can be found that in both sections, the cladding would not experience dryout in the calculation without radial connections, while in the base calculation the fuel rods do experience dryout and temperature excursions resulted consequently.

The resulting fuel quench time along the fuel of both high and low power rods from both calculations are shown in Figures 4-46 and 4-47. For the high power rods, other than the difference in the bottom section which did not experience dryout in sensitivity calculation, the quench time of lower part of fuel in the calculation without radial connection was all postponed by about 6-10 seconds. While for the low power rods, except the central section, the quench time was postponed a little in the calculation without radial connections.

The core inlet flow rates and collapsed water levels from both calculations are also compared, as shown in Figures 4-48 and 4-49 respectively. It can be observed that there were no noticeable differences for these two parameters. In addition, the CPU time used in the two calculations was also compared as shown in Figure 4-50. The costs of the two calculations were quite close.

4.2.3 The Maximum Number of Heat Slab Axial Interval for 2-D Reflood Calculation

In the base modeling the heat slab axial maximum interval was set to 8. To investigate the effect of this number, it was timed and divided by a factor of 4. The resulting peak cladding temperatures along the fuel rod elevations for both high and low power rods are shown in Figures 4-51 and 4-52 respectively. It can be observed that there is no noticeable difference for both high and low power rods. The resulting quench time on each different elevation of both high and low power rods is also shown in Figures 4-53 and 4-54. It can be seen that the effect of the maximum axial number on the reflood calculation was not obvious. Even though, there is an interesting tendency revealed from the results implying that the larger the maximum number, the later the rewetting that may occur. The difference probably was resulted from the rewetting rate featured in Semiscale test facility. As revealed from the test results, the rewetting rate was about 1.8 cm/sec. In addition, the resulting cladding temperature histories of the highest power sections of both high and lower power rods are also put together for comparison and shown in Figures 4-55 and 4-56. Both trends and magnitudes from those different modelings were quite matched. Again, it can be said that the effect of the maximum number on the integral cladding temperature response was obscure. Finally, the CPU time used in three cases is compared in Figure 4-57. It can be seen that once the reflood calculation began, the difference appeared. However, the difference was not noticeable.

4.2.4 Number of Axial Hydraulic Volumes Representing the Core

In this study, the axial number of hydraulic volumes representing the core was changed from the base model numbered 11 to 5 and 22. Several important parameters associated with the hot channel were compared. The resulting peak cladding temperatures versus the hot fuel elevations are shown in Figure 4-58. It can be found that results from three modelings were quite matched except a dip in the calculation with 22 axial volumes representing the core. To illustrate such difference, the cladding temperature responses at this location are compared in Figure 4-59. It can be seen that although in all cases the fuel has experienced dryout at this location, dryout time from the modeling having 22 volumes was a little postponed and the resulted magnitude of temperature excursion was smaller.

The quench time versus fuel elevations is also compared in Figure 4-60. It can be seen that other than at ends of fuel rods, there existed a tendency showing that fine noding of the core may result in a later quench. The temperature responses of the highest power section from three modeling are compared too, as shown in Figure 4-61. The noding difference seemed to have no effect on the integral cladding temperature response on the hot spot.

Comparison of core collapsed water levels from three modelings are shown in Figure 4-62. Also, no noticeable difference was noted. Nevertheless, the CPU time cost in the

calculation of 22 axial nodes was much more than the other two did, as shown in Figure 4-63.

4.2.5 Cross-Flow Junctions on Reactor Vessel Entrances

In the base calculation the entrances of four legs entering the reactor vessel were modelled with normal junctions. In this study, those normal junctions were replaced by four cross-flow junctions to investigate the effect of momentum flux in loops. Resulting break flow rates are shown in Figures 4-64 and 4-65 and compared to what was obtained from the base calculations. It can be seen that it had almost no effect on break flow rates especially for the break flow near the pump side. As for downcomer and lower plenum collapsed water levels, shown in Figures 4-66 and 4-67, it can be seen that trends were quite matched. However, the associated filled-up time was a little delayed in the calculation with cross-flow junctions. As a result, the core water level ascending in the sensitivity calculation was a little postponed too, as shown in Figure 4-68. The quench time of high power rods versus fuel elevations is also compared and shown in Figure 4-69. It can be seen that other than on the ends of the fuel, the fuel quench time was a little put off in the calculation with cross-flow junctions. This postponement basically was caused by the associated delayed ascending of core water level depicted above. Other than the quench time, the highest cladding temperature along the fuel elevation is also compared and results are shown in Figure 4-70.

It can be found that both curves were almost identical. To investigate the effect on the integral cladding temperature responses, the cladding temperatures of the highest power section versus time are shown in Figure 4-71. As revealed, both trend and magnitude were quite matched except a little delay of the quench in the sensitivity calculation which already has been described. Finally, the costs of CPU time for both calculations are also compared and shown in Figure 4-72. It can be observed that the calculation with cross-flow junction modeling used more CPU time than base calculation by a factor about 1.15.

4.2.6 Reflood Calculation

In the base modeling, reflood calculation is actuated when the core is nearly empty. As addressed in Reference 2, a two-dimensional conduction scheme and different heat transfer correlations known to apply for the reflood process are employed. In this study, normal reflood calculation is intentionally defeated to investigate associated effects. Resulting high power rod hot spot cladding temperature is shown in Figure 4-73 and compared with result from base calculation. It can be observed that after the actuation of reflood calculation in the base case, difference between both calculations appeared and it was enlarged after the fill of the lower plenum. Such difference basically was caused by the effect of axial conduction along the fuel and different heat transfer package used. To further identify which one plays the key role in making this difference, a reflood unit

consisting of 11 sections in the base modeling to represent fuel rods was changed to 11 reflood unit in series consisting of 1 section in each. The result is such that the two-dimensional conduction effect can almost be suppressed in this alter modeling while still using the same reflood heat transfer package. Resulting temperature is shown in Figure 4-74 and compared to the result from base modeling. From comparison, it can be deduced that the effect of two-dimensional conduction was rather small and the difference shown in Figure 4-73 was mainly caused by the usage of different heat transfer package when defeating of normal reflood calculation. The comparison of CPU time used is shown in Figure 4-75. It is clear that the cost of CPU time is very close even without reflood calculation.

REACTOR EXCURSION AND LEAK ANALYSIS PROGRAM(RELAP5/MOD2/36.04)

SIMULATION OF SEMISCALE S-06-3 LARGE LOCA TEST

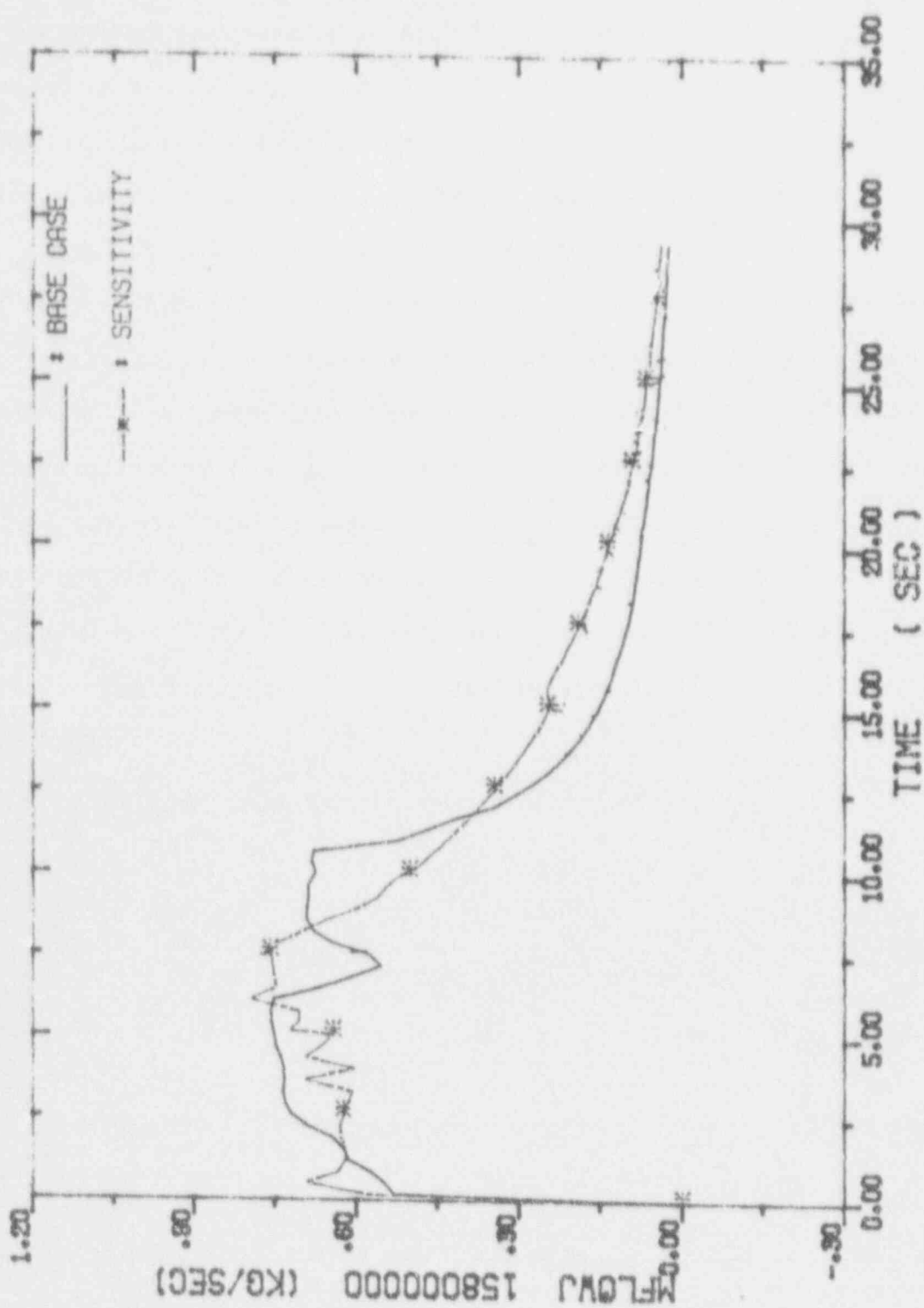


Fig. 4-40. Pressurizer Outsurge Flow Rates

REACTOR EXCURSION AND LEAK ANALYSIS PROGRAM(RELAPS/MOD2/36.04)

SIMULATION OF SEMISCALE S-06-3 LARGE LOCA TEST

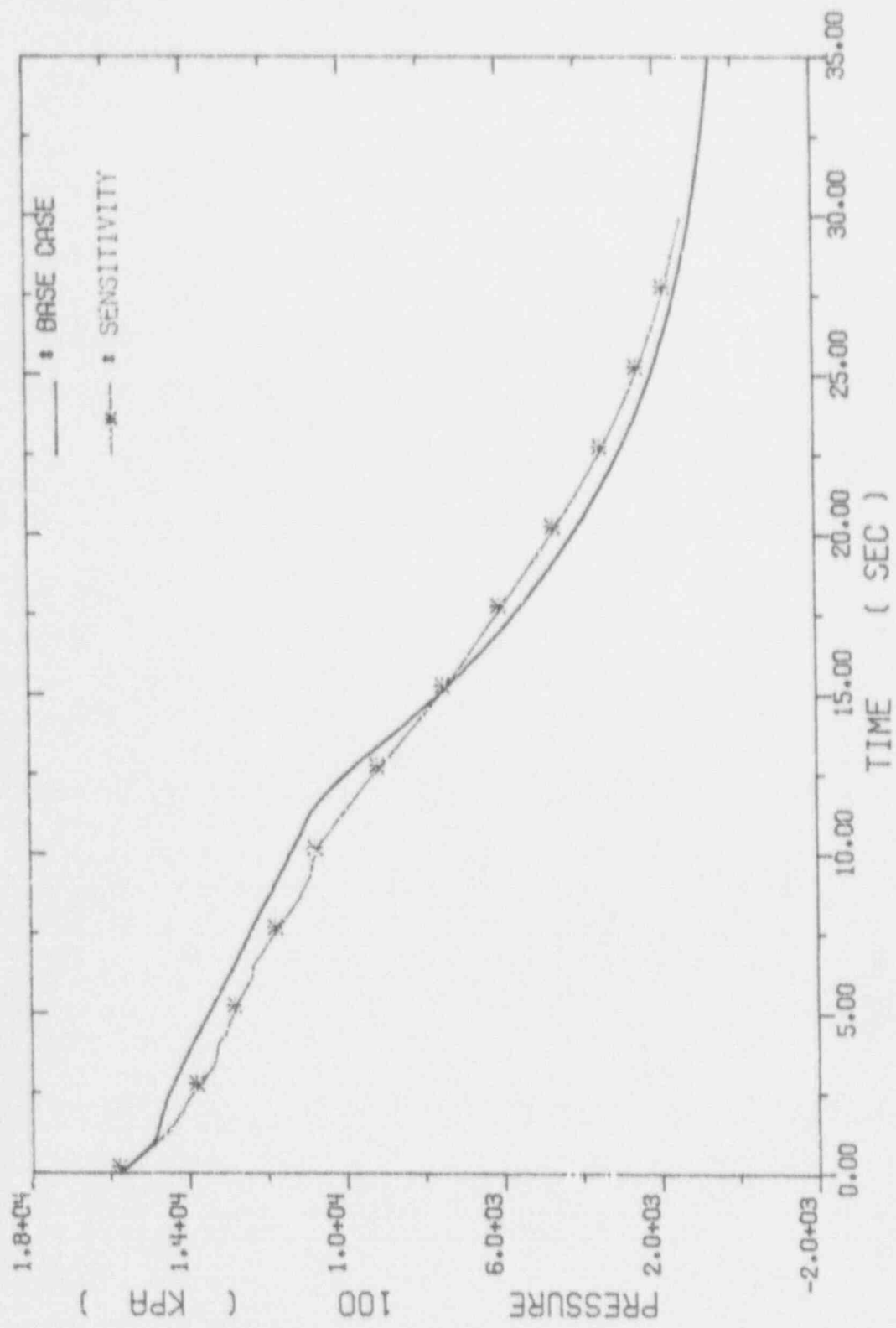


Fig. 4-41. Pressurizer Pressures

REACTOR EXCURSION AND LEAK ANALYSIS PROGRAM(RELAPS/MOD2/36.04)

SIMULATION OF SEMISCALE S-06-3 LARGE LOCA TEST

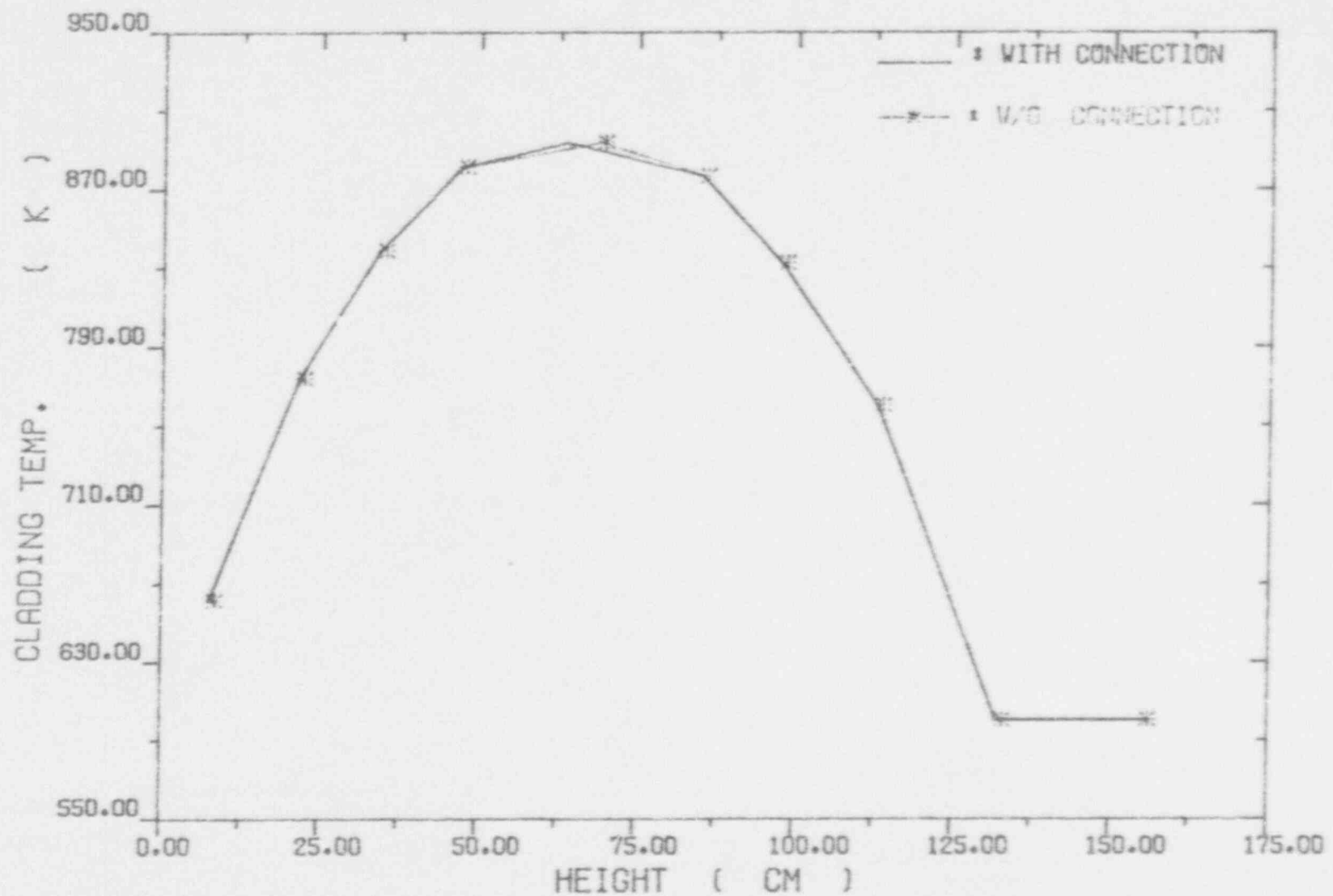


Fig. 4-42. Low Power Rod Peak Cladding Temperatures
versus Elevation

REACTOR EXCURSION AND LEAK ANALYSIS PROGRAM(RELAPS/MOD2/36.04)

SIMULATION OF SEMISCALE S-06-3 LARGE LOCA TEST

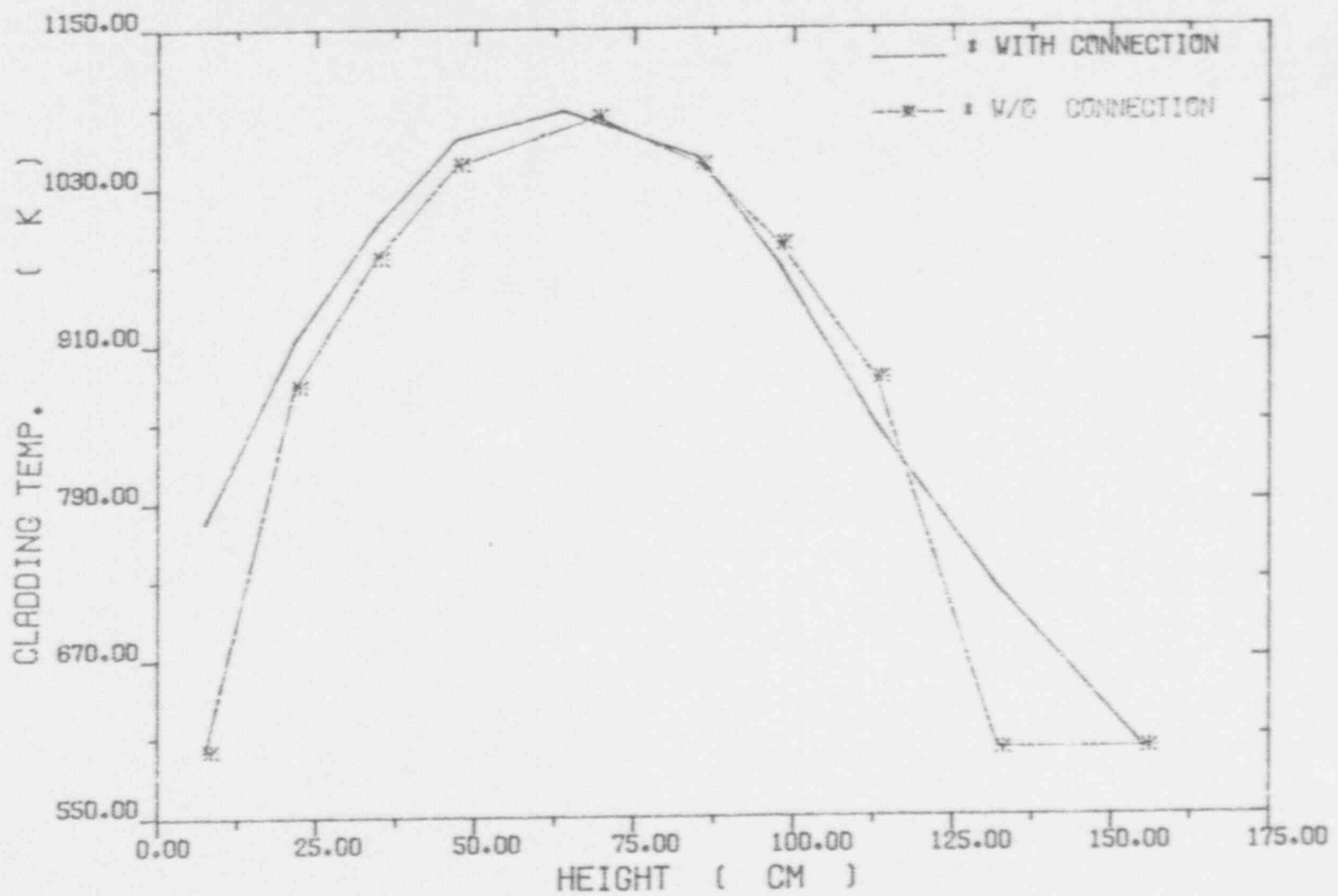


Fig. 4-43. High Power Rod Peak Cladding Temperatures versus Elevation

REACTOR EXCURSION AND LEAK ANALYSIS PROGRAM (RELAPS/MOD2/36.04)

SIMULATION OF SEMISCALE S-06-3 LARGE LOCA TEST

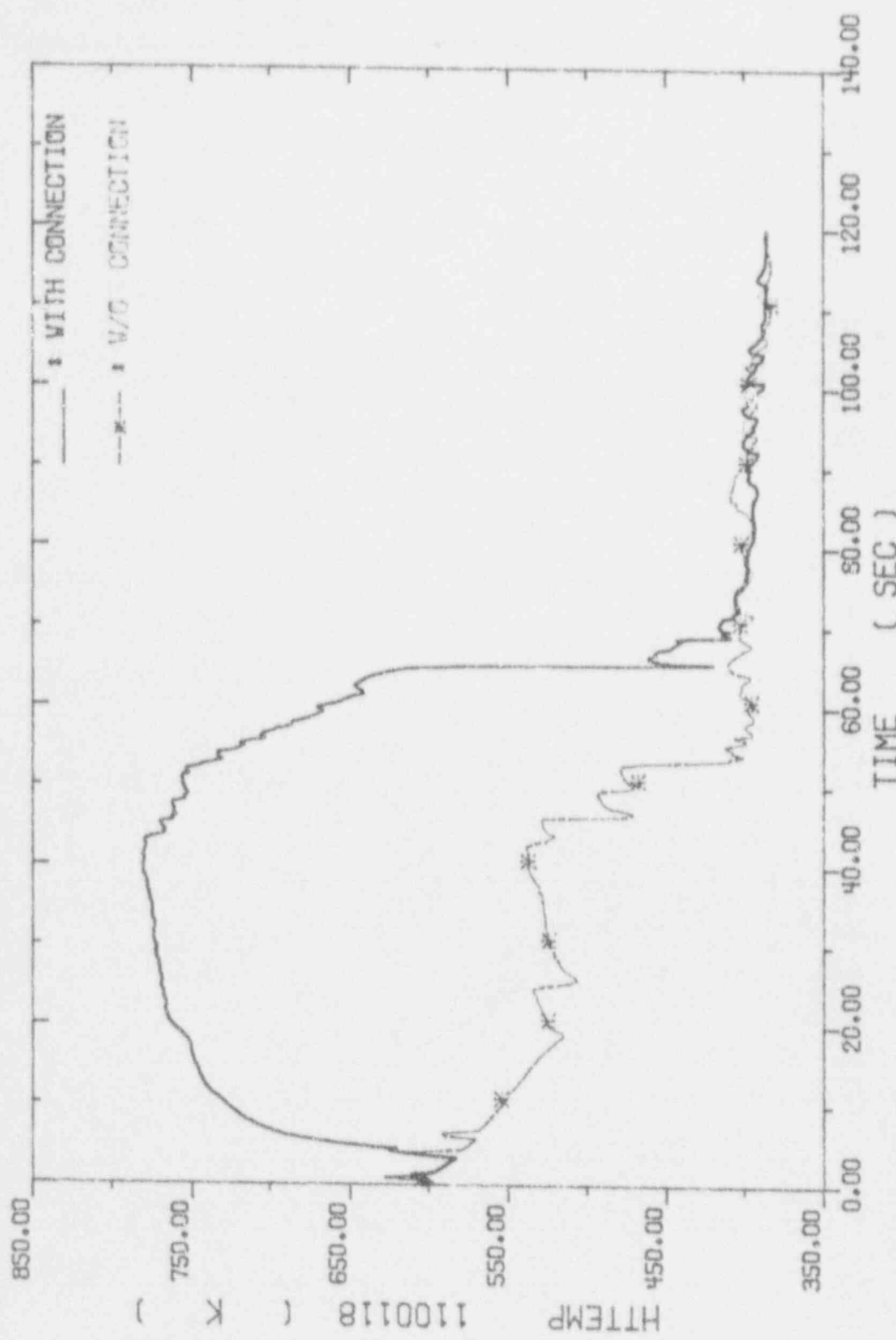


Fig. 4-44. High Power Rod Bottom Section Cladding Temperatures

REACTOR EXCURSION AND LEAK ANALYSIS PROGRAM (RELAPS/MOD2/36.0)

SIMULATION OF SEMISCALE S-06-3 LARGE LOCA TEST

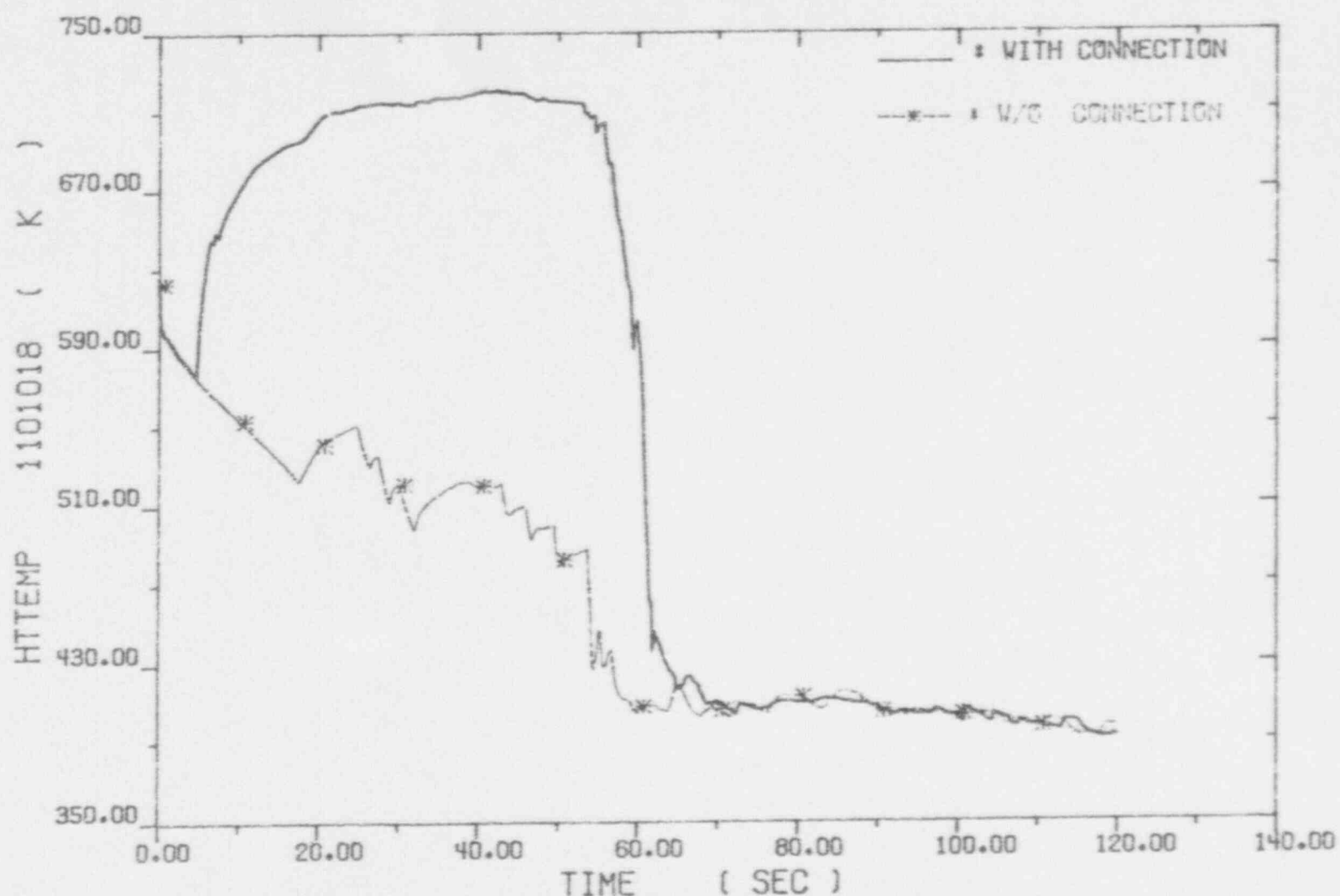


Fig. 4-45. High Power Rod Top Section Cladding Temperatures

SIMULATION OF SEMISCALE S-06-3 LARGE LOCA TEST

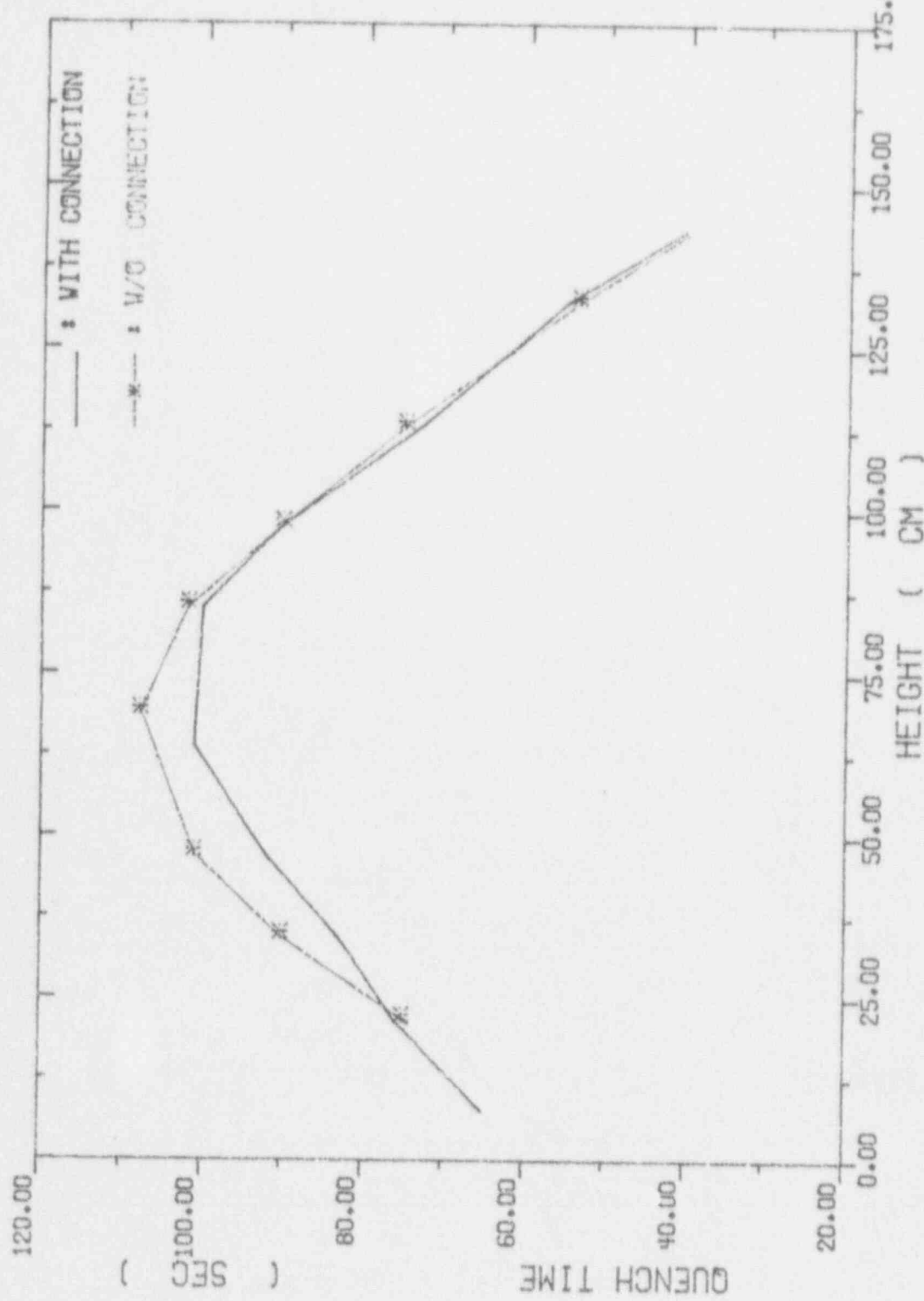


Fig. 4-46. High Power Rod Quench Time versus Elevation

REACTOR EXCURSION AND LEAK ANALYSIS PROGRAM (RELAP5/MOD2/36.04)

SIMULATION OF SEMISCALE S-06-3 LARGE LOCA TEST

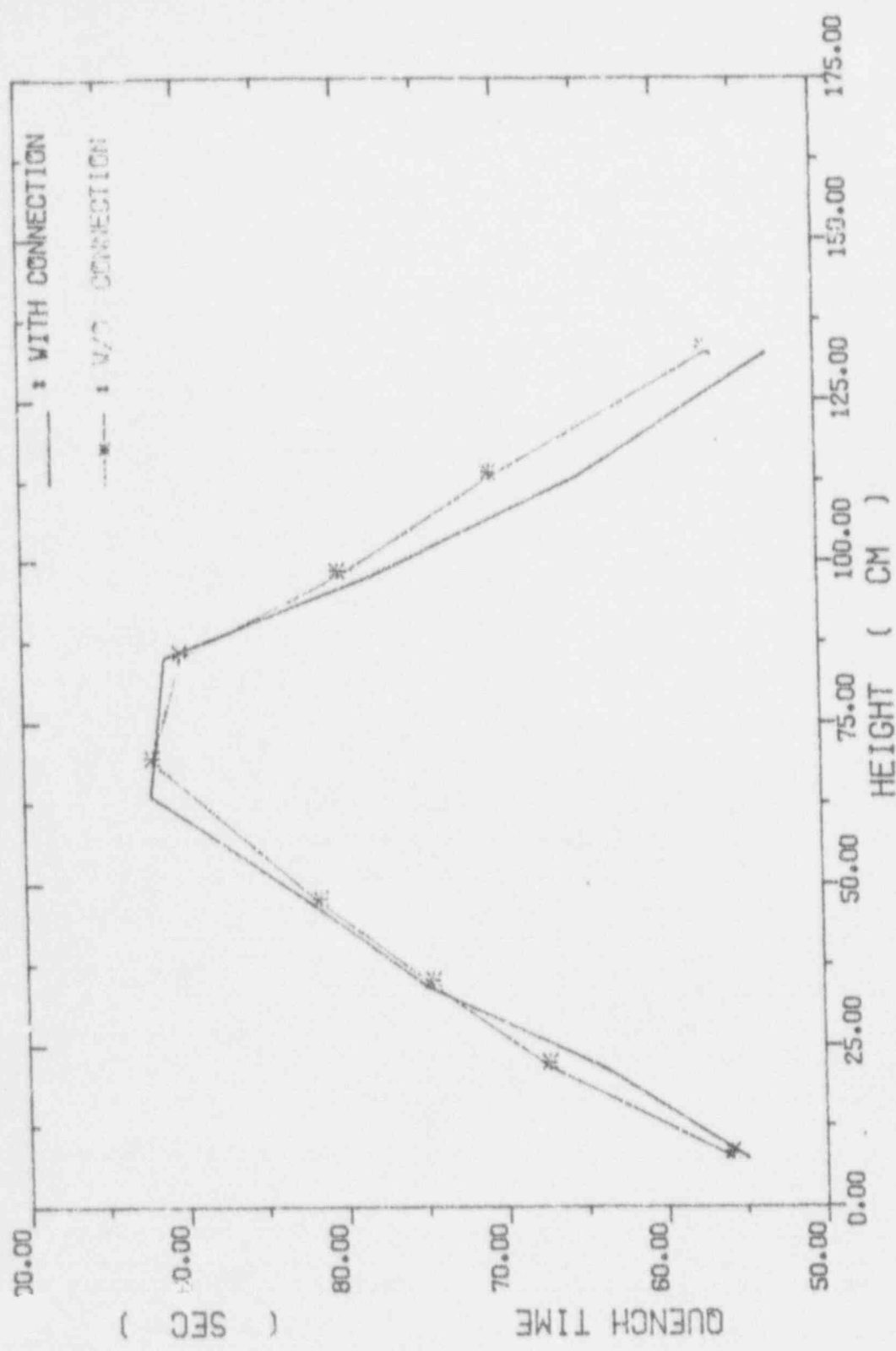


Fig. 4-47. Low Power Rod Quench Time versus Elevation

REACTOR EXCISSION AND LEAK ANALYSIS PROGRAM(RELAPS/MOD2/36.04)

SIMULATION OF SEMISCALE S-06-3 LARGE LOCA TEST

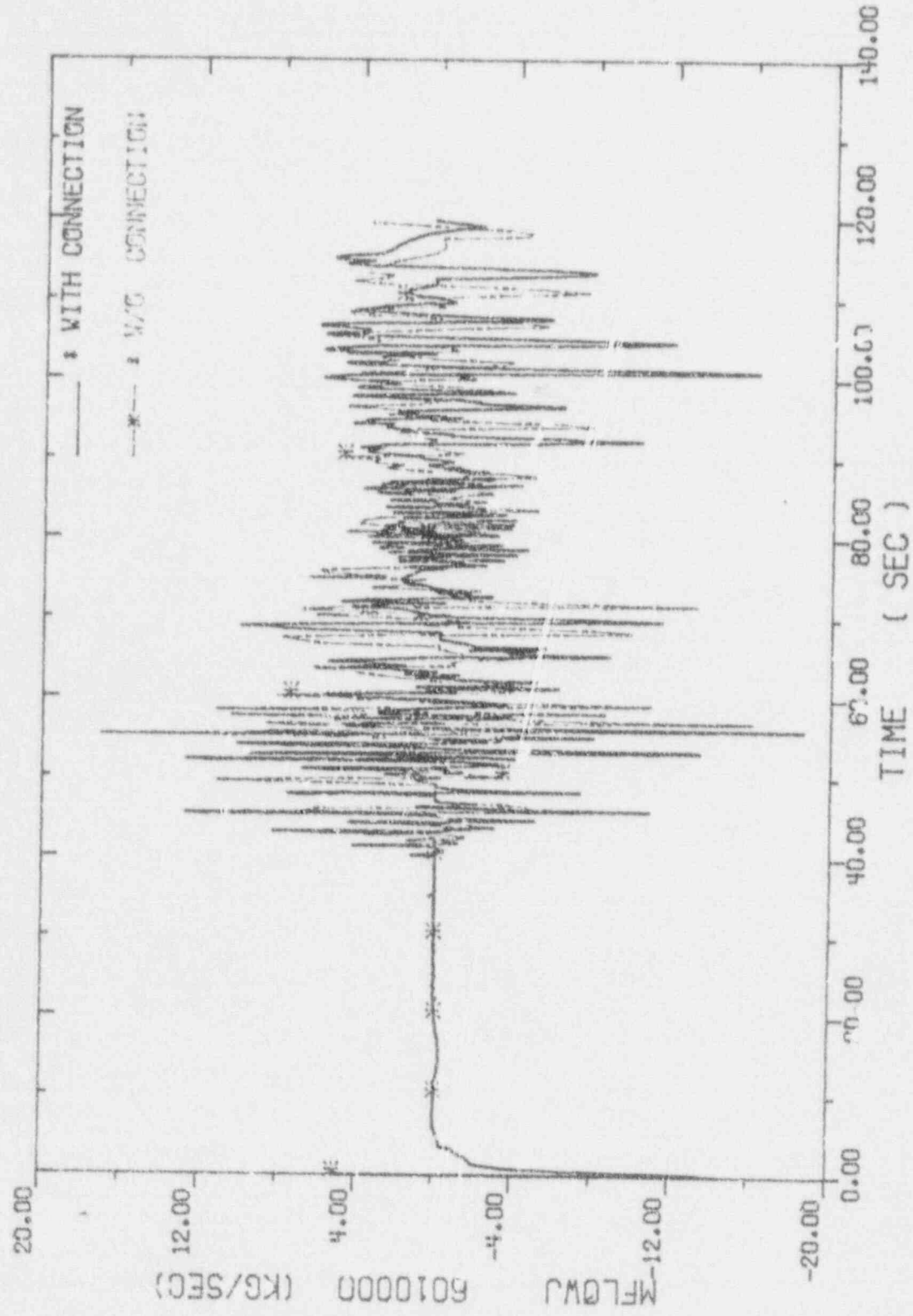


Fig. 4-48. Core Inlet Flow Rates

REACTOR EXCURSION AND LEAK ANALYSIS PROGRAM (RELAPS/MOD/1.05.04)

SIMULATION OF SEMISCALE S-06-3 LARGE LOCA TEST

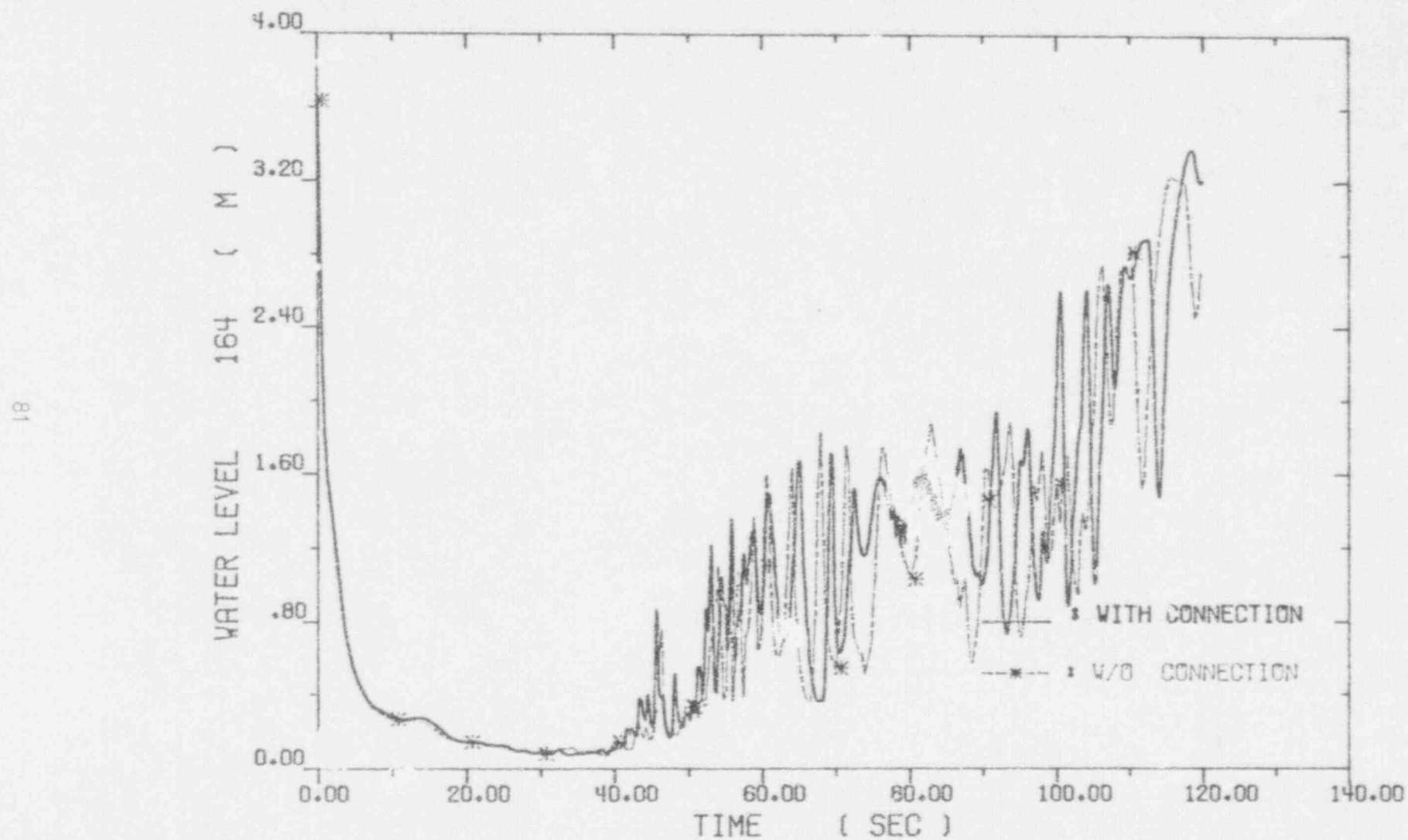


Fig. 4-49. Collapsed Water Levels across the Core

REACTOR EXCURSION AND LEAK ANALYSIS PROGRAM(RELAP5/MOD2/36.64)

SIMULATION OF SEMISCALE S-06-3 LARGE LOCA TEST

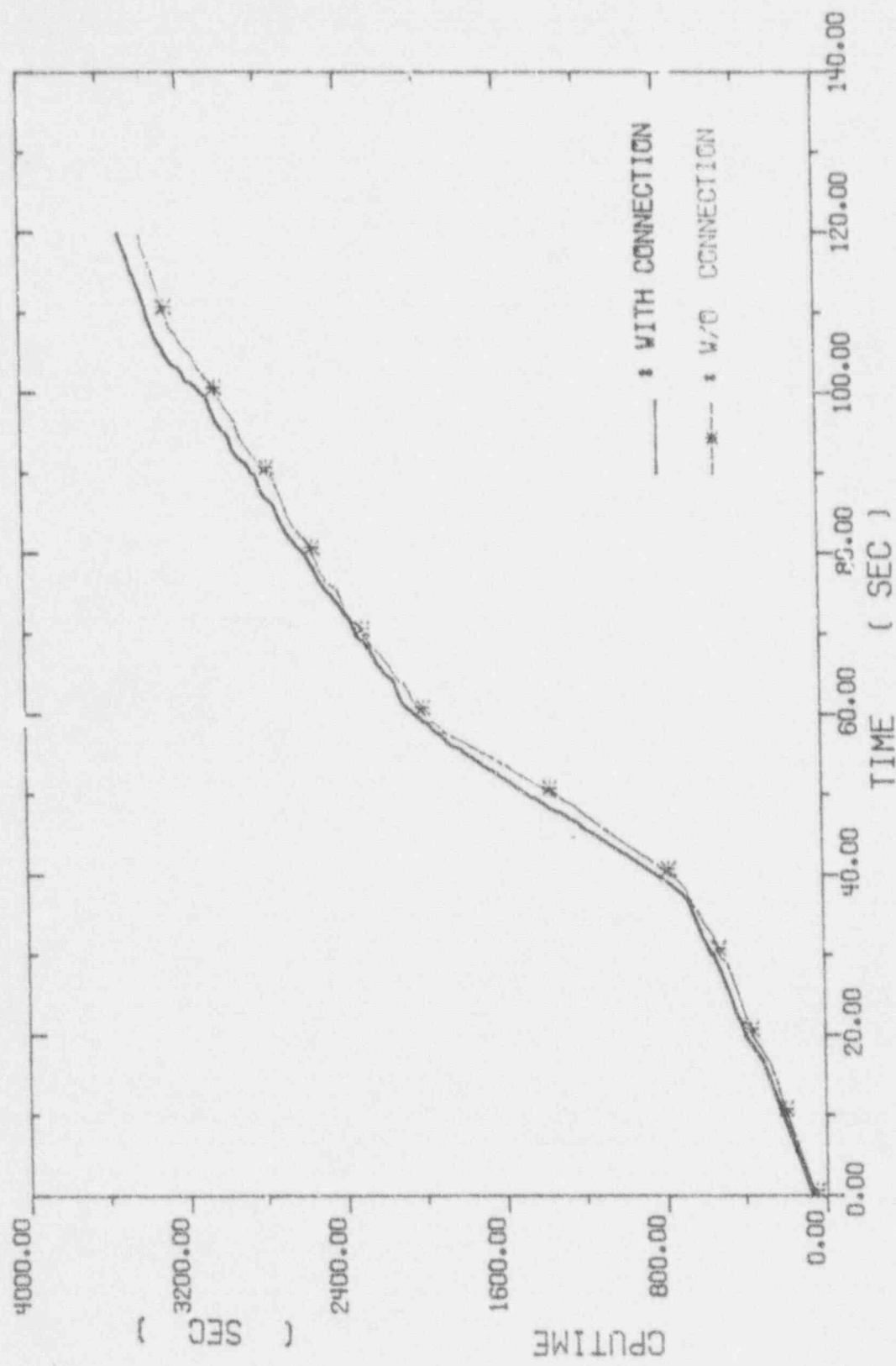


Fig. 4-50. Comparison of CPU Time

SIMULATION OF SEMISCALE S-06-3 LARGE LOCA TEST

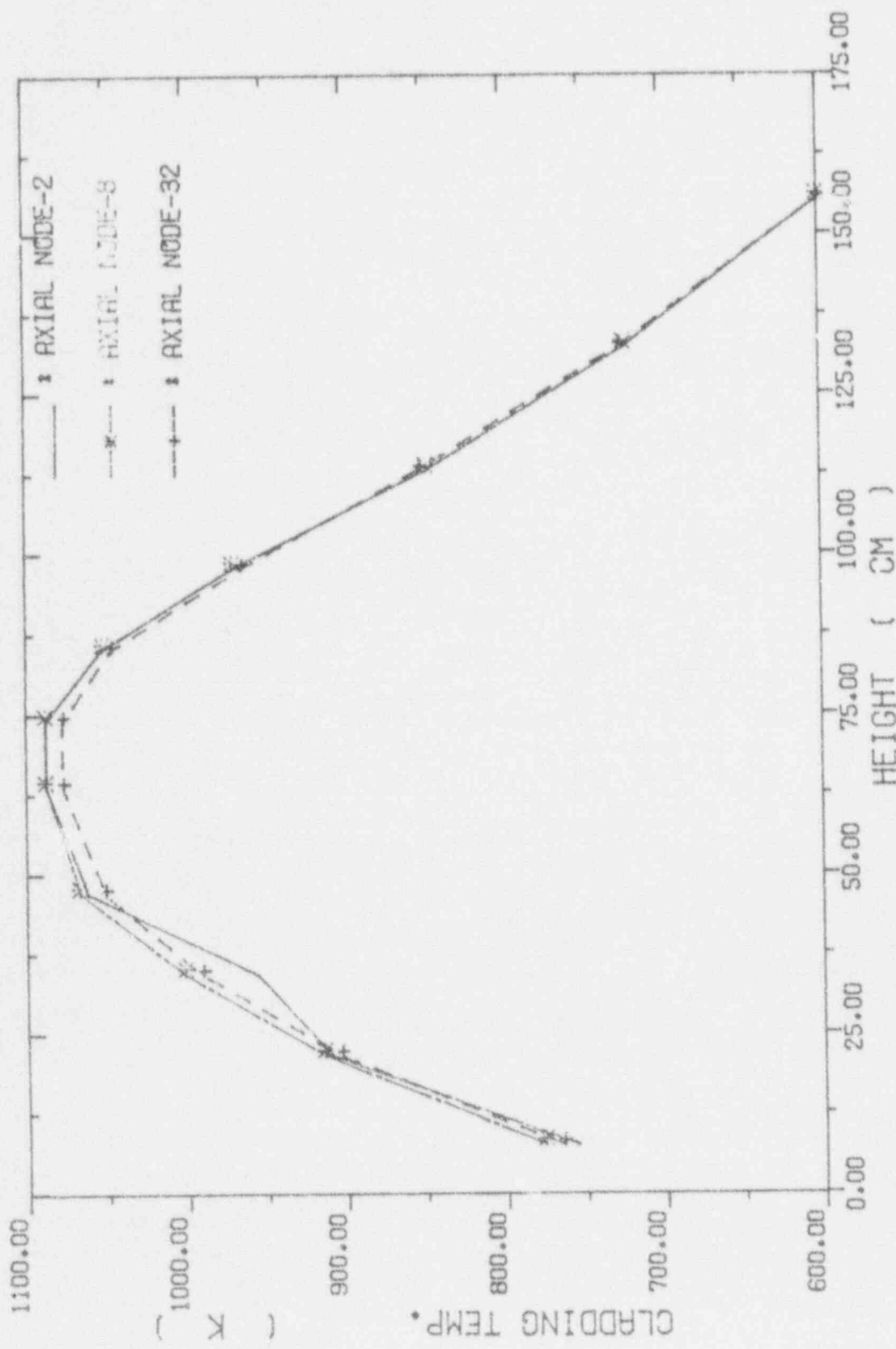


Fig. 4-51. High Power Rod Peak Cladding Temperatures
versus Elevation

REACTOR EXCURSION AND LEAK ANALYSIS PROGRAM(RELAPS/MOD2/36.04)

SIMULATION OF SEMISCALE S-06-3 LARGE LOCA TEST

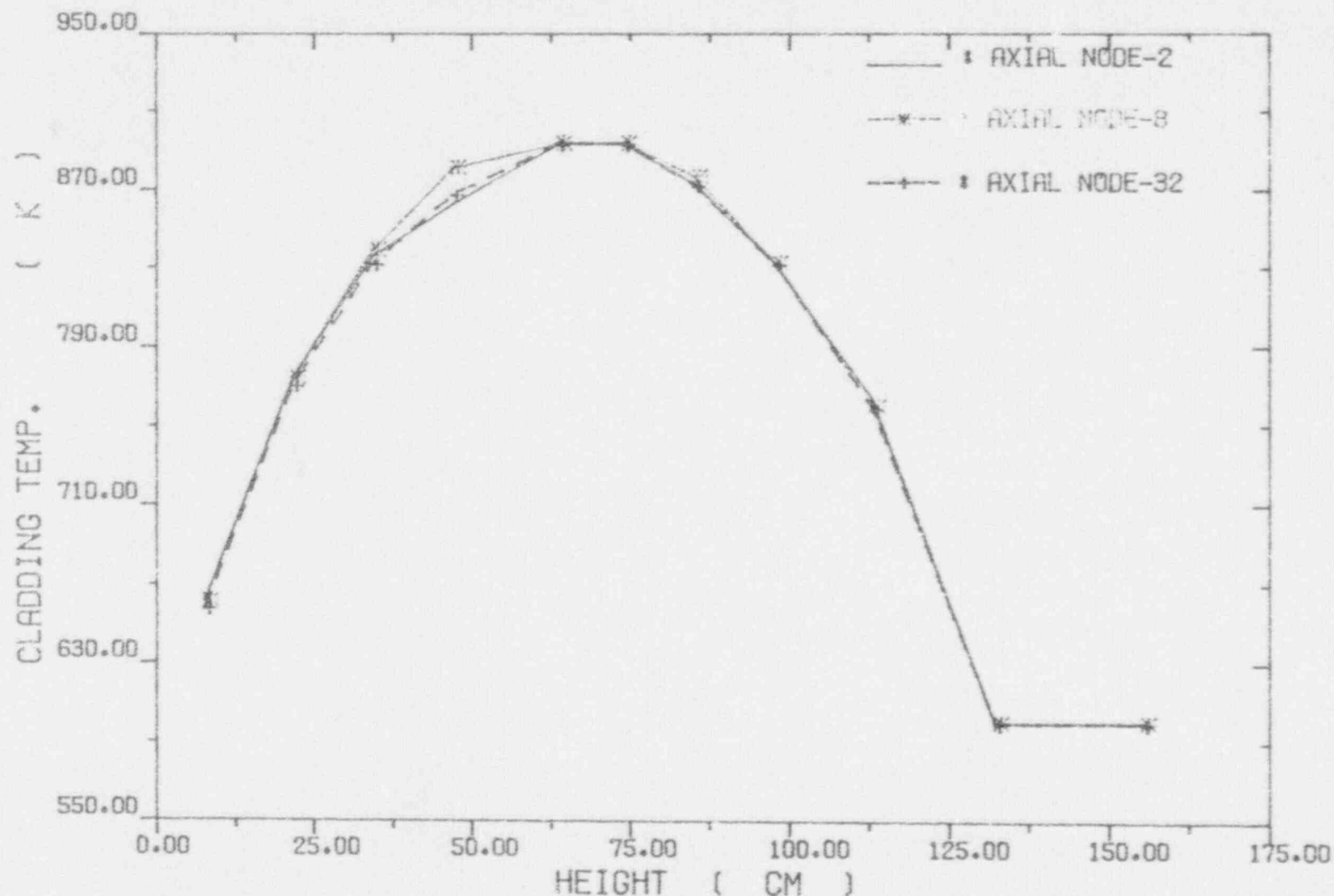


Fig. 4-52. Low Power Rod Peak Cladding Temperatures versus Elevation

REACTOR EXCURSION AND LEAK ANALYSIS PROGRAM (RELAPS/MOD2/36.04)

SIMULATION OF SEMISCALE S-06-3 LARGE LOCA TEST

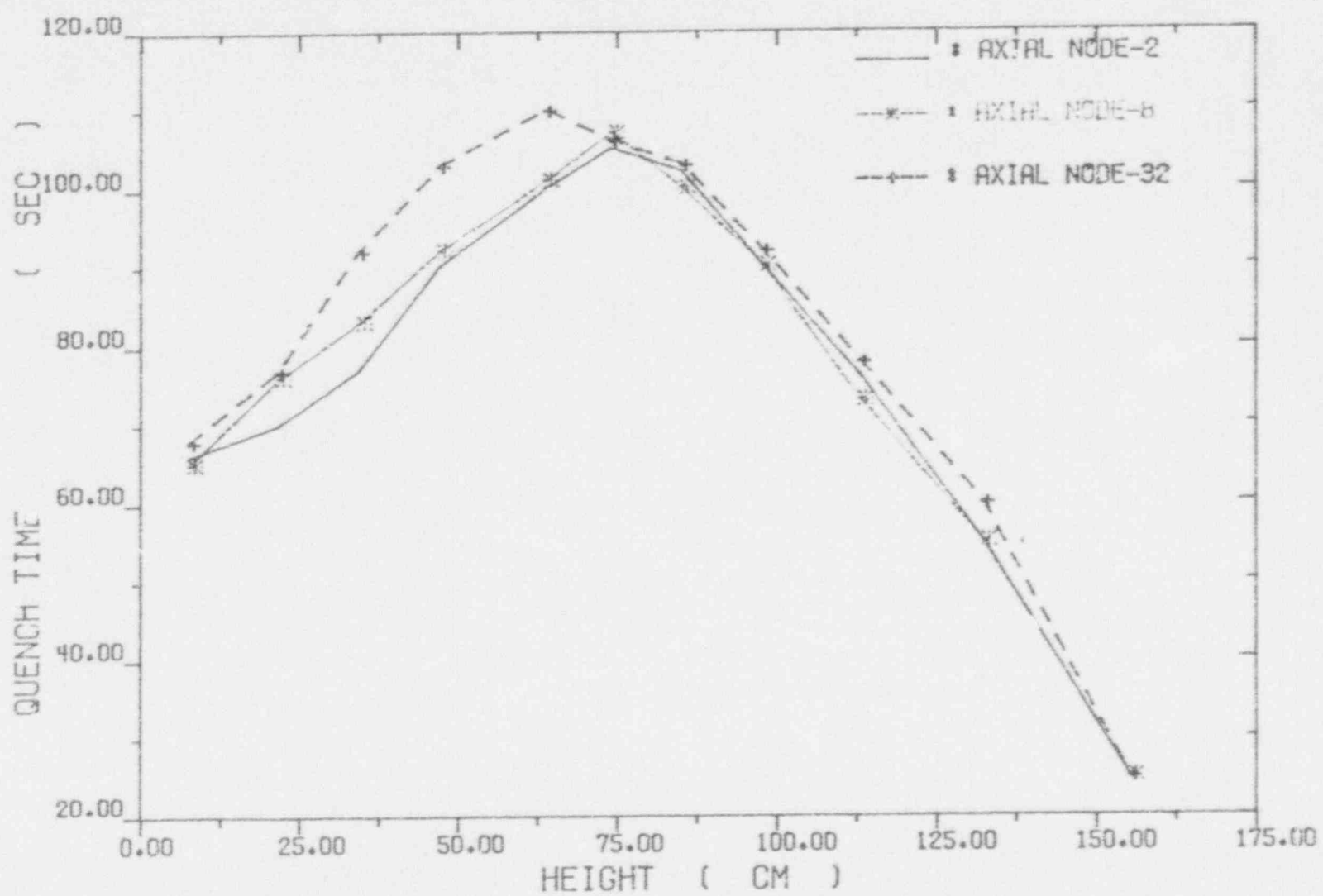


Fig. 4-53. High Power Rod Quench Time versus Elevation

REACTOR EXCURSION AND LEAK ANALYSIS PROGRAM (RELAP5/MOD2/36.04)

SIMULATION OF SEMISCALE S-06-3 LARGE LOCA TEST

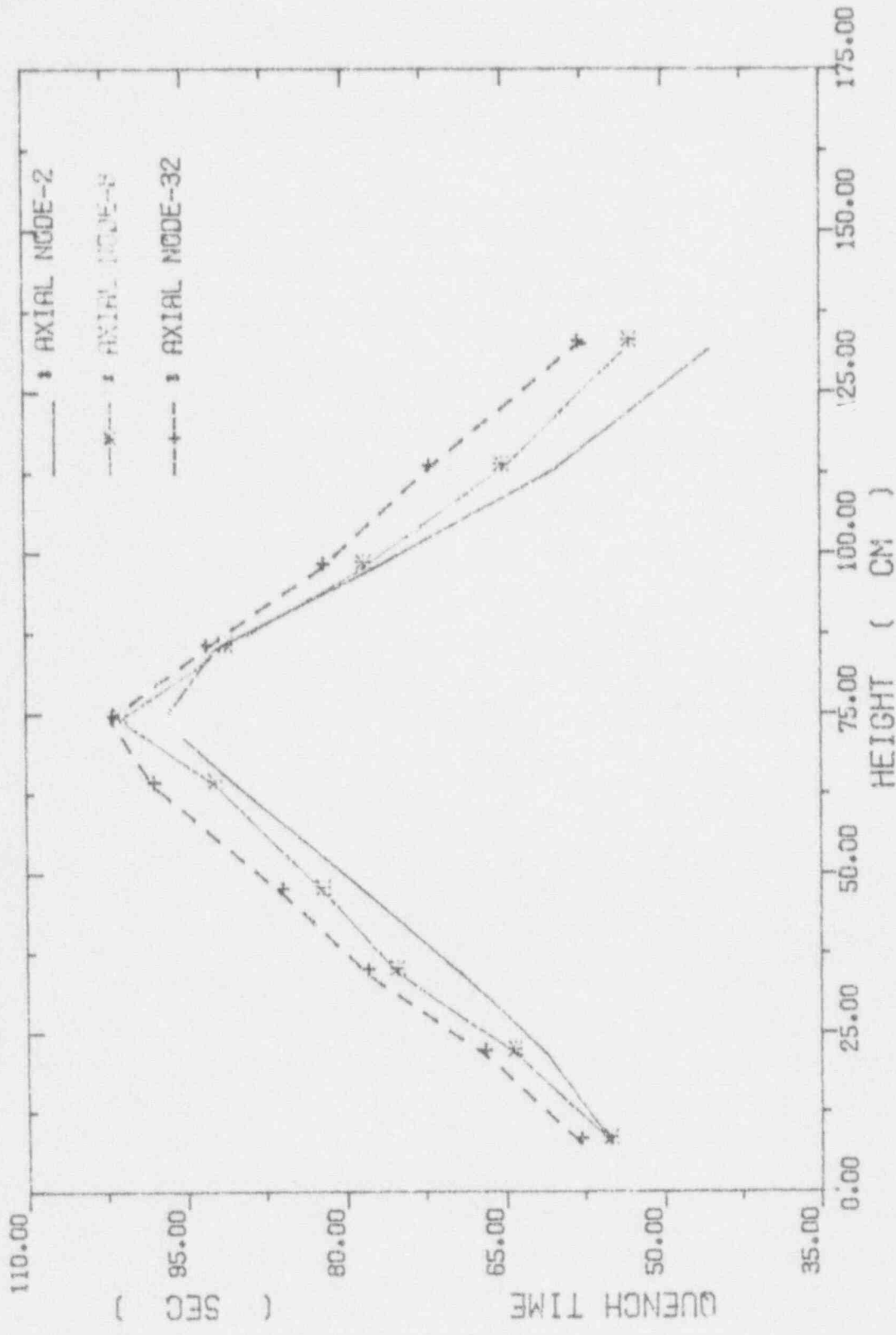


Fig. 4-54. Low power Rod Quench Time versus Elevation

REACTOR EXPLOSION AND THERMAL RADIATION FROM THE HOT SPOT

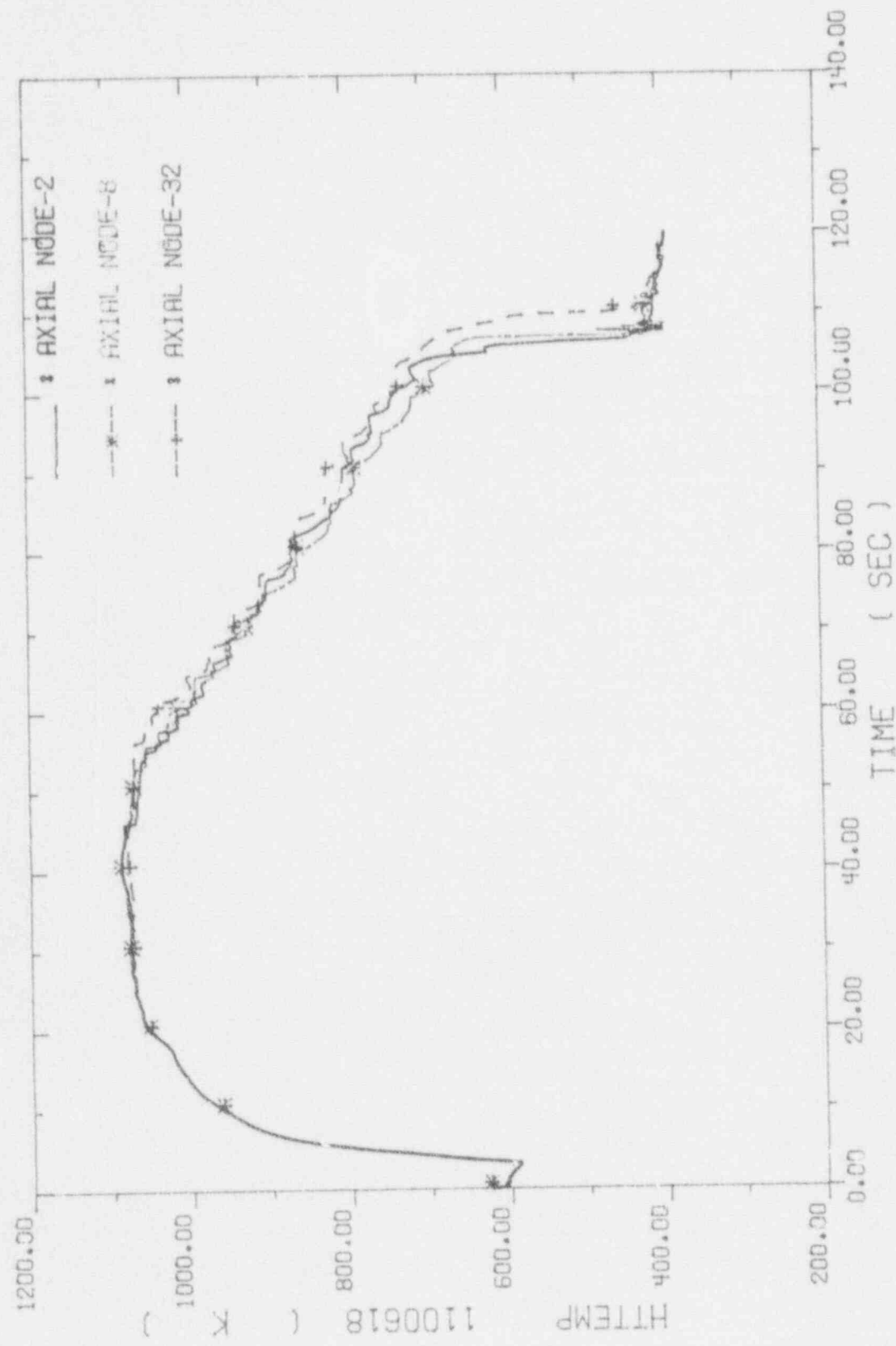


Fig. 4-55. High Power Rod Hot Spot Cladding Temperatures

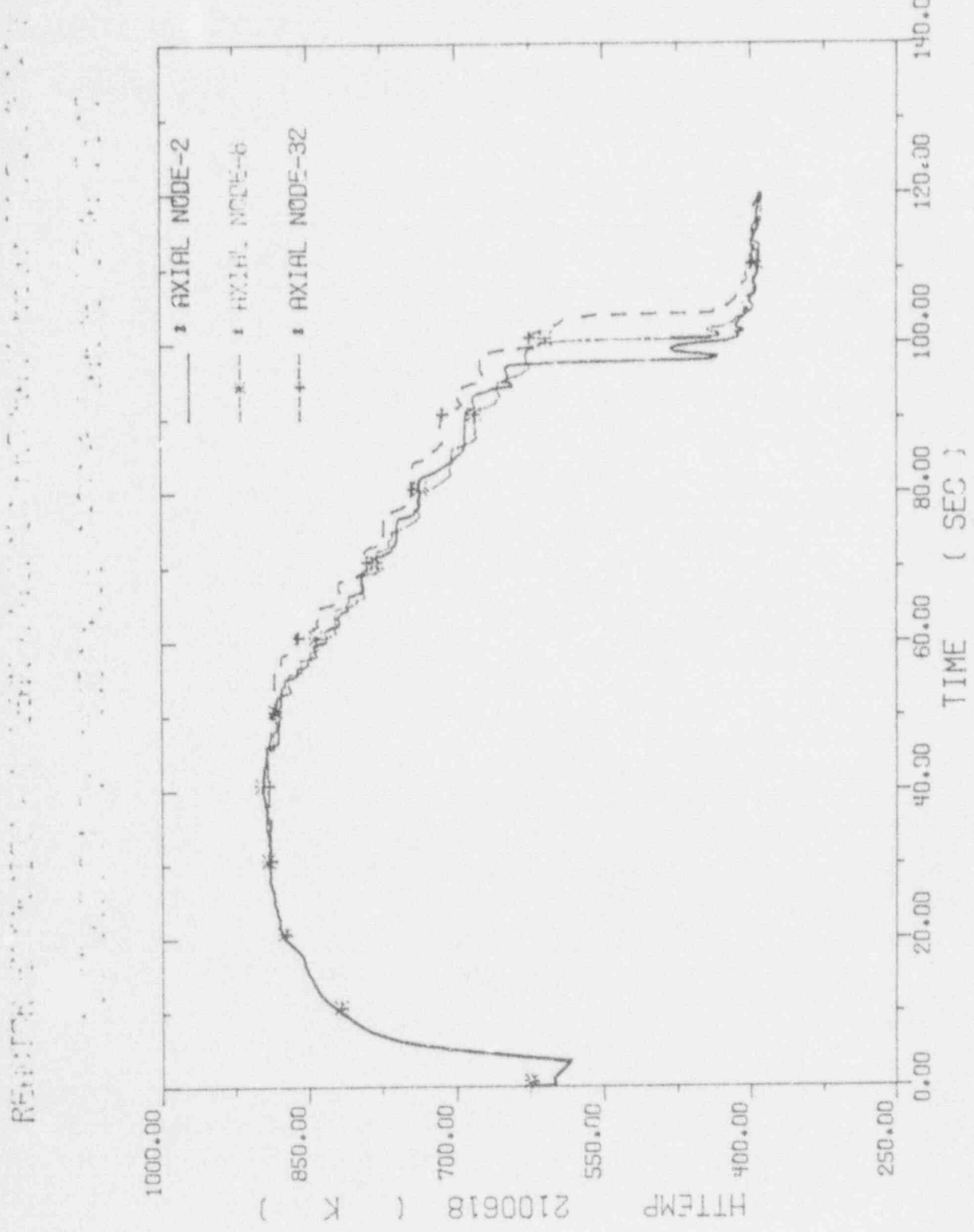


Fig. 4-56. Low Power Rod Hot Spot Cladding Temperatures

REACTOR EXCURSION AND LEAK ANALYSIS PROGRAM (RELAP5/MOD2/36.04)

SIMULATION OF SEMISCALE S-06-3 LARGE LOCA TEST

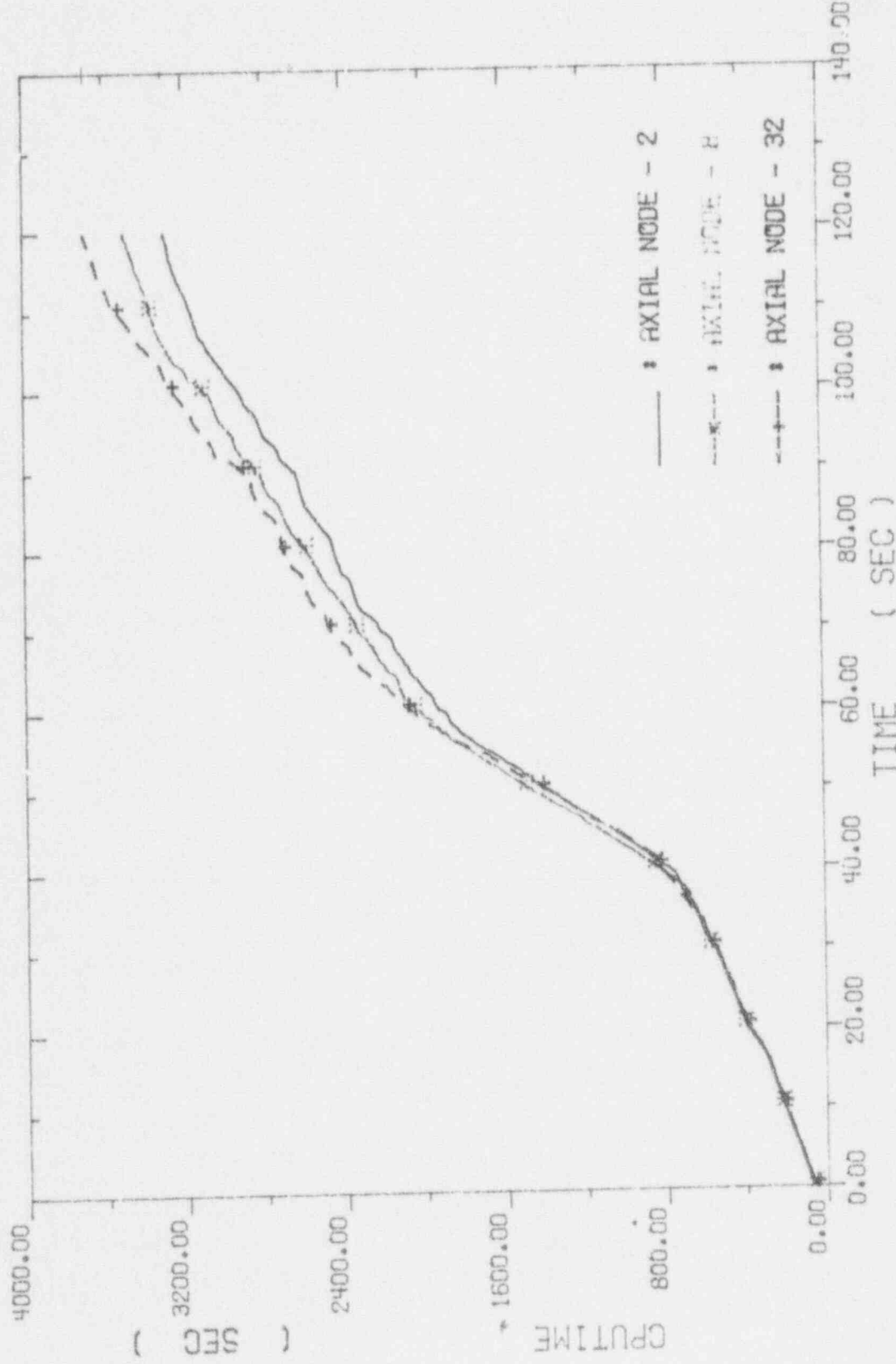


Fig. 4-57. Comparison of CPU Time

REACTOR EXCURSION AND LEAK ANALYSIS PROGRAM (RELAPS/MOD2/36.04)

SIMULATION OF SEMISCALE S-06-3 LARGE LOCA TEST

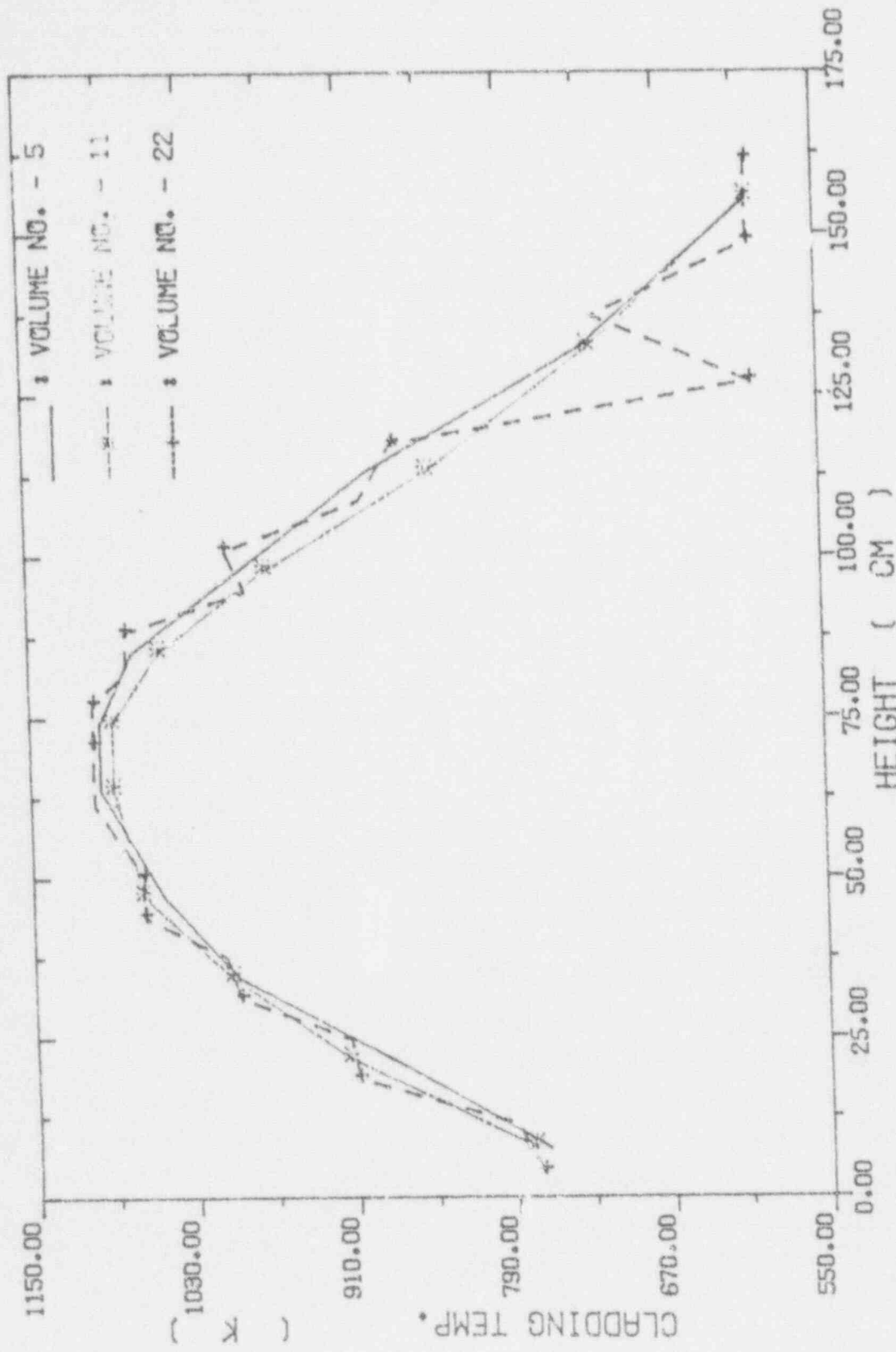


Fig. 4-58. High Power Rod Peak Cladding Temperatures
versus Elevation

REACTOR EXCURSION AND LEAK ANALYSIS PROGRAM (RELAP5/MOD2/36.04)

SIMULATION OF SEMISCALE S-06-3 LARGE LOCA TEST

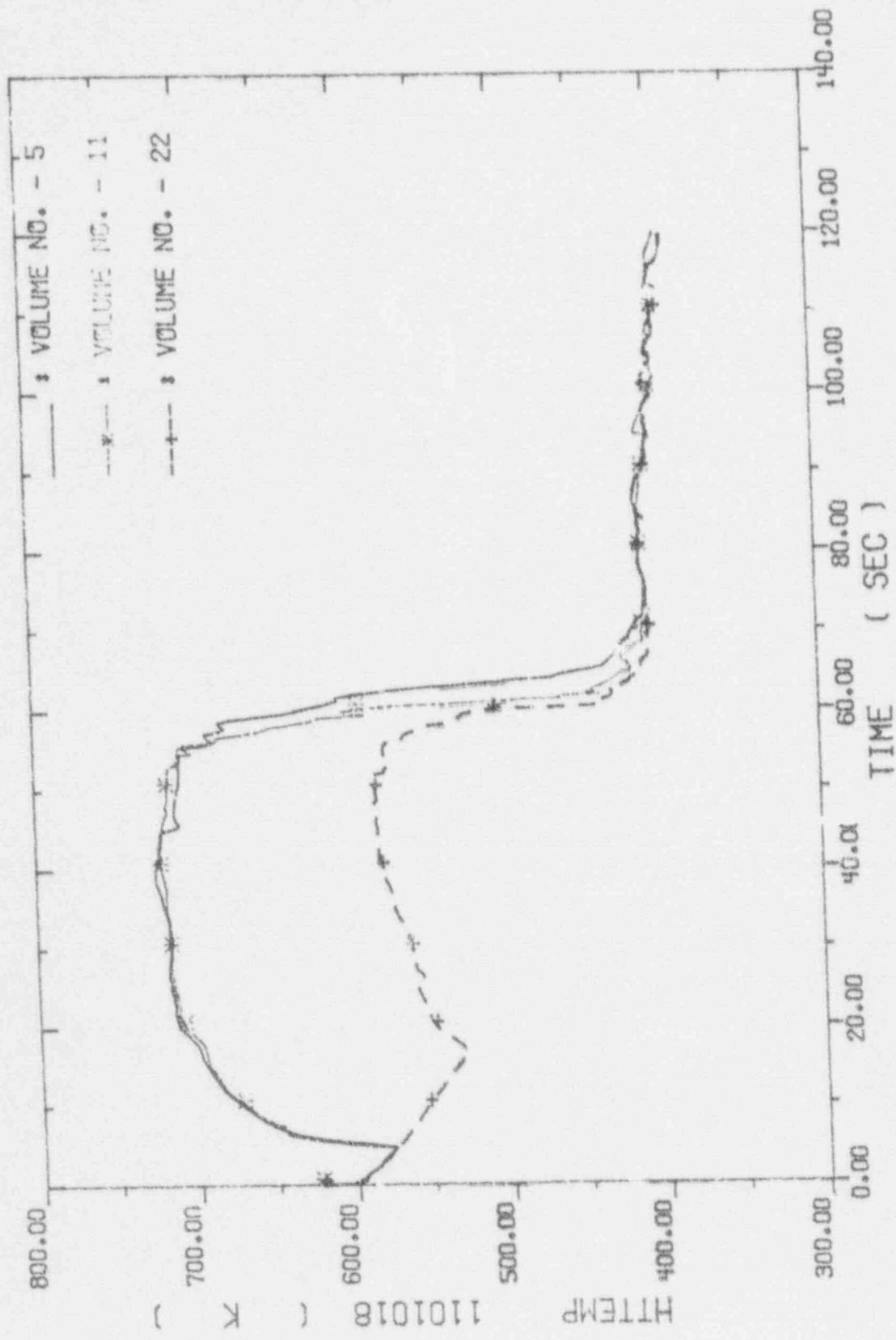


Fig. 4-59. High power Rod Top Section Cladding Temperatures

REACTOR EXCURSION AND LEAK ANALYSIS PROGRAM (RELAP5/MOD2/36.04)

SIMULATION OF SEMISCALE S-06-3 LARGE LOCA TEST

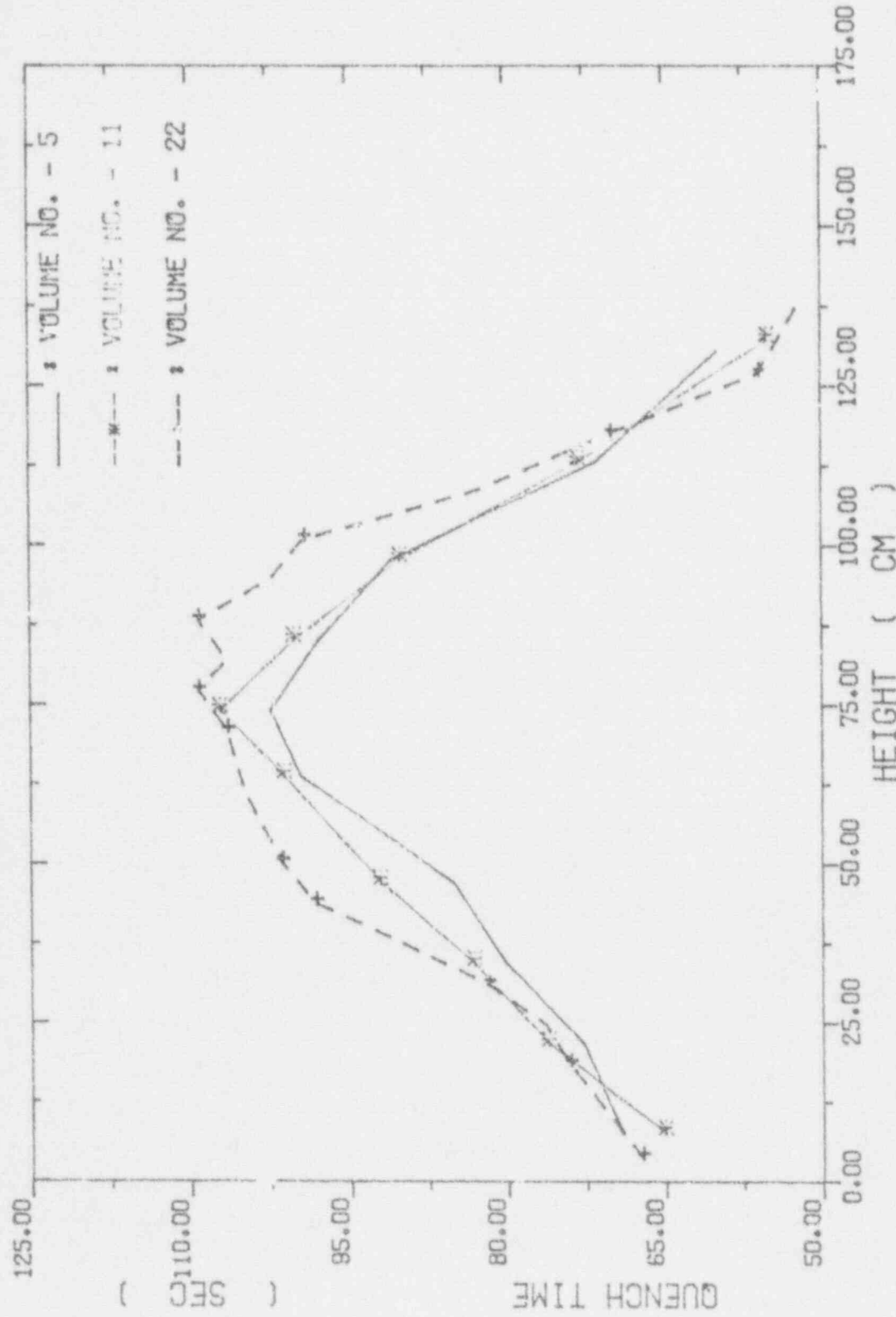


Fig. 4-60. High Power Rod Quench Time versus Elevation

REACTOR EXCURSION AND LEAK ANALYSIS PROGRAM (RELAP^r) 2/36.04)

SIMULATION OF SEMISCALE S-06-3 LARGE LOCA TEST

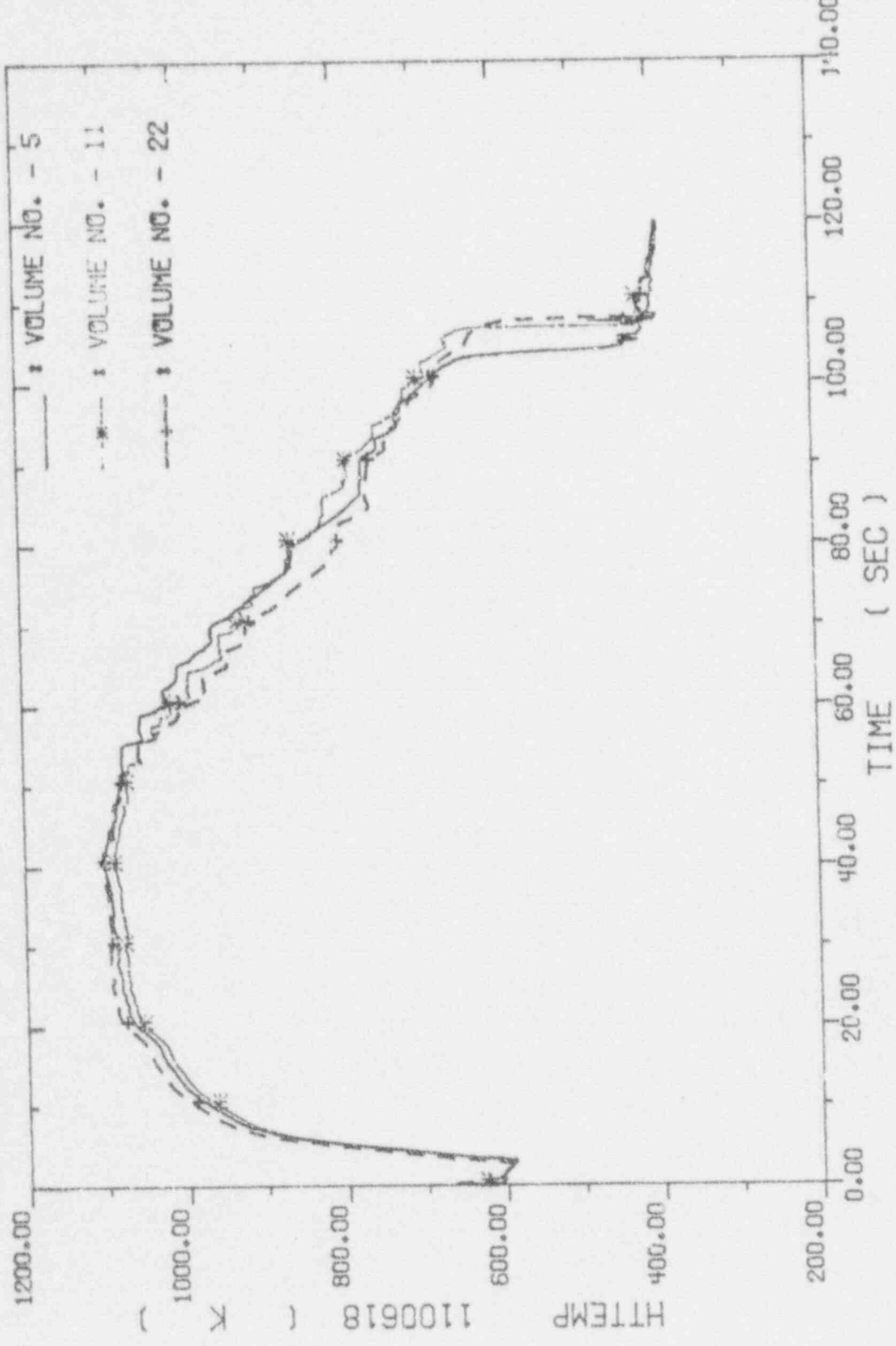


Fig. 4-61. High Power Rod Cladding Temperatures

REACTOR EXCURSION AND LEAK ANALYSIS PROGRAM (RELAP5/MOD2/36.04)

SIMULATION OF SEMISCALE S-06-3 LARGE LOCA TEST

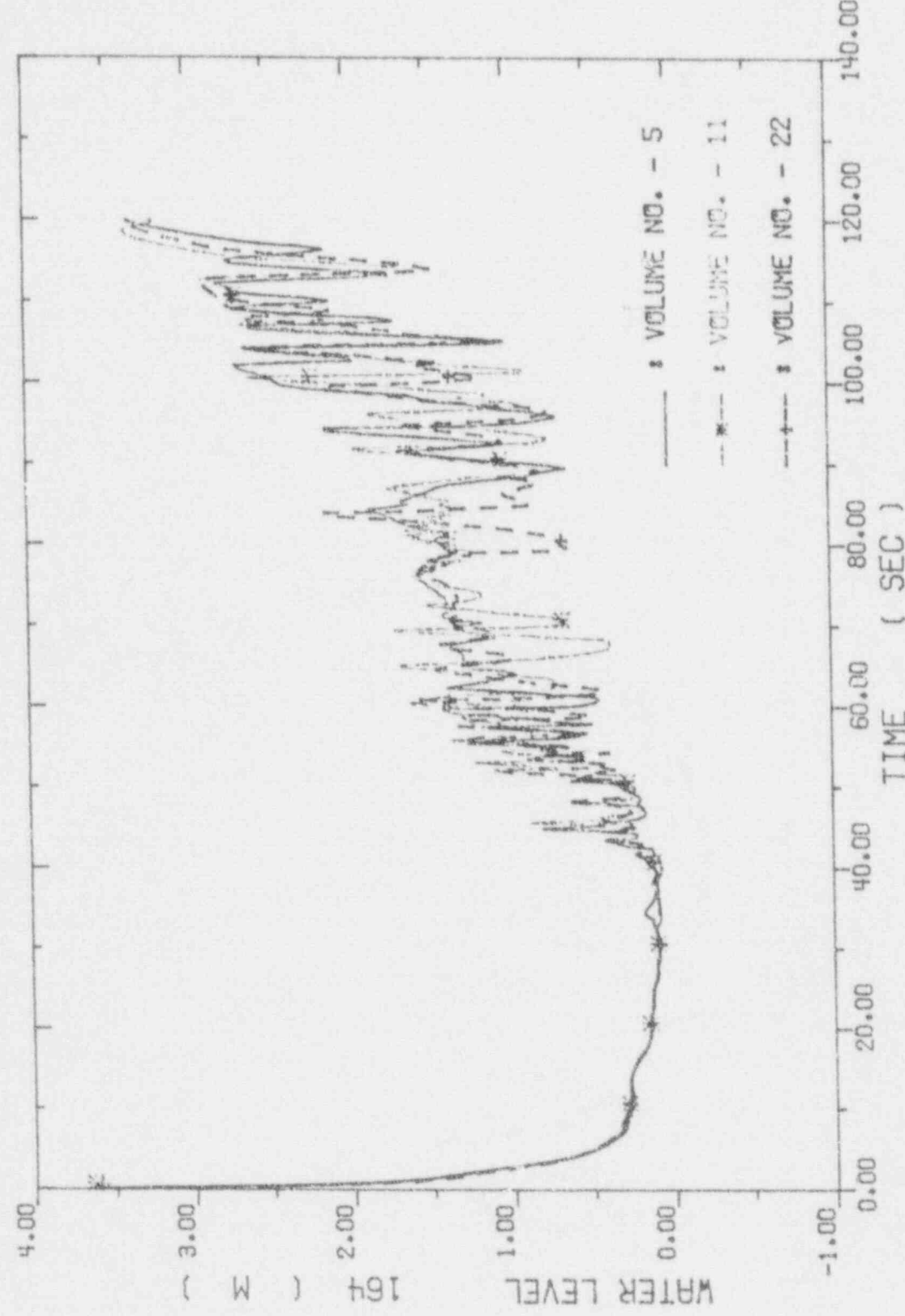


Fig. 4-62. Collapsed Water Levels across The Core

REACTOR EXCURSION AND LEAK ANALYSIS PROGRAM(RELAPS/MOD2/36.04)

SIMULATION OF SEMISCALE S-06-3 LARGE LOCA TEST

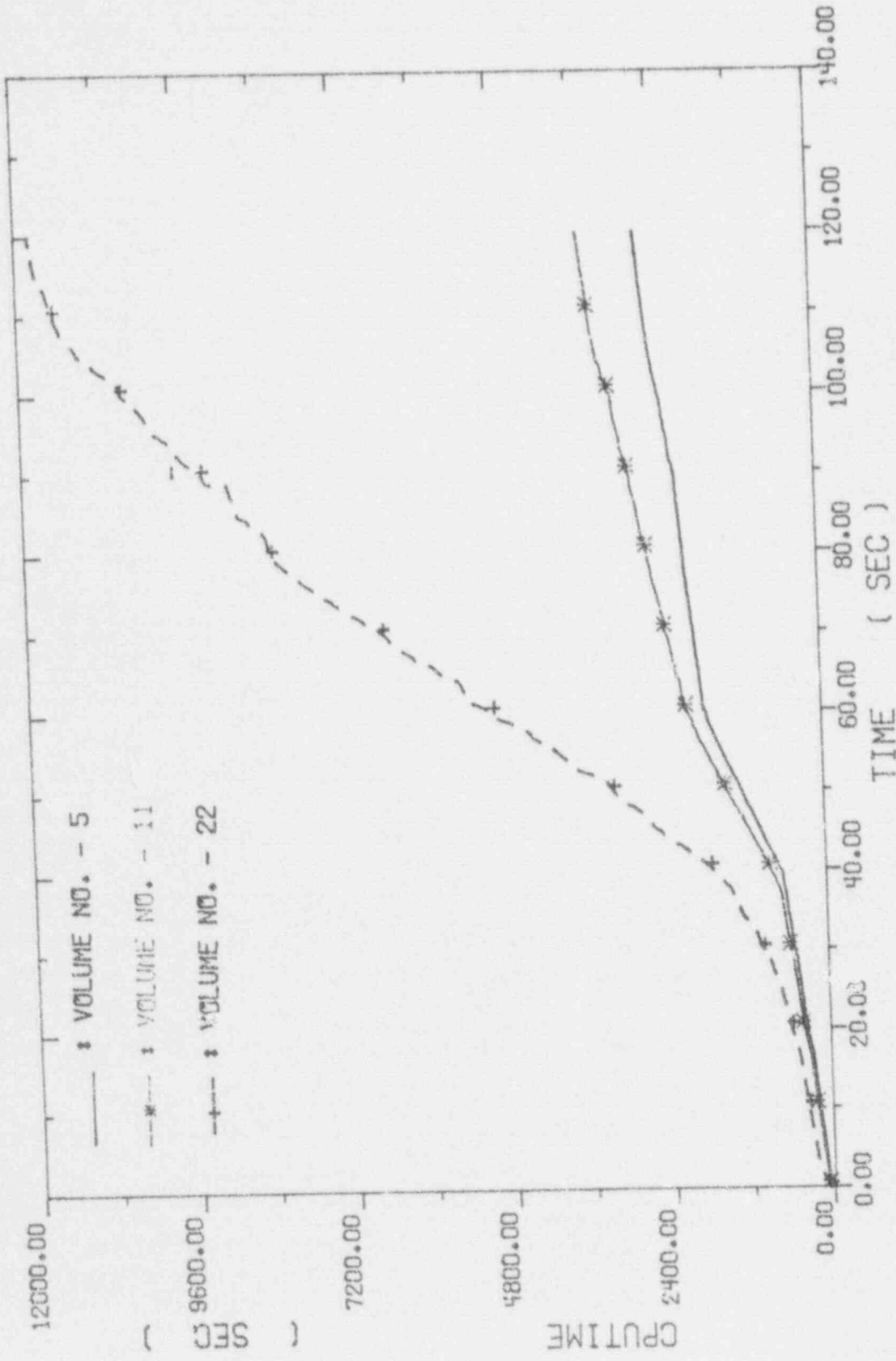


Fig. 4-63. Comparison of CPU Time

REACTOR EXCURSION AND LEAK ANALYSIS PROGRAM(RELAPS/MOD2/36.04)

SIMULATION OF SEMISCALE S-06-3 LARGE LOCA TEST

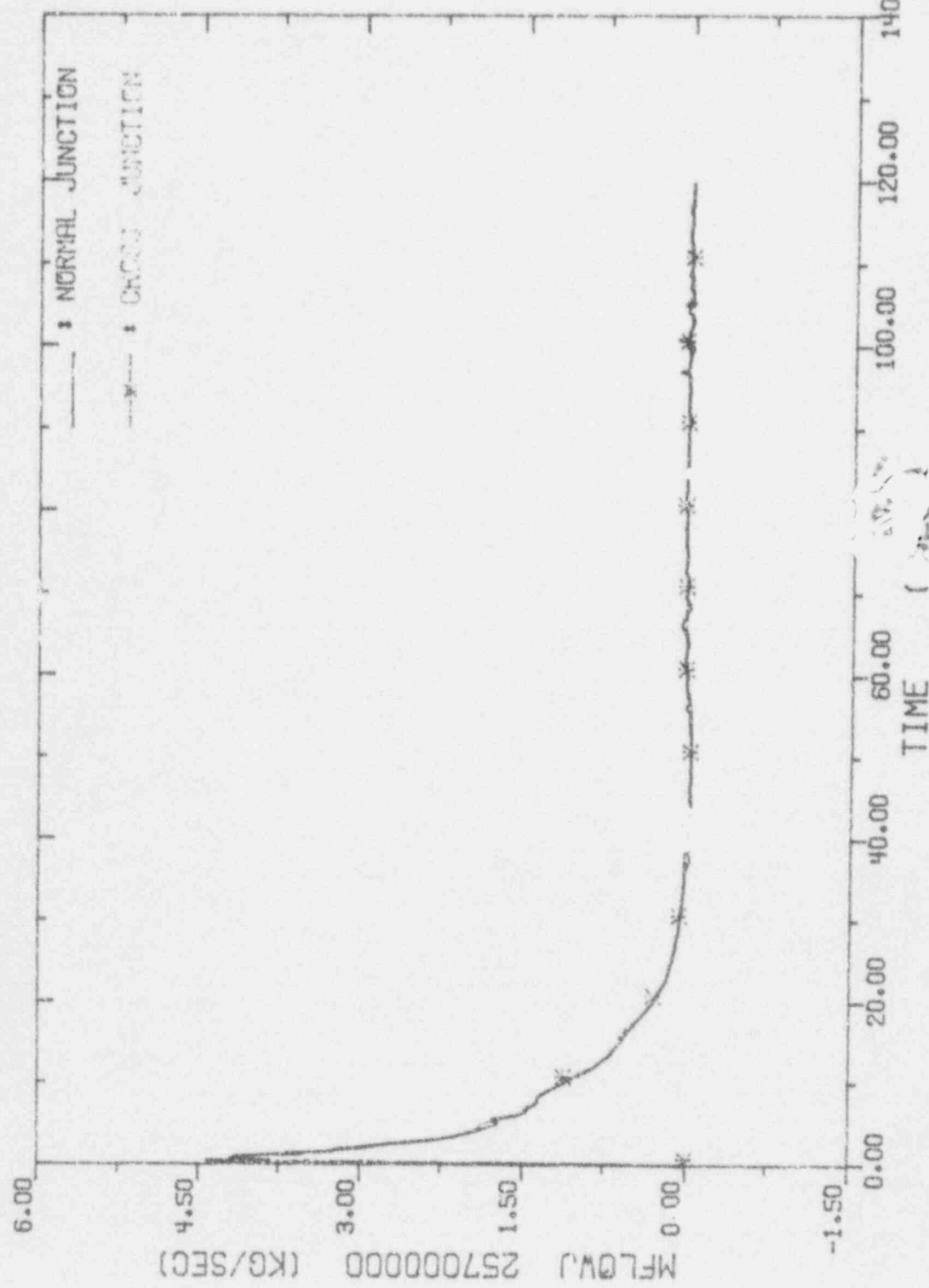


Fig. 4-64. Break Flow Rate, near ΔP_{max} Side

REACTOR EXCURSION AND LEAK ANALYSIS PROGRAM (RELAP5/MOD2/36.04)

SIMULATION OF SEMISCALE S-06-3 LARGE LOCA TEST

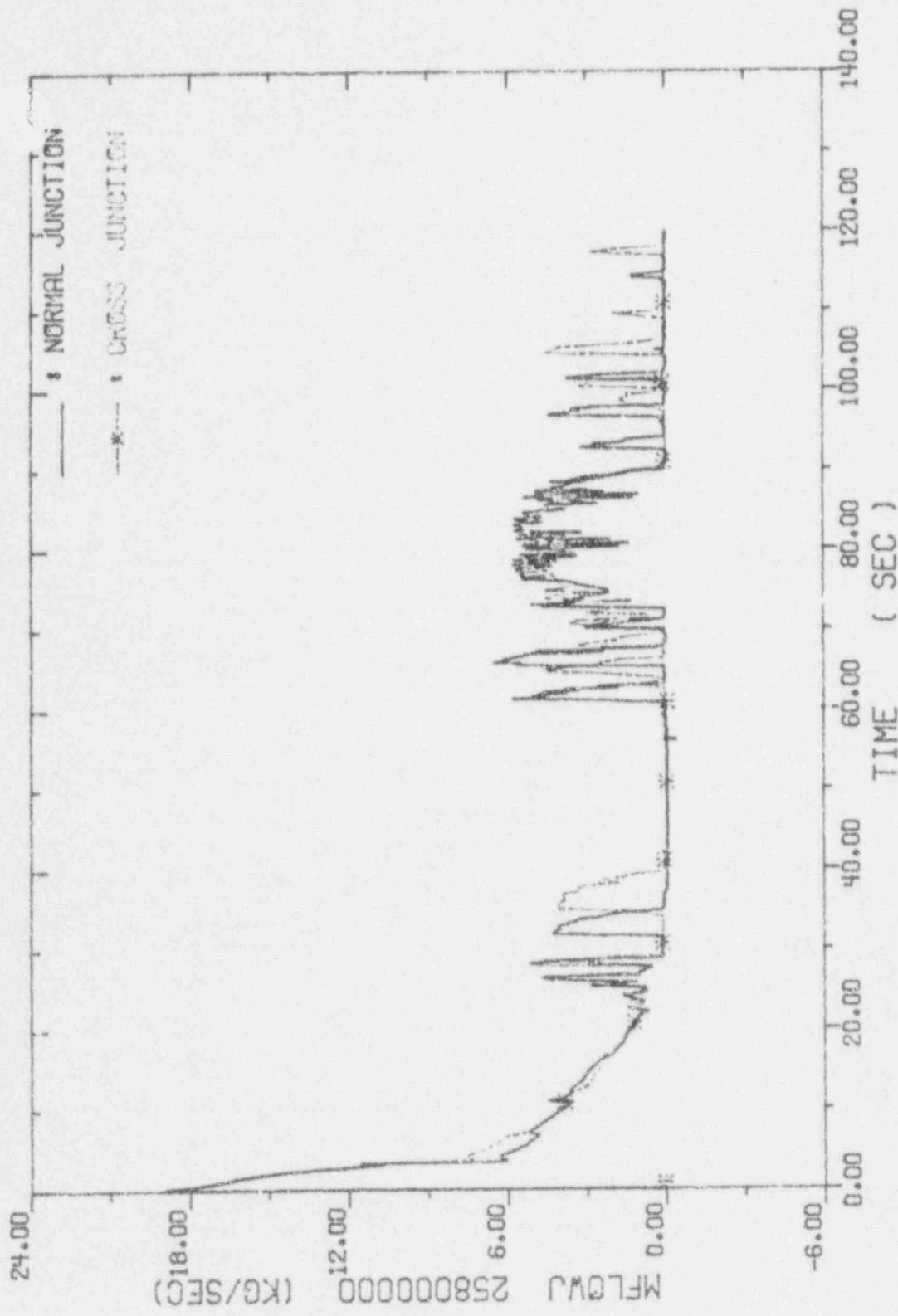


Fig. 4-65. Break Flow Rate near Vessel Side

REACTOR EXCURSION AND LEAK ANALYSIS PROGRAM : ELAP5/MOD2/36.04)

SIMULATION OF SEMISCALE S-06-3 LARGE LOCA TEST

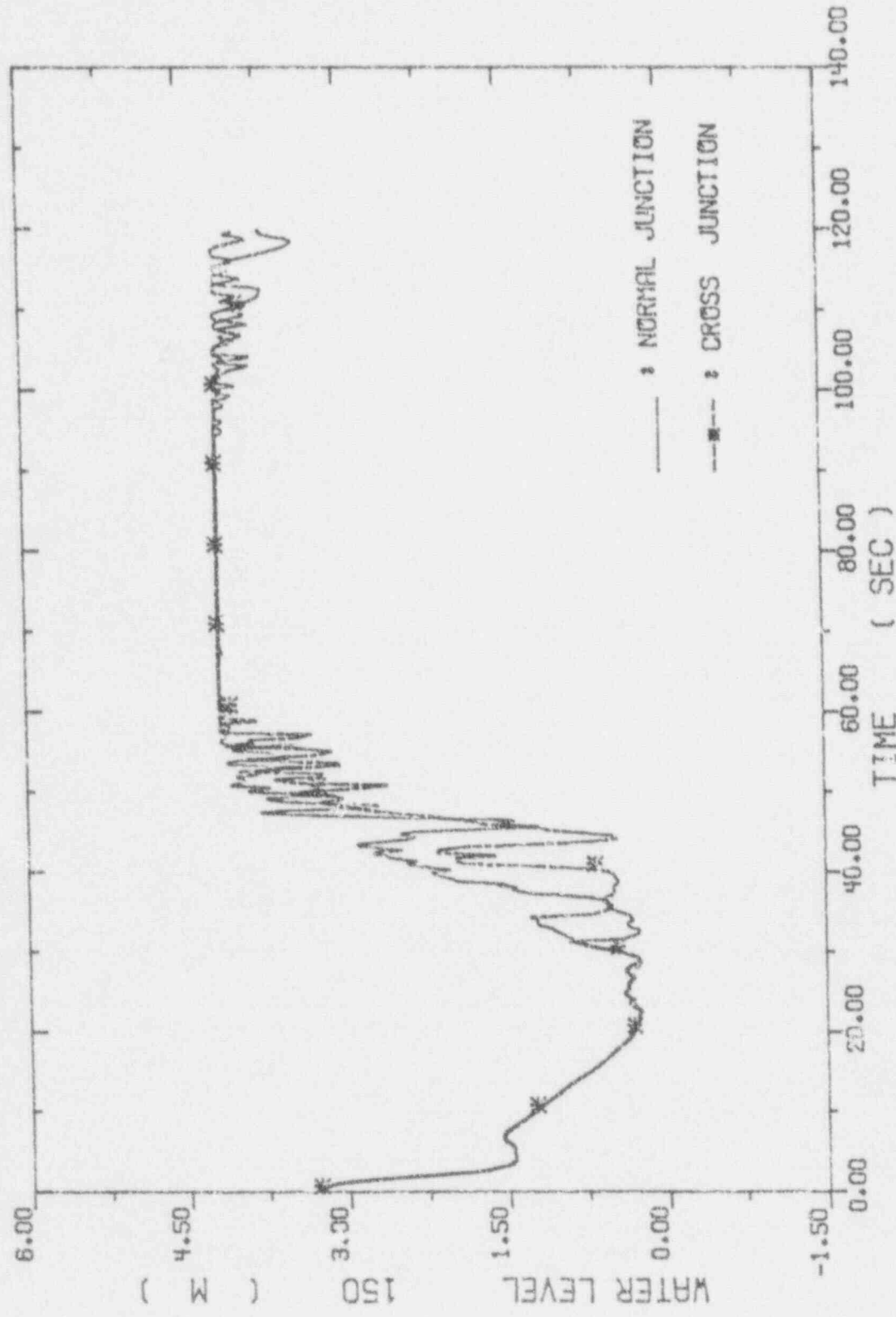


Fig. 4-66. Collapsed Water Levels across The Downcomer

REACTOR EXCURSION AND LEAK ANALYSIS PROGRAM(RELAPS/MOD2/36.04)

SIMULATION OF SEMISCALE S-06-3 LARGE LOCA TEST

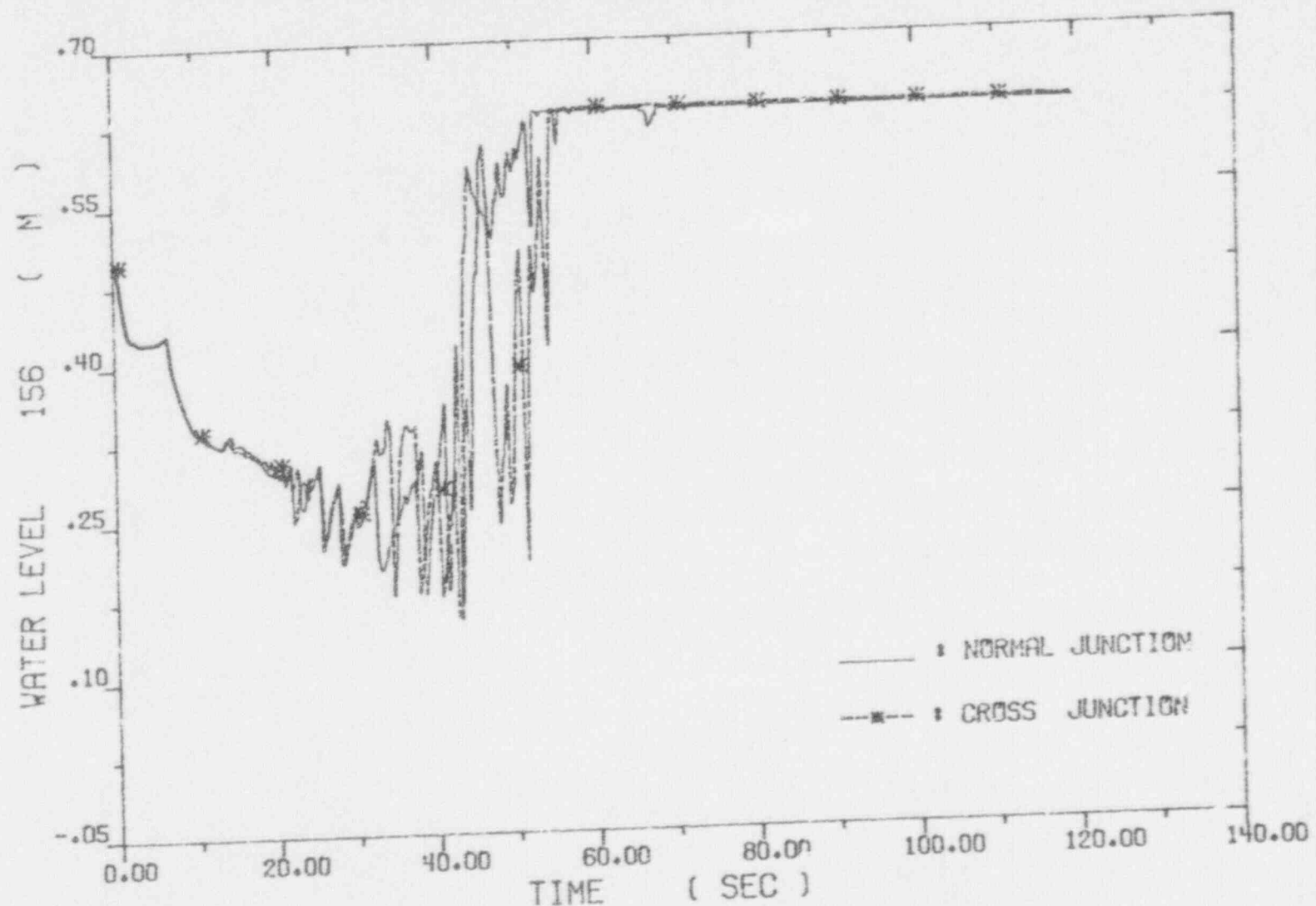


Fig. 4-67. Collapsed Water Levels across The Lower Plenum

REACTOR EXCURSION AND LEAK ANALYSIS PROGRAM (RELAP5/MOD2/36.04)

SIMULATION OF SEMISCALE S-06-3 LARGE LOCA TEST

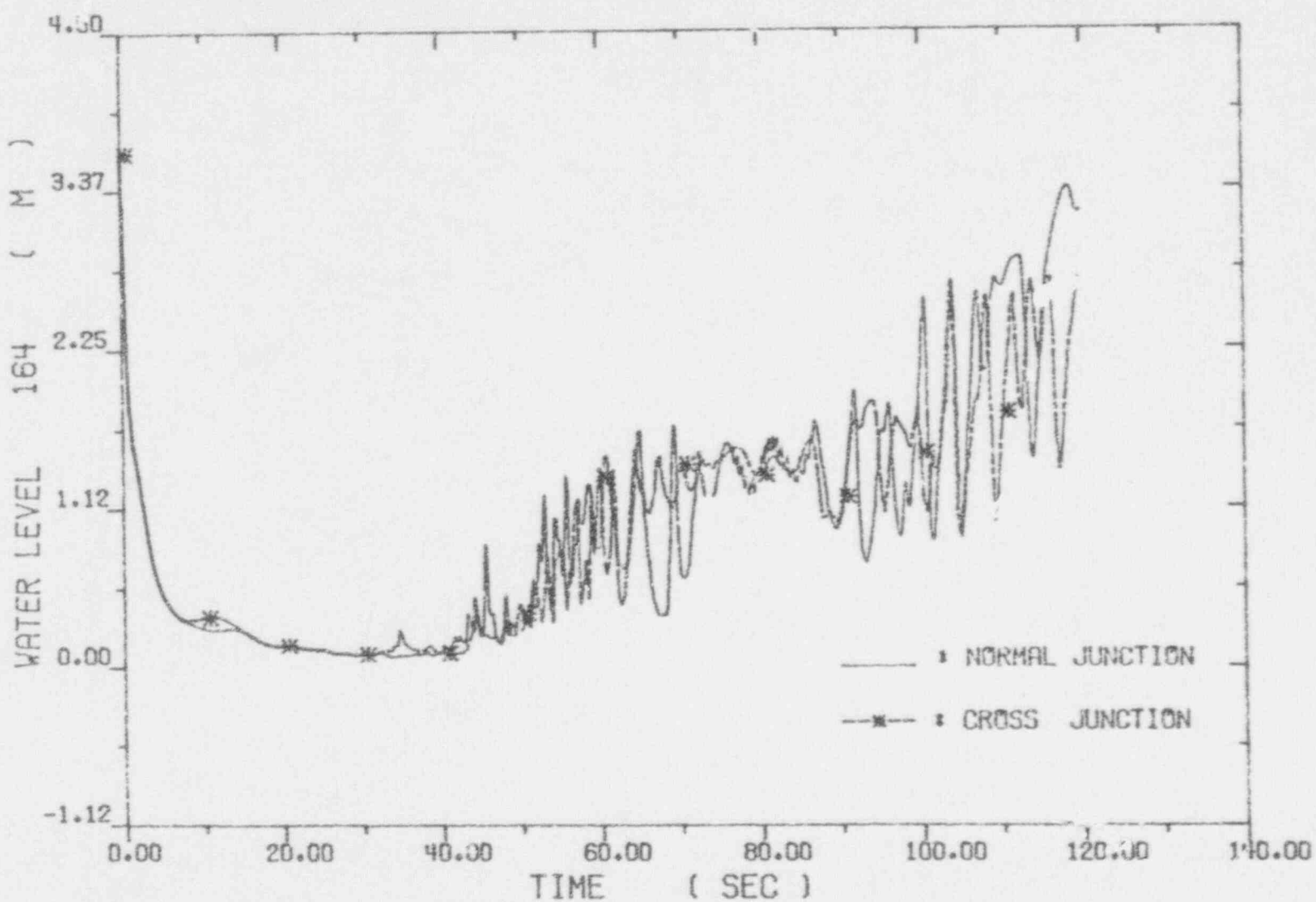


Fig. 4-68. Collapsed Water Levels across The Core

REACTOR EXCURSION AND LEAK ANALYSIS PROGRAM(RELAPS/MOD2/36.04)

SIMULATION OF SEMISCALE S-06-3 LARGE LOCA TEST

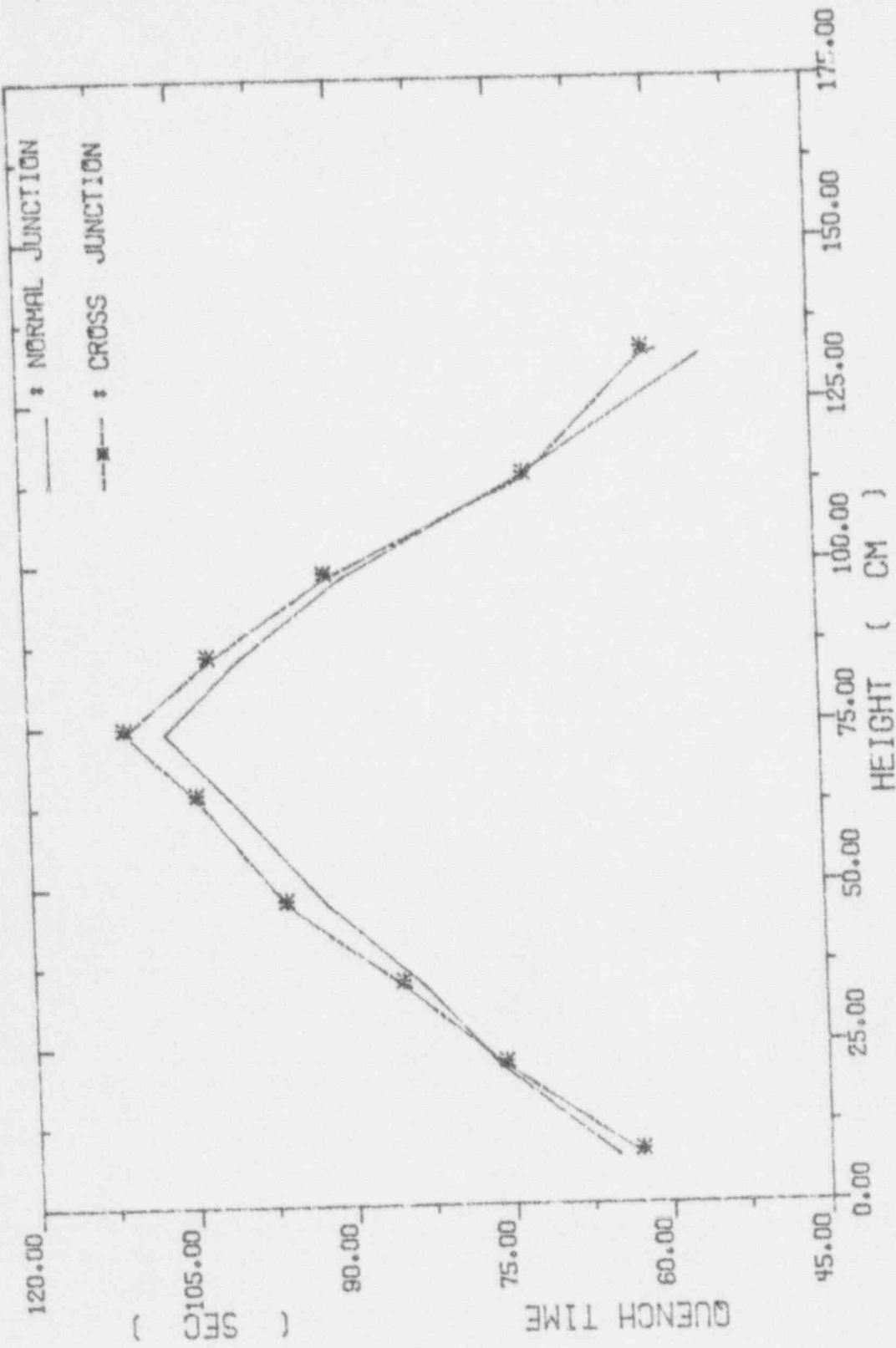


Fig. 4-69. High Power Rod Quench time versus Elevation

REACTOR EXCURSION AND LEAK ANALYSIS PROGRAM (RELAPS/MOD2/36.04)
SIMULATION OF SEMISCALE S-06-3 LARGE LOCA TEST

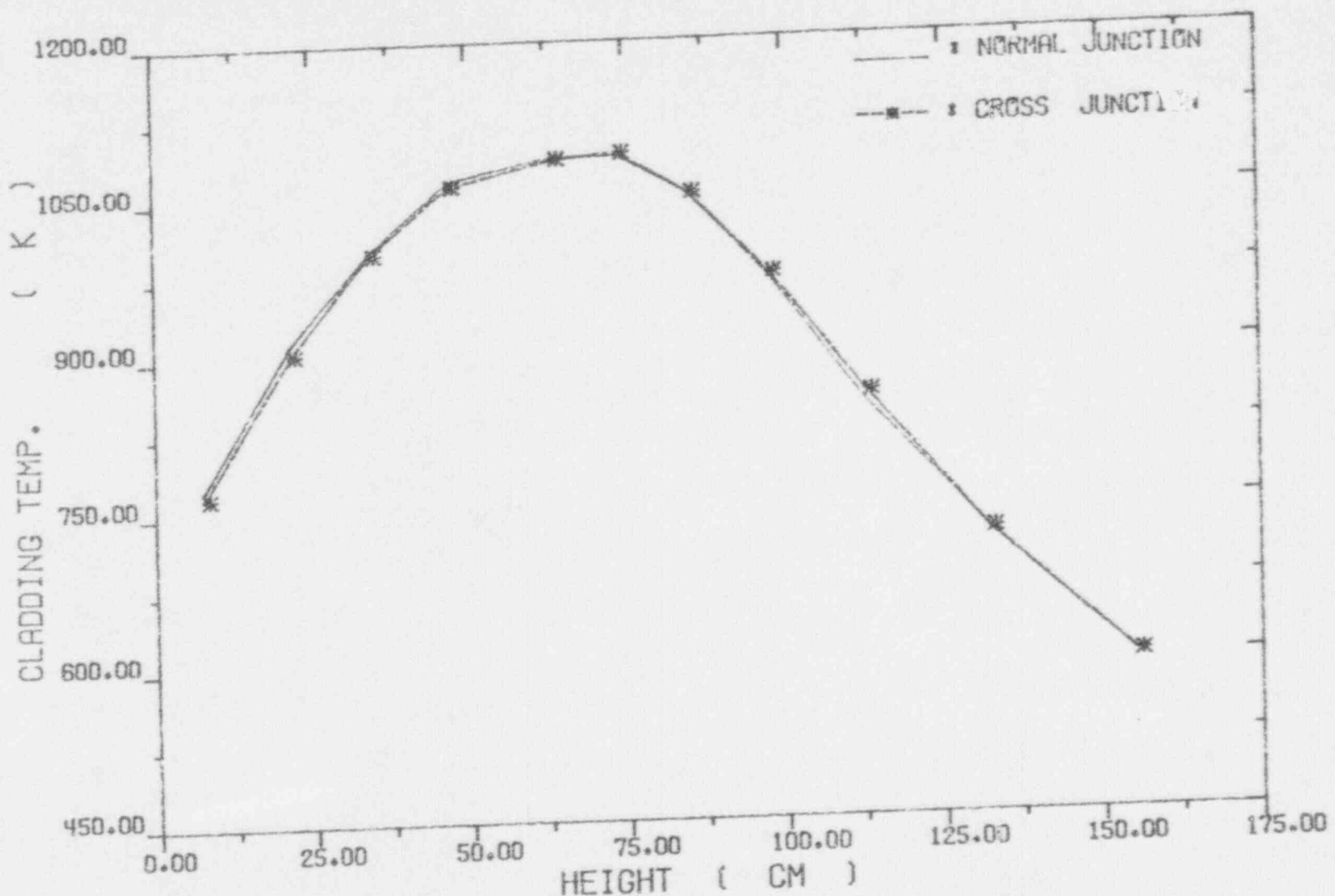


Fig. 4-70. High Power Rod Peak Cladding Temperatures
versus Elevation

REACTOR EXCURSION AND LEAK ANALYSIS PROGRAM (RELAPS/MOD2/36.04)

SIMULATION OF SEMISCALE S-06-3 LARGE LOCA TEST

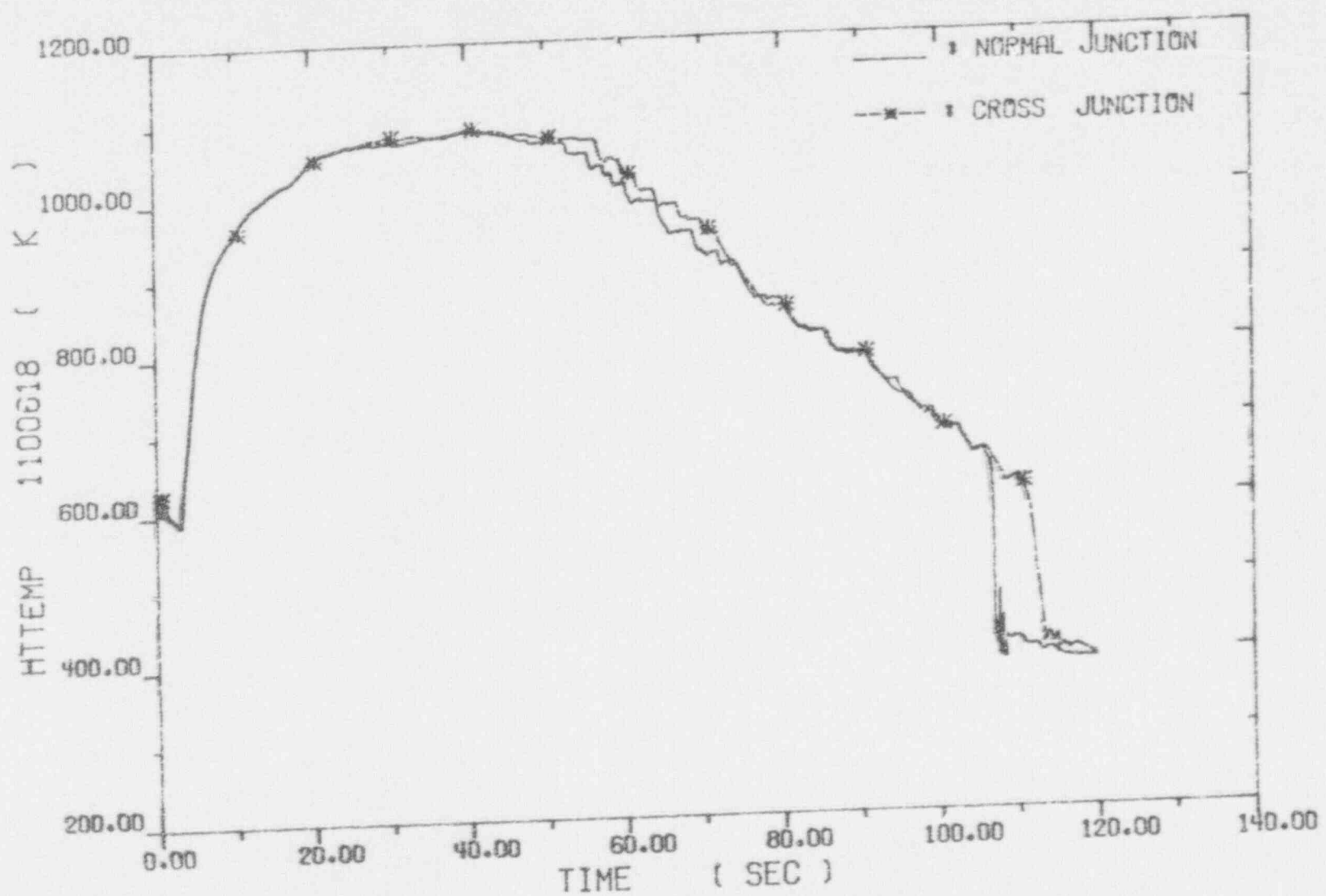


Fig. 4-71. High Power Rod Hot Spot Cladding Temperatures

REACTOR EXCURSION AND LEAK ANALYSIS PROGRAM(RELAPS/MOD2/36.04)

SIMULATION OF SEMISCALE S-06-3 LARGE LOCA TEST

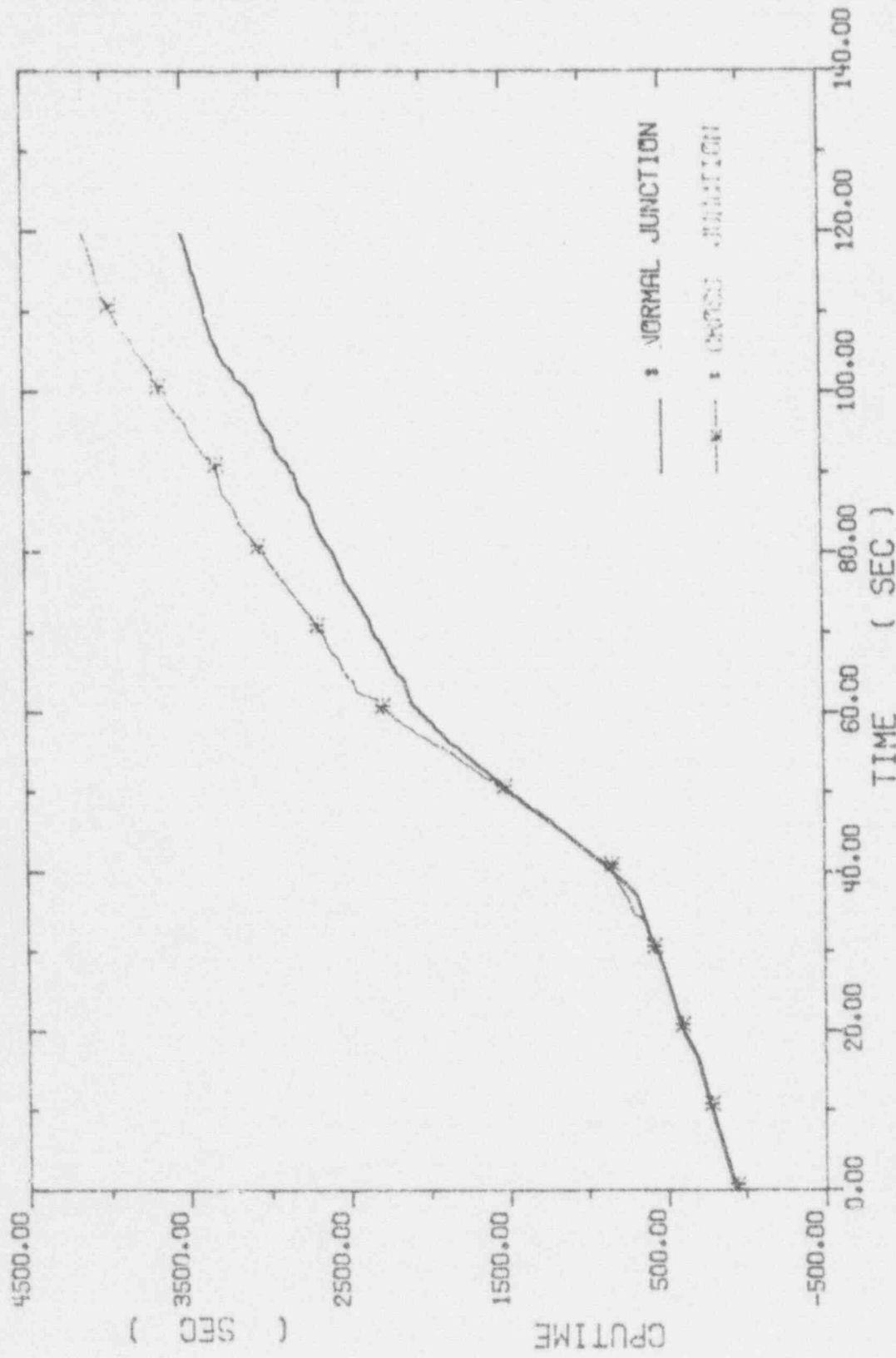


Fig. 4-72. Comparison of CPU Time

REACTOR EXCURSION AND LEAK ANALYSIS PROGRAM (RELAP5/MOD2/36.04)

SIMULATION OF SEMISCALE S-06-3 LARGE LOCA TEST

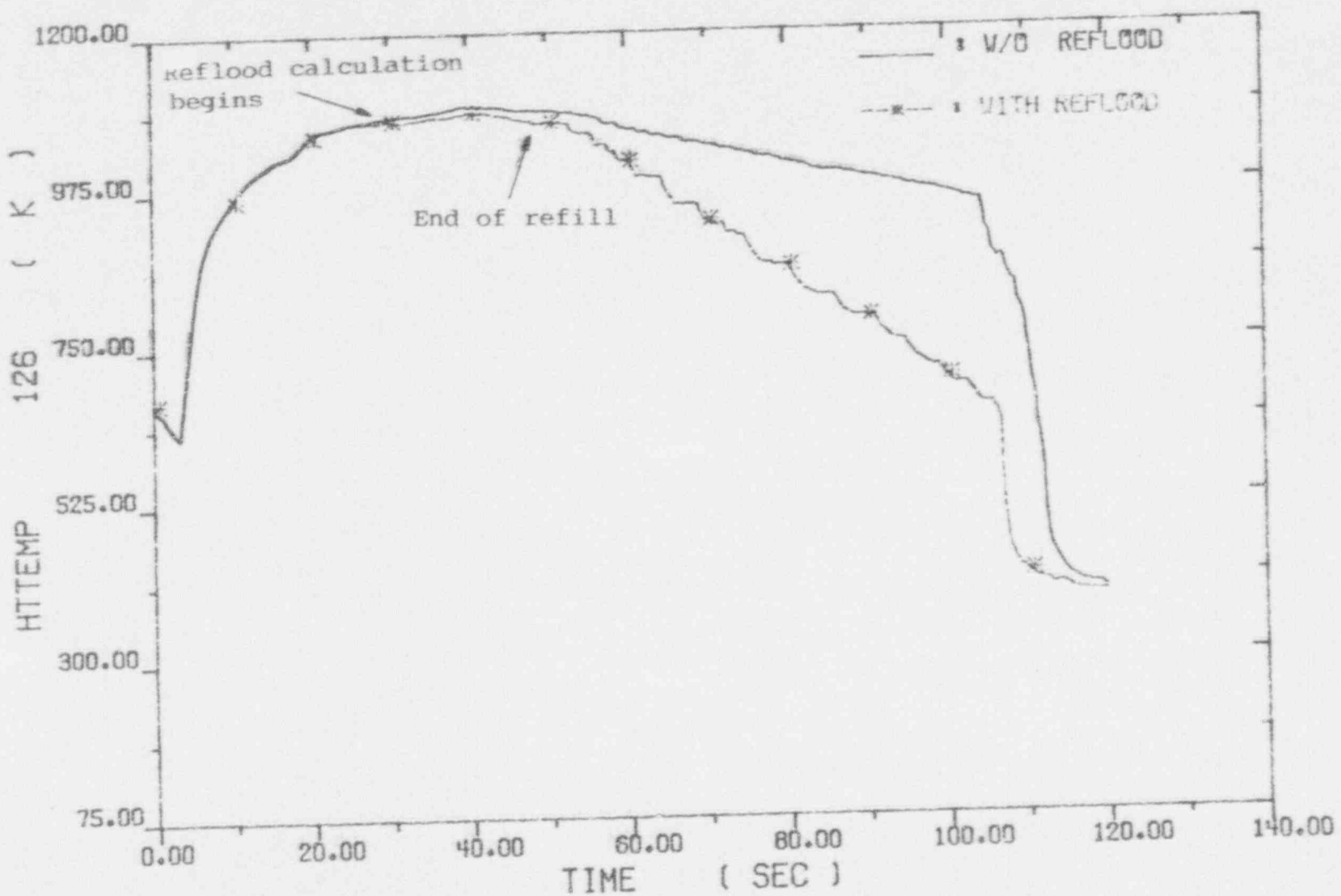


Fig. 4-73. Comparison of Peak Cladding Temperatures from with and without Reflood Calculations

REACTOR EXCURSION AND LEAK ANALYSIS PROGRAM(RELAPS/MOD2/36.04)

SIMULATION OF SEMISCALE S-06-3 LARGE LOCA TEST

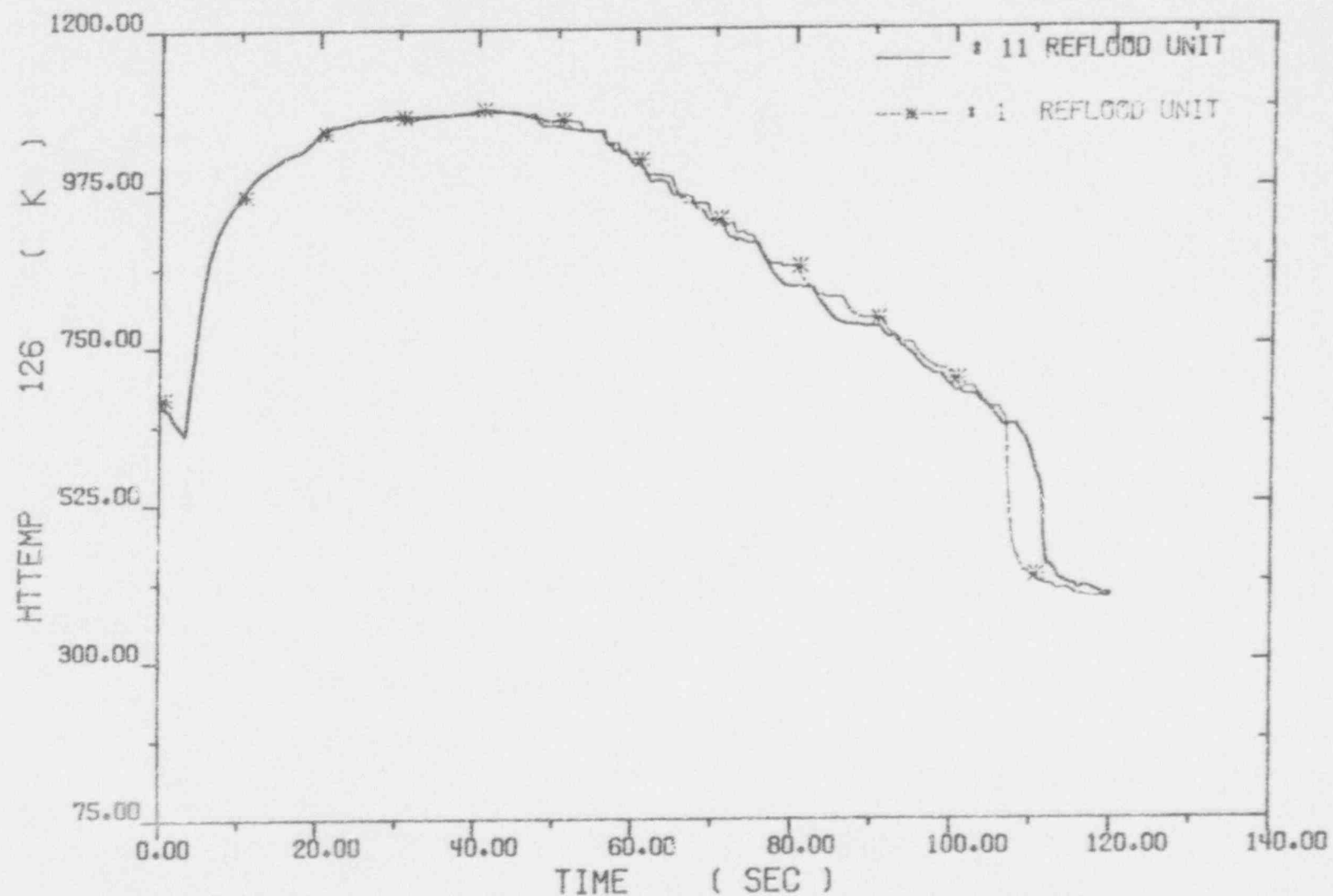


Fig. 4-74. Comparison of Peak Cladding Temperatures from 1 Reflood Unit and 11 Reflood Unit in Series

REACTOR EXCURSION AND LEAK ANALYSIS PROGRAM: RELAP5/MOD2/36.04]

SIMULATION OF SEMISCALE S-06-3 LARGE LOCA TEST

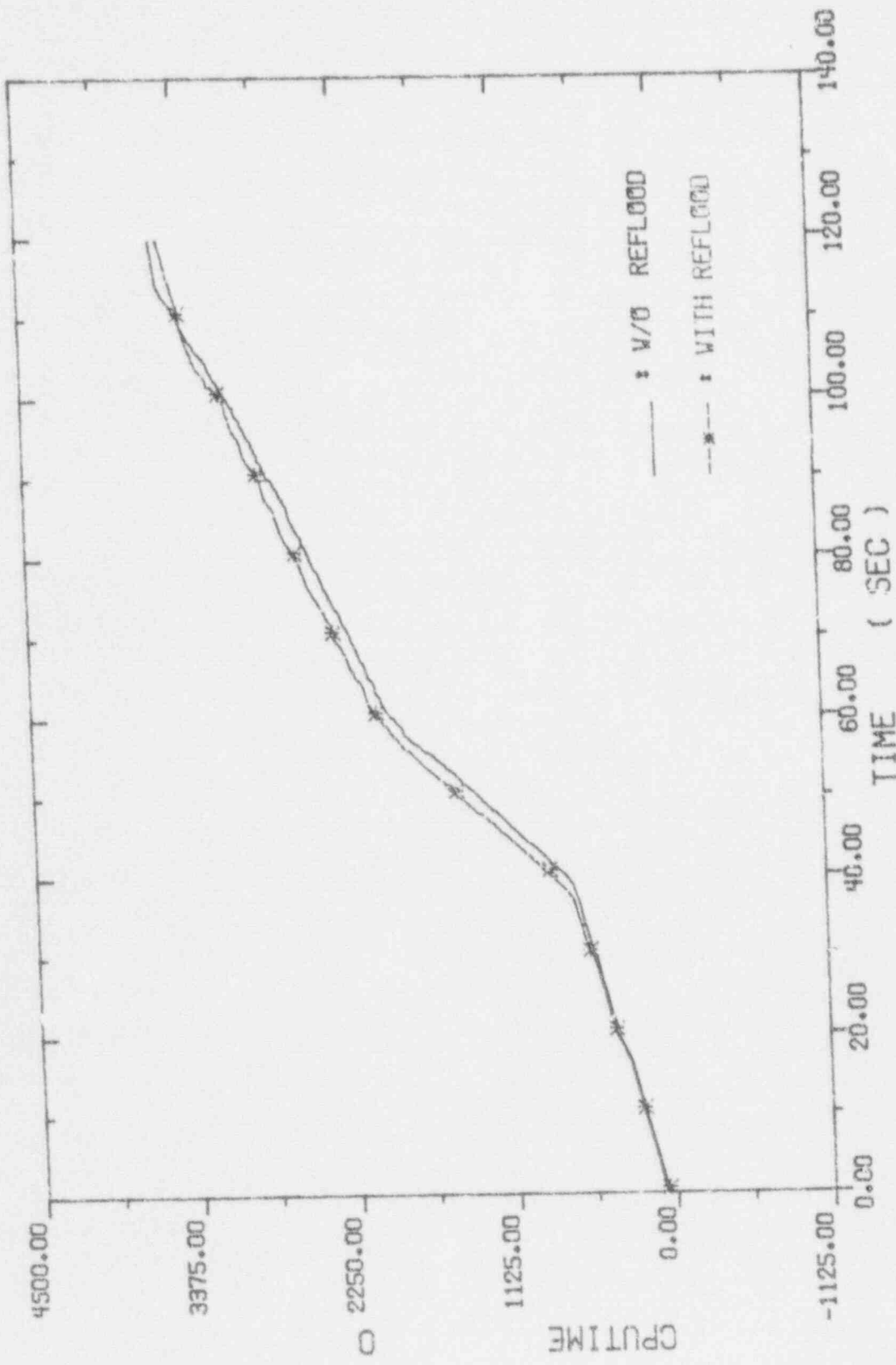


Fig. 4-75. Comparison of CPU Time

5. RUN STATISTICS

The computer run statistics of the RELAPS simulations is summarized in Table 5-1. The CPU time is for a FACOM M200 computer which is compatible to IBM MVS system. All simulations were calculated using same maximum and minumum time steps, and was 5.0×10^{-2} and 1.0×10^{-2} seconds respectively.

Table 5-1 Run Time Statistics for S-06-3 Simulations

6. CONCLUSIONS AND RECOMMENDATIONS

Generally speaking, RELAP5 calculation correctly simulates responses of vital parameters and catches associated important phenomena except the CCFL which takes place in the blowdown and refill periods and makes the latter-on consequence deviated. Through extensive comparisons with measurement and important sensitivity studies elaborated in the previous section, the following conclusions are reached with suggestions :

1. The calculated break flow rates from both sides matched the data very well especially for the break near the pump side. As for the flow from the break near the vessel side, before the accumulator injection began, it also matched the data well. However, owing to the inability to simulate CCFL and the over-estimation of liquid downflow for a given steam upflow [11], some differences appeared between the calculated and measured break flow rates after the accumulator injection. Once ECC bypass and downcomer penetration phenomena can be caught well via the installation of CCFL model and the modification of interfacial drag between vapor and liquid in the code, prediction of the break flow from the vessel side probably can be improved.
2. Pressurizer responses under large LOCA were simulated well provided the noding of pressurizer was fine enough. As revealed from our sensitivity study, if the noding is fine enough the pressure two-slope behavior resulted from the

pressurizer emptiness can even be calculated.

3. Before the accumulator injection began, water levels within the reactor vessel were predicted well. However, due to the inability to simulate ECC bypass and downcomer penetration phenomena, calculated water levels rose again earlier than what were measured. Therefore, the termination of refill phase and the begining of reflood phase were all shifted ahead in the calculation.
4. Superheated steam in the lower and upper plena was predicted reasonably well as compared to test data. Besides, core flow reversal phenomenon caused by the condensation induced from the ECC injection was also simulated, which was elucidated in the comparison of lower plenum coolant temperature responses.
5. The prediction of the highest cladding temperatures along the fuel elevations was quite well especially for the low power rods. As for the high power rods, the peak position moved a little upward and the value was lower about 30 K. Also concluded are the more effective precursor cooling prior to the quench and the earlier rewet of fuel rods in the calculation. Once the current interfacial drag model and film boiling correlation can be improved, and the CCFL model can be installed, those deficiencies probably can be diminished.
6. Whether the radial connections between the hot and average channels were milled or not almost had no effect on the

predictions of peak cladding temperatures. However, cladding temperature responses of both ends of high power rods were affected. In the base calculation in which the radial connections were simulated, both ends experienced CHF soon after breaks occurred, while in the calculation without radial connection both ends remained in the status of no temperature excursion throughout the simulation. Besides, the radial disconnection between the hot and average channels caused the lower part of high power rods rewetted a little late as compared to results with radial connections.

7. The maximum number of heat slab axial interval for 2-D reflood calculation almost had no effect on the calculation of peak cladding temperatures along the fuel. Nevertheless, it had a little effect on the calculation of fuel quench time. Generally speaking, refinement of 2-D reflood calculation made the fuel rewetted a little late. This tendency probably was resulted from the special feature of Semiscale MOD-1 system. The rewetting rate of Semiscale MOD-1 is about 1.8 cm/sec.
8. The number of axial hydraulic volumes representing the core showed some influence upon the thermal responses of fuel rods. As depicted in the previous section, the number of axial hydraulic volumes representing the core did not affect the prediction of peak cladding temperatures too much. However, it resulted in a tendency showing that except at

ends of fuel, fine noding of the core might result in a later quench, but the postponed time was only about several seconds.

9. In the base calculation, the entrances of four legs entering the vessel were modelled with normal junctions. The effect of using cross-flow junctions to replace those has been investigated. Although the replacement had no effect on the break flow calculation, the filled-up time of lower plenum was postponed a little and so was the core water level asending time. As a result, the fuel quench time was a little put off in the calculation with cross-flow junction, but the peak cladding temperature prediction was not affected at all.
10. Defeating normal reflood calculation would heavily affect the response of hot spot cladding temperature. Through sensitivity study, it was identified that different heat transfer package used majorly contributed to such difference instead of the effect of two-dimensional conduction. Since such discrepancy appears in the stage of film boiling which is not necessarily related to the reflood, it is suggested that the difference and the applicability of these two packages should be further verified.
11. Generally speaking, modelings with in-core radial connection, larger number of heat slab axial interval for 2-D reflood calculation, larger number of hydraulic volumes

representing the core, or cross-flow junctions on vessel entrances would cost more CPU time, especially for the last two modelings. Particularly the total CPU time used in the calculation with 22 axial volumes representing the core was about 3.4 times of that used in the base calculation in which only 11 axial volumes were involved.

7. REFERENCE

1. Brent L. Collins, Morris L. Patton, Jr. et. al., "Experiment Data Report for Semiscale Mod-1 Test S-06-3 (LOFT Counterpart test)," NUREG/CR-0251, TREE-1123, July 1987
2. V. Ransom et. al., "RELAP5/MOD2 Code Manual," NUREG/CR-4312, EGG-2396, August 1985
3. E. M. Feldman and D. J. Olson, "Semiscale Mod-1 Program and System Description for the Blowdown Heat Transfer Tests (Test Series 2)," ANCR-1230, August 1975
4. C. G. Branson Ltr to L. P. Leach, "Transmittal of Configuration Control Writeup for LOFT Simplified Hot Pin Model," CGB-8-75, October 2, 1975
5. L. E. Hochreiter, K. Riedle, "Reflood Heat Transfer and Hydraulics in Pressurizer Water Reactors," Symposium on the Thermal and Hydraulic Aspects of Nuclear Reactor Safety, Atlanta, U. S., Nov. 1977
6. G. G. Loomis, "Summary of the Semiscale Program (1965-1986)," NUREG/CR-4945, EGG-2509, July 1987
7. U. S. Nuclear Regulatory Commission, "Compendium of ECCS Research for Realistic LOCA Analysis," NUREG-1230, April 1987
8. Private Communication, "Code Improvement Plan for TRAC-PF1 and RELAP5," U.S. Nuclear Regulatory Commision, November 1987
9. Yassin A. Hassan, "Analysis of Flecht and Flecht-Seaset Reflood Tests with RELAPS/MOD2," Nuclear Technology, Vol. 74 Aug. 1986

10. George E. Forsythe, Michael A. Malcolm, and Cleve B. Moler,
Computer Methods for Mathematical Computations, Prentice-Hall, Inc. 1987
11. M. Dillistone & C. G. Richards, "Counter-Current Flow Modelling in RELAP5," Third International Code Assessment and Application Program (ICAP) Specialist Meeting, Grenoble, France, March 1988

APPENDIX A

INPUT DATA LISTING

*
886 CIRCUIT TEMPERATURES IN LOOPS (K)

*
316 TEMPF 214010000 * PL = COLD LEG
317 TEMPF 201010000 * PL = HOT LEG
*
318 TEMPF 112010000 * IL = COLD LEG
319 TEMPF 101010000 * IL = HOT LEG
*

*
888 COOLANT TEMPERATURE IN VESSEL (K)

*
320 TEMPF 007010000 * CORE INLET
321 TEMPF 029010000 * UPPER PLN.
*
322 TEMPF 002010000 * DEC. 1
323 TEMPF 003010000 * DEC. 2
324 TEMPF 004010000 * DEC. 3
325 TEMPF 004020000 * DEC. 4
326 TEMPF 004030000 * DEC. 4
*

*
890 PEAK CLADDING TEMPERATURES (HOT CHANNEL) (K)

*
327 CNTRLVAR 122 * DEC. 2
328 CNTRLVAR 123 * DEC. 3
329 CNTRLVAR 124 * DEC. 4
330 CNTRLVAR 126 * DEC. 5
331 CNTRLVAR 128 * DEC. 7
332 CNTRLVAR 130 * DEC. 9
*

*
898 PEAK CLADDING TEMPERATURES (AVERAGE CHANNEL) (K)

*
333 CNTRLVAR 133 * DEC. 3
334 CNTRLVAR 136 * DEC. 5
335 CNTRLVAR 138 * DEC. 7
*

*
899 DIFFERENTIAL PRESSURE

*
336 CNTRLVAR 141 * ACROSS DOWNCOMER
337 CNTRLVAR 142 * ACROSS LOK PLN.
338 CNTRLVAR 143 * ACROSS CRP
*

*
***** HYDRAULIC MODELING *****
***** REACTOR VESSEL *****

*

0010000 UPPER BRANCH

0010001 1 0
0010101 0.110896 0.0 0.032404 0.0 90. 0.2922 0.0 0.2153 0
0010200 3 2291.1 556.07
0011101 001000000 002000000 0.110896 0.0 0.0 01000
0011201 -4.5404e-9 -4.6086e-9 0.0
*

***** DOWNCOMER *****

* 0020000 DCH-1 ANNULUS

0020001 1
0020101 0.110896 1
0020301 0.0 1
0020401 0.0363961 1
0020501 0.0 1
0020601 -90.0 1
0020701 -0.3382 1
0020801 0.0 0.2153 1
0031001 0.0 1
0021201 3 2291.2 553.72 0.0 0.0 0.0 1

*

* 0510000 DCH-2 SNGLJUN

0510101 002010000 003000000 0.110896 0.0 0.0 01000
0510201 0 2.1277 2.1277 0.0

*

* 0030000 DCH-2 ANNULUS

0030001 1
0030101 0.110896 1
0030301 0.0 1
0030401 0.1032 1
0030501 0.0 1
0030601 -90.0 1
0030701 -0.9306 1
0030801 0.0 0.2153 1
0031001 0.0 1
0031201 3 2291.4 553.72 0.0 0.0 0.0 1

*

* 0520000 DCH-3 SNGLJUN

0520101 003010000 004000000 0.0583 1.5 1.5 01000
0520201 0 4.0473 4.0473 0.0

*

* 0040000 DCH-3 ANNULUS

0040001 3
0040101 0.0583 3
0040201 0.0583 2
0040301 0.0 1
0040401 0.258 3
0040501 0.0 3
0040601 -90.0 3
0040701 -4.19 3
0040801 0.0 0.078 3
0040901 0.3 0.3 2
0041001 0 3
0041101 01000 2
0041201 3 2292.0 553.73 0.0 0.0 0.0 1
0041202 3 2293.3 553.75 0.0 0.0 0.0 2
0041203 3 2294.5 553.76 0.0 0.0 0.0 3
0041300 0
0041301 4.0473 4.0473 0.0 1
0041302 4.0473 4.0473 0.0 2

*

* 0050000 LPLNUM-1 SNGLVOL

0050101 0.138779 0.0 0.2324 0.0 90. 1.6746 0.0 0.5508 0
0050200 3 2295.7 256.08

*

0060000 LFLNUM=2 BRANCH
 0060001 3 0
 0060101 0.2383 0.0 0.5306 0.0 90. 0.7333 0.0 0.5508 0
 0060200 3 2295.3 553.77
 0061001 006010000 007000000 0.03142 0.1697 0.3144 01000
 0061201 7.5096 7.5096 0.0
 0062101 005010000 006000000 0.2383 0.0 0.0 01000
 0062201 3.46981-5 3.52281-9 0.0
 0063101 00-0100000 006010000 0.0583 1.5 1.5 01000
 0063201 4.0472 4.0472 0.0
 *
 0070000 LFLNUM=3 BRANCH
 0070001 4 0
 0070101 0.0687 0.0 0.1310 0.0 90. 1.777 0.0 0.3053 0
 0070200 3 2294.7 553.76
 0071001 007010000 018000700 0.00231 1.25 1.25 01000
 0071201 10.101 10.101 0.0
 0072101 007010000 008000000 0.02106 1.25 1.25 01000
 0072201 10.081 10.081 0.0
 *
 ***** REACTOR CORE *****

 *
 888 AVERAGE CHANNEL
 *
 0080000 AVG-1 BRANCH
 0080001 1 0
 0080101 0.046251 0.0 0.0231255 0.0 90. 0.500 0.0 0.0352 0
 0080200 3 2293.7 557.19
 0081101 008010000 009000000 0.046251 0.000 0.000 01000
 0081201 4.5950 4.5950 0.0
 *
 0080000 AVG-2 BRANCH
 0080001 1 0
 0080101 0.046251 0.0 0.01928667 0.0 90. 0.417 0.0 0.0352 0
 0080200 3 2293.5 562.05
 0081101 009010000 010000000 0.046251 0.189 0.189 01000
 0081201 4.6236 4.6236 0.0
 *
 0100000 AVG-3 BRANCH
 0100001 1 0
 0100101 0.046251 0.0 0.01928667 0.0 90. 0.4165 0.0 0.0352 0
 0100200 3 2293.3 568.24
 0101101 010010000 011000000 0.046251 0.000 0.000 01000
 0101201 4.7547 5.0434 0.0
 *
 0110000 AVG-4 BRANCH
 0110001 1 0
 0110101 0.046251 0.0 0.01928667 0.0 90. 0.4165 0.0 0.0352 0
 0110200 0 2293.2 569.86 1049.2 7.3050-4
 0111101 011010000 121000000 0.046251 0.189 0.189 01000
 0111201 4.7052 5.2194 0.0
 *
 1210000 AVG-5 BRANCH
 1210001 1 0
 1210101 0.046251 0.0 0.0241431 0.0 90. 0.522 0.0 0.0352 0
 1210200 0 2293.0 581.70 1049.3 2.7016-3
 1211101 121010000 122000000 0.046251 0.000 0.000 01000
 1211201 4.7808 5.2677 0.0
 *
 1220000 AVG-5 BRANCH

0230200 0 2292.7 627.67 1049.3 6.6750E-2
 0231101 023010000 024000000 5.139E-3 0.189 0.189 01000
 0231201 5.0319 6.5635 0.0
 *
 7230000 HDT-6 SNGLJUN
 7230101 023000000 013000000 0.0 0.0 0.0 01003
 7230201 0 0.12113 0.12114 0.0
 *7230300 TRPVLV
 *7230301 502
 *
 0240000 HDT-7 BRANCH
 0240001 1 0
 0240101 5.139E-3 0.0 2.142063E-3 0.0 00. 0.417 0.0 0.0465 0
 0240200 0 2292.5 636.62 1049.3 8.791E-1
 0241101 024010000 025000000 5.139E-3 0.000 0.000 01000
 0241201 6.4234 7.0303 0.0
 *
 7240000 HDT-7 SNGLJUN
 7240101 024000000 014000000 0.0 0.000 0.000 01003
 7240201 0 -0.26137 -0.26137 0.0
 *7240300 TRPVLV
 *7240301 502
 *
 0250000 HDT-8 BRANCH
 0250001 1 0
 0250101 5.139E-3 0.0 2.996037E-3 0.0 00. 0.583 0.0 0.0465 0
 0250200 0 2292.3 647.23 1049.3 0.10824
 0251101 025010000 026000000 5.139E-3 0.189 0.189 01000
 0251201 6.4754 7.5740 0.0
 *
 7250000 HDT-8 SNGLJUN
 7250101 025000000 015000000 0.0 0.0 0.0 01003
 7250201 0 0.17333 -0.17334 0.0
 *7250300 TRPVLV
 *7250301 502
 *
 0260000 HDT-9 BRANCH
 0260001 0
 0260101 5.139E-3 0.0 3.427713E-3 0.0 00. 0.667 0.0 0.0465 0
 0260200 0 2292.1 651.37 1049.3 0.10184
 0261101 026010000 027000000 5.139E-3 0.000 0.000 01000
 0261201 7.3318 8.8039 0.0
 *
 7260000 HDT-9 SNGLJUN
 7260101 026000000 016000000 0.0 0.000 0.000 01003
 7260201 0 -0.74936 -0.74840 0.0
 *7260300 TRPVLV
 *7260301 502
 *
 0270000 HDT-10 BRANCH
 0270001 1 0
 0270101 5.139E-3 0.0 4.280787E-3 0.0 00. 0.533 0.0 0.0465 0
 0270200 0 2291.8 655.73 1049.3 8.7247E-2
 0271101 027010000 028000000 5.139E-3 5.48 5.48 01000
 0271201 5.0912 8.0134 0.0
 *
 7270000 HDT-10 SNGLJUN
 7270101 027000000 017000000 0.0 0.0 0.0 01003
 7270201 0 1.2947 1.2948 0.0
 *7270300 TRPVLV
 *7270301 502
 *

00000 BREAK VALVE NEAR VESSEL

0

25F0000 BREAK VALVE

25F0101 211010000 210000000 0.00262 0.053 0.053 00000

25F0201 1.0.0 0.0 0.0

25F0300 TRPVLV

25F0301 402

0

00000 BREAK VALVE NEAR PUMP

0

2570000 BREAK VALVE

2570101 20F010000 209000000 0.00262 0.053 0.053 00000

2570201 1.0.0 0.0 0.0

2570300 TRPVLV

2570301 402

0

00000 ISOLATED CONTAINMENT 00000

00000 ISOLATED CONTAINMENT 00000

0

2100000 FIRE-SUPP TMDPVOL

2100101 7.79 0.0 1.1+2 0.0 -90. -8.3 0.0 3.4 0

2100200 2 402

2100201	-1.00000	35.7617	1.0
2100202	0.00000	35.7617	1.0
2100203	0.684931	27.7347	1.0
2100204	5.342465	40.3288	1.0
2100205	7.534246	35.0697	1.0
2100206	9.726027	36.0385	1.0
2100207	10.54794	35.0697	1.0
2100208	12.46575	36.7305	1.0
2100209	13.56164	34.9313	1.0
2100210	15.20547	36.4537	1.0
2100211	16.84931	35.0697	1.0
2100212	17.94520	35.6233	1.0
2100213	19.04109	35.9001	1.0
2100214	20.13692	34.5161	1.0
2100215	21.23217	34.9313	1.0
2100216	24.24657	34.7929	1.0
2100217	26.71232	35.4849	1.0
2100218	29.17808	34.1010	1.0
2100219	30.00000	34.9313	1.0
2100220	30.54794	35.2081	1.0
2100221	34.10958	34.6545	1.0
2100222	36.84931	34.9313	1.0
2100223	37.67123	34.6545	1.0
2100224	39.04109	34.7929	1.0
2100225	39.58904	34.1010	1.0
2100226	40.41095	34.7929	1.0
2100227	49.45205	34.7929	1.0
2100228	500.0000	34.7929	1.0

0

2090000 FIRE-SUPP TMDPVOL

2090101 7.79 0.0 1.1+2 0.0 -90. -9.058 0.0 3.4 0

2090200 2 402

2090201	-1.00000	35.7617	1.0
2090202	0.00000	35.7617	1.0
2090203	0.684931	27.7347	1.0
2090204	5.342465	40.3288	1.0
2090205	7.534246	35.0697	1.0
2090206	9.726027	36.0385	1.0
2090207	10.54794	35.0697	1.0

2090208	12.46575	36.7305	1.0
2090209	13.56164	34.9313	1.0
2090210	15.20547	36.4537	1.0
2090211	16.84931	35.0697	1.0
2090212	17.94520	35.6230	1.0
2090213	19.04109	35.9001	1.0
2090214	20.13698	34.5161	1.0
2090215	21.23287	34.9313	1.0
2090216	24.24657	34.7929	1.0
2090217	26.71232	35.4849	1.0
2090218	29.17808	34.1010	1.0
2090219	30.00000	34.9313	1.0
2090220	30.54794	35.2081	1.0
2090221	34.10953	34.6545	1.0
2090222	36.84931	34.9313	1.0
2090223	37.67123	34.6545	1.0
2090224	39.04109	34.7929	1.0
2090225	39.55904	34.1710	1.0
2090226	40.41095	34.7929	1.0
2090227	49.45205	34.7929	1.0
2090228	500.0000	34.7929	1.0

b

oooooooooooooo PRESSURIZER ooooooooooooooo
oooooooooooooo PRESSURIZER SURGE LINE ooooooooooooooo
b

b

ooooo PRESSURIZER SURGE LINE oooooo
b
ooooo PRZ SURGE LINE oooooo
b

1140000	SUR-LINE PIPE						
1140001	3						
1140101	0.0030	3					
1140201	0.0030	2					
1140301	0.0	3					
1140401	0.004333333	3					
1140501	0.0	3					
1140601	-90.0	1					
1140602	0.0	2					
1140603	90.0	3					
1140701	-0.6963	1					
1140702	0.0	2					
1140703	0.6963	3					
1140801	0.0 0.0613	3					
1140901	0.0 0.0	2					
1141001	0	3					
1141101	01000	?					
1141201	0	2287.4	626.78	1049.6	2.3130-9	0.0	1
1141202	3	2287.5	617.74	0.0	0.0	0.0	2
1141203	3	2287.4	625.98	0.0	0.0	0.0	3
1141300	0						
1141301	2.2406-2	2.2381-2	0.0	1			
1141302	2.2406-2	2.2406-2	0.0	2			

c

ooooo PRZ ISOLATION VALVE (36.0 SEC CLOSED)

c

1580000	TO/PRESS VALVE						
1580101	113000000 114010000	0.003	486.0	486.0	01000		
1580201	0	-2.2388-2	-2.2388-2	0.0			
1580300	TRPVLV						

3530222	22.7825012	3.07957840	0.0	0.0
3530223	24.1737976	3.24961567	0.0	0.0
3530224	25.5650940	3.39359951	0.0	0.0
3530225	26.9564056	3.40354824	0.0	0.0
3530226	28.3477020	3.38010406	0.0	0.0
3530227	29.7389984	3.47554111	0.0	0.0
3530228	30.7823944	3.39810085	0.0	0.0
3530229	32.1737051	3.47435570	0.0	0.0
3530230	32.8694000	3.36234188	0.0	0.0
3530231	33.5650024	3.26429939	0.0	0.0
3530232	34.2606964	3.32018757	0.0	0.0
3530233	35.3041992	3.36281400	0.0	0.0
3530234	35.9998016	3.46133327	0.0	0.0
3530235	37.7389069	3.46441078	0.0	0.0
3530236	38.4347008	3.45043755	0.0	0.0
3530237	39.1302032	3.45706940	0.0	0.0
3530238	40.1737061	3.39310085	0.0	0.0
3530239	41.9127960	3.42699528	0.0	0.0
3530240	42.6085052	3.43291187	0.0	0.0
3530241	43.3040924	3.41609659	0.0	0.0
3530242	43.6519928	3.39218044	0.0	0.0
3530243	44.3475952	3.37299919	0.0	0.0
3530244	46.0867004	3.39199904	0.0	0.0
3530245	46.7823944	3.36329079	0.0	0.0
3530246	48.1737061	3.36196856	0.0	0.0
3530247	49.9127960	3.34126472	0.0	0.0
3530248	50.9562988	3.32350540	0.0	0.0
3530249	51.6519012	3.31663704	0.0	0.0
3530250	52.3475952	3.25482559	0.0	0.0
3530251	53.7389069	3.23422146	0.0	0.0
3530252	54.0867004	3.22332859	0.0	0.0
3530253	54.4344940	3.20414829	0.0	0.0
3530254	54.7823944	3.19798946	0.0	0.0
3530255	55.4779968	3.1851852	0.0	0.0
3530256	55.8258057	3.20201588	0.0	0.0
3530257	56.8692932	3.14494228	0.0	0.0
3530258	57.5650024	3.12002300	0.0	0.0
3530259	57.9127960	3.11747169	0.0	0.0
3530260	58.9562988	3.08573723	0.0	0.0
3530261	59.9996948	3.06750202	0.0	0.0
3530262	61.7389069	3.02795219	0.0	0.0
3530263	63.4779968	3.00687790	0.0	0.0
3530264	64.1735992	3.00166798	0.0	0.0
3530265	64.5214996	2.98627567	0.0	0.0
3530266	64.8692932	2.99266911	0.0	0.0
3530267	66.2606049	2.97774982	0.0	0.0
3530268	67.6519012	2.99195862	0.0	0.0
3530269	67.9996948	2.67698956	0.0	0.0
3530270	68.6954041	2.27037334	0.0	0.0
3530271	69.0431976	2.64999104	0.0	0.0
3530272	69.3910065	2.53324127	0.0	0.0
3530273	69.7388000	3.10752487	0.0	0.0
3530274	70.4344940	3.83242512	0.0	0.0
3530275	70.7823029	4.10832024	0.0	0.0
3530276	71.4779968	4.72451782	0.0	0.0
3530277	71.8258057	5.31372261	0.0	0.0
3530278	72.5213928	5.95005512	0.0	0.0
3530279	72.8692932	6.12885094	0.0	0.0
3530280	73.5648956	6.81941414	0.0	0.0
3530281	73.9127045	7.12348747	0.0	0.0
3530282	74.6083984	7.85857010	0.0	0.0
3530283	74.9562073	8.08710098	0.0	0.0

3520231	212.347107	0.689884484	0.0	0.0
3520232	212.694901	0.610256596	0.0	0.0
3520233	213.390594	0.6899106584	0.0	0.0
3520234	214.173203	0.690188825	0.0	0.0
3520235	216.520996	0.689749241	0.0	0.0
3520236	217.912292	0.691203773	0.0	0.0
237	216.607895	0.690899312	0.0	0.0
238	218.755795	0.688971221	0.0	0.0
3520240	219.651398	0.689952135	0.0	0.0
3520240	219.999207	0.689985812	0.0	0.0
3520241	221.042692	0.691305220	0.0	0.0
3520242	221.390503	0.688768089	0.0	0.0
3520243	222.434006	0.691914022	0.0	0.0
3520244	222.781799	0.659140320	0.0	0.0
	223.825302	0.690459371	0.0	0.0
	224.175094	0.689850569	0.0	0.0
	227.651395	0.694180489	0.0	0.0
	228.347000	0.690662503	0.0	0.0
	300.000000	0.693233192	0.0	0.0

L P I S P S O L T M D P V O

1.0 0.0 1.44 0.0 0.0 0.0 0.0 0.0 1.0 0

1
0.0 85.0 0.0

HIGH PRESSURE INJECTION

3510000 HPJS TMDP JUN

3510101 301000000 112000000 0.00499

3510200 1 402 * 405

3510201	0.0	0.0	0.0	0.0
3510202	0.173799992	0.528852269E-01	0.0	0.0
3510203	0.869499981	0.218777098E-01	0.0	0.0
3510204	1.21725042	0.219791532E-01	0.0	0.0
3510205	1.91000011	0.319373980E-01	0.0	0.0
3510206	2.26000000	0.298240146E-01	0.0	0.0
3510207	2.95634492	0.392074399E-01	0.0	0.0
3510208	3.30430031	0.389030986E-01	0.0	0.0
3510209	3.99909986	0.359781832E-01	0.0	0.0
3510210	4.3470012	0.399175324E-01	0.0	0.0
3510211	5.0433998	0.408135951E-01	0.0	0.0
3510212	6.08689976	0.399682447E-01	0.0	0.0
3510213	6.78250027	0.402387679E-01	0.0	0.0
3510214	7.47819996	0.408305116E-01	0.0	0.0
3510215	8.52130977	0.330233587E-01	0.0	0.0
3510216	8.86050016	0.291477405E-01	0.0	0.0
3510217	10.2608004	0.277051695E-01	0.0	0.0
3510218	10.6085997	0.215395652E-01	0.0	0.0
3510219	12.3477001	0.218438953E-01	0.0	0.0
3510220	13.3912001	0.229090378E-01	0.0	0.0
3510221	13.7390003	0.228245035E-01	0.0	0.0
3510222	14.4347000	0.250900462E-01	0.0	0.0
3510223	15.1302996	0.403063893E-01	0.0	0.0
3510224	16.8694000	0.37030986E-01	0.0	0.0
3510225	18.2606964	0.407628827E-01	0.0	0.0
3510226	20.3477000	0.325122438E-01	0.0	0.0
3510227	21.0430000	0.348623283E-01	0.0	0.0
3510228	22.0868000	0.248195343E-01	0.0	0.0
3510229	23.1302948	0.210154429E-01	0.0	0.0
3510230	24.8694000	0.279473364E-01	0.0	0.0

3510231	25.2171936	0.299254581E+01	0.0	0.0
3510232	25.9129028	0.208632767	0.0	0.0
3510233	26.9564056	0.141799271	0.0	0.0
3510234	27.3041942	0.501124784E-01	0.0	0.0
3510235	28.6954956	0.915178051E-01	0.0	0.0
3510236	29.3910980	0.111704826	0.0	0.0
3510237	29.7389984	0.932761431E-01	0.0	0.0
3510238	30.0868073	0.854820013E-01	0.0	0.0
3510239	30.4346005	0.131739676	0.0	0.0
3510240	30.7823944	0.153279126	0.0	0.0
3510241	31.1302948	0.727509856E-01	0.0	0.0
3510242	31.8258972	0.909598470E-01	0.0	0.0
3510243	32.1737061	0.4891208195E-01	0.0	0.0
3510244	32.8694000	0.55235311-E-01	0.0	0.0
3510245	33.2171936	0.854650736E-01	0.0	0.0
3510246	34.2606964	0.163068+14	0.0	0.0
3510247	34.9562988	0.161005516	0.0	0.0
3510248	35.9998016	0.134565922E-01	0.0	0.0
3510249	36.3475952	0.7525324825E-01	0.0	0.0
3510250	37.0433044	0.884745717E-01	0.0	0.0
3510251	37.3910980	0.7572662835E-01	0.0	0.0
3510252	38.4346005	0.720747113E-01	0.0	0.0
3510253	38.7823944	0.114173234	0.0	0.0
3510254	39.1302032	0.915685296E-01	0.0	0.0
3510255	39.4781036	0.146972895	0.0	0.0
3510256	40.1737061	0.143181079	0.0	0.0
3510257	40.5214996	0.148781836	0.0	0.0
3510258	41.2171936	0.120750129	0.0	0.0
3510259	41.5650024	0.9371572735E-01	0.0	0.0
3510260	41.9127960	0.121815264	0.0	0.0
3510261	42.9562988	0.148632679	0.0	0.0
3510262	43.6519928	0.157235324	0.0	0.0
3510263	43.9998016	0.105888784	0.0	0.0
3510264	45.0433044	0.131435335	0.0	0.0
3510265	45.7389069	0.159450293	0.0	0.0
3510266	46.7823944	0.162290633	0.0	0.0
3510267	47.4779968	0.162341356	0.0	0.0
3510268	48.8692932	0.121003687	0.0	0.0
3510269	49.2171936	0.146144271	0.0	0.0
3510270	49.9127960	0.12174033	0.0	0.0
3510271	50.2606049	0.158749915	0.0	0.0
3510272	50.9562988	0.990245342E-01	0.0	0.0
3510273	51.3040924	0.104231894	0.0	0.0
3510274	58.9562988	0.170642674	0.0	0.0
3510275	59.9996948	0.163051307	0.0	0.0
3510276	65.9127960	0.165739715	0.0	0.0
3510277	69.0431976	0.150726080	0.0	0.0
3510278	69.7388000	0.161749482	0.0	0.0
3510279	72.8692932	0.153279126	0.0	0.0
3510280	73.2171021	0.150066653	0.0	0.0
3510281	86.7823025	0.158266723	0.0	0.0
3510282	89.9127045	0.178081751	0.0	0.0
3510283	95.4779053	0.165722726	0.0	0.0
3510284	95.8256989	0.167075157	0.0	0.0
3510285	97.5648041	0.172248840	0.0	0.0
3510286	107.939603	0.176052988	0.0	0.0
3510287	111.477798	0.173499942	0.0	0.0
3510288	124.347397	0.205318987	0.0	0.0
3510289	150.434204	0.216917157	0.0	0.0
3510290	174.78199	0.217542887	0.0	0.0
3510291	190.434077	0.206570089	0.0	0.0
3510292	193.216705	0.230679512	0.0	0.0


```

4060000  OUTLET THDPVOL
4060101  1.0 0.0 1.0 0.0 0.0 0.0 0.0 1.0 0
4060200  2
4060201  0.0 947.0 1.0
*
***** S/G DESIRED MASS CNTRL *****
*
4530000  S/GMASS THDPVOL
4530101  407000000 403000000 0.0
4530200  1 501 CNTRLVAR 6
4530201  -1.01+3 0.0 0.0 0.0
4530202  -1.0+3 -1.0+3 0.0 0.0
4530203  0.0 0.0 0.0 0.0
4530204  1.0+3 1.0+3 0.0 0.0
*
4070000  S/GMASS THDPVOL
4070101  1.0 0.0 1.0 0.0 0.0 0.0 0.0 1.0 00
4070200  3
4070201  0.0 950.0 434.93
*
***** CONTROL VARIABLES *****
*****
***** PUMP SPEED CTR FOR FLOW(4.993 KG/S) *****
*****
20500100 ILMERR SUM 1.0 0.0 1
20500101 4.993 -1.0 MFLDRJ 110020000
*
20500200 ILPSPD INTEGRAL 190.98 3650.0 1
20500201 CNTRLVAR 1
*
*
***** S/G DESIRED MASS CNTRL(22.128 KG) *****
*
20500500 S/G SUM 1.0 0.0 1
20500501 0.0 0.064510 RHD 402010000
20500502 0.032270 RHD 402020000
20500503 0.014210 RHD 402030000
20500504 0.012470 RHD 404010000
20500505 0.012470 RHD 405010000
20500506 0.012470 RHD 405020000
20500507 0.012470 RHD 405030000
20500508 0.012470 RHD 405040000
20500509 0.012470 RHD 405050000
20500510 0.012338 RHD 403010000
*
20500600 SG-ERR SUM 0.66138 1.0 1
20500601 22.128 -1.0 CNTRLVAR 5
*
***** PUMP SPEED CTR FOR TEST SIMULATION *****
*
20500700 PUMP FUNCTION 1811.7 0.0 1

```

20500701 TIME 0 1

*

***** TEMP DIFFERENCE ACROSS CORE *****

*

20501000 DT SUM 1.0 0.0 1

20501001 0.0 1.0 TEMPF 101010000

20501002 -1.0 TEMPF 111010000

*

***** DESIRED PATH FOR COMPARISON *****

*

***** SYSTEM PRESSURES

*

*** UPPER PLENUM PRESSURE

*

20509900 UP-PLN-P SUM 1.0+3 0.0 1

20509901 0.0 1.0 P 029010000

*

*** PRZ PRESSURE

*

20510000 PRZ-P SUM 1.0-3 0.0 1

20510001 0.0 1.0 P 113130000

*

*** S/G PRESSURE

*

20510100 SG-P SUM 1.0-3 0.0 1

20510101 0.0 1.0 P 405010000

*

***** VOLUMATRIC FLOW RATES

*

*** INTACT LOOP HOT LEG

*

20510200 ILHLG-VF MULT 1.0 0.0 1

20510201 VELFJ 101030000 VD1DFJ 101030000

*

20510300 ILHLG-VG MULT 1.0 0.0 1

20510301 VELGJ 101030000 VD1DGJ 101030000

*

20510400 ILHLG-V SUM 28.316 0.0 1

* 28.316=FT**3/L

20510401 0.0 0.02058 CNTRLVAR 102

20510402 0.02058 CNTRLVAR 103

*

*** INTACT LOOP COLD LEG

*

20510500 ILCLG-VF MULT 1.0 0.0 1

20510501 VELFJ 112020000 VD1DFJ 112020000

*

20510600 ILCLG-VG MULT 1.0 0.0 1

20510601 VELGJ 112020000 VD1DGJ 112020000

*

20510700 ILCLG-V SUM 28.316 0.0 1

* 28.316=FT**3/L

20510701 0.0 0.0378 CNTRLVAR 105

20510702 0.0378 CNTRLVAR 106

*

*** INTACT PRZ SURGE FLOW

20513101 0.0 1.0 HTTEMP 002100112

*

20513202 AF-2 SUM 1.0 0.0 1

20513201 0.0 1.0 HTTEMP 002100212

*

20513302 AF-3 SUM 1.0 0.0 1

20513301 0.0 1.0 HTTEMP 002100312

*

20513400 AF-4 SUM 1.0 0.0 1

20513401 0.0 1.0 HTTEMP 002100412

*

20513500 AF-5 SUM 1.0 0.0 1

20513501 0.0 1.0 HTTEMP 002100512

*

20513602 AF-6 SUM 1.0 0.0 1

20513601 0.0 1.0 HTTEMP 002100612

*

20513700 AF-7 SUM 1.0 0.0 1

20513701 0.0 1.0 HTTEMP 002100712

*

20513800 AF-8 SUM 1.0 0.0 1

20513801 0.0 1.0 HTTEMP 002100812

*

20513903 AF-9 SUM 1.0 0.0 1

20513901 0.0 1.0 HTTEMP 002100912

*

20514000 AF-10 SUM 1.0 0.0 1

20514001 0.0 1.0 HTTEMP 002101012

*

***** DIFFERENTIAL PRESSURE

* ACROSS DOWNCOMER

*

20514100 DCH-DP SUM 1.0-3 0.0 1

20514101 0.0 1.0 P 005010000 -1.2152 RHO 005010000

20514102 -1.0 P 003010000 0.1176 RHO 003010000

*

* * * ACROSS LOX PLEN.

*

20514200 LPN-DF SUM 1.0-3 0.0 1

20514201 0.0 1.0 P 005010000 2.5015 RHO 005010000

20514202 -1.0 P 006010000 0.3724 RHO 006010000

*

* * * ACROSS CORE

*

20514300 CORE-DP SUM 1.0-3 0.0 1

20514301 0.0 1.0 P 005010000 -1.2152 RHO 005010000

20514302 -1.0 P 029010000 -2.5284 RHO 029010000

*

***** COLLAPSED WATER LEVEL (DESITY=990.0 KG/M³ × 100.0 F)

*

* * * * ACROSS DOWNCOMER

*

* * * W/L D-P

*

20514500 DCH-WLI SUM 1.0307-4 0.0 1 1.0307-4=1/(9.8*990.0)

20514501 0.0 1.0+3 CNTRLVAR 141

*

*** V/L CALCULATED BY VOID

*
20514600 DCH-WLII SUM 1.0 0.0 1
20514601 0.0 0.1537 VOIDF 003010000
20514602 1.771 VOIDF 004010000
20514603 1.2771 VOIDF 004020000
20514604 1.2771 VOIDF 004030000
20514605 0.2235 VOIDF 006010000
20514606 0.1315 VOIDF 005010000

*
20514700 DCH-WLIII SUM 1.0 0.0 1
20514701 0.0 0.1537 VOIDG 003010000
20514702 1.2771 VOIDG 004010000
20514703 1.2771 VOIDG 004020000
20514704 1.2771 VOIDG 004030000
20514705 0.2235 VOIDG 006010000
20514706 0.1315 VOIDG 005010000

*
20514800 DCH-WLIII MULT 0.0010101 0.0 1 * 0.0010101=1/990.0
20514801 RHDF 005010000
20514802 CNTRLVAR 146

*
20514900 DCH-WLII MULT 0.0010101 0.0 1
20514901 RHOG 005010000
20514902 CNTRLVAR 147

*
20515000 DCH-WLII JN 1.0 0.0 1
20515001 0.0 1.0 CNTRLVAR 148
20515002 1.0 CNTRLVAR 149

*
***** ACROSS LOW PLENUM

*
*** V/L CALCULATED BY D-P

*
20515100 LPN-WLI SUM 1.0307-4 0.0 1 * 1.0307-4=1/(9.8+990.0)
20515101 0.0 1.0+3 CNTRLVAR 142

*
*** V/L CALCULATED BY VOID

*
20515200 LPN-WLII SUM 1.0 0.0 1
20515201 0.0 0.1496 VOIDF 006010000
20515202 0.5104 VOIDF 005010000

*
20515300 LPN-WLII SUM 1.0 0.0 1
20515301 0.0 0.1496 VOIDG 006010000
20515302 0.5104 VOIDG 005010000

*
20515400 LPN-WLII MULT 0.0010101 0.0 1
20515401 RHDF 005010000
20515402 CNTRLVAR 152

*
20515500 LPN-WLII MULT 0.0010101 0.0 1
20515501 RHOG 005010000
20515502 CNTRLVAR 153

*
20515600 LPN-WLII SUM 1.0 0.0 1
20515601 0.0 1.0 CNTRLVAR 154
20515602 1.0 CNTRLVAR 155

*
***** ACROSS CORE

*
*** V/L CALCULATED BY D-P

20515700 COR-WL1 SUM 1.0307-4 0.0 1 1.0307-4=1/(9.8995,0)
 20515701 0.0 1.0*3 CNTRLVAR 143
 *
 *** V/L CALCULATED BY VOID
 *
 20515800 COR-WL1I SUM 1.0 0.0 1
 20515801 0.0 0.1315 VOIDF 005010000
 20515802 0.2235 VOIDF 006010000
 20515803 0.5416 VOIDF 007010000
 20515804 0.1524 VOIDF 008010000
 20515805 0.1271 VOIDF 009010000
 20515806 0.1269 VOIDF 010010000
 20515807 0.1269 VOIDF 011010000
 20515808 0.1591 VOIDF 121010000
 20515809 0.0948 VOIDF 122010000
 20515810 0.1271 VOIDF 013010000
 *
 20515900 COR-WL1II SUM 1.0 0.0 1
 20515901 0.0 0.1271 VOIDF 014010000
 20515902 0.1777 VOIDF 015010000
 20515903 0.2033 VOIDF 016010000
 20515904 0.2539 VOIDF 017010000
 20515905 0.7043 VOIDF 028010000
 20515906 0.7043 VOIDF 028020000
 20515907 0.7043 VOIDF 028030000
 20515908 0.1541 VOIDF 029010000
 20515909 1.0 CNTRLVAR 158
 *
 20516000 COR-WL1II SUM 1.0 0.0 1
 20516001 0.0 0.1315 VOIDG 005010000
 20516002 0.2235 VOIDG 006010000
 20516003 0.5416 VOIDG 007010000
 20516004 0.1524 VOIDG 008010000
 20516005 0.1271 VOIDG 009010000
 20516006 0.1269 VOIDG 010010000
 20516007 0.1269 VOIDG 011010000
 20516008 0.1591 VOIDG 121010000
 20516009 0.0948 VOIDG 122010000
 20516010 0.1271 VOIDG 013010000
 *
 20516100 COR-WL1II SUM 1.0 0.0 1
 20516101 0.0 0.1271 VOIDG 014010000
 20516102 0.1777 VOIDG 015010000
 20516103 0.2033 VOIDG 016010000
 20516104 0.2539 VOIDG 017010000
 20516105 0.7043 VOIDG 028010000
 20516106 0.7043 VOIDG 028020000
 20516107 0.7043 VOIDG 028030000
 20516108 0.1541 VOIDG 029010000
 20516109 1.0 CNTRLVAR 160
 *
 20516200 COR-WL1II MULT 0.0010101 0.0 1
 20516201 RHOF 005010000
 20516202 CNTRLVAR 159
 *
 20516300 COR-WL1II MULT 0.0010101 0.0 1
 20516301 RHOG 005010000
 20516302 CNTRLVAR 161
 *
 20516400 COR-WL1II SC 1.0 0.0 1
 20516401 0.0 1.0 CNTRLVAR 162

20521408 1.093-3 CNTRLVAR 205
 20521409 1.093-3 CNTRLVAR 206
 20521410 1.093-3 CNTRLVAR 207
 20521411 1.093-3 CNTRLVAR 208
 20521412 1.093-3 CNTRLVAR 209
 20521413 1.093-3 CNTRLVAR 210
 20521414 5.465-3 CNTRLVAR 211
 20521415 5.465-3 CNTRLVAR 212
 20521416 5.465-3 CNTRLVAR 213

 20521500 PRZERR SUM 0.4613E 0.0 1
 20521501 9.09 -1.0 CNTRLVAR 214
 HEAT STRUCTURES
 10011000 11 18 2 1 0.0 1 1 8
 10011100 0 1
 10011101 1 0.002917 4 0.010084 4 0.014334 8 0.017554
 10011201 1 1 3 5 1 9 2 17
 10011301 0.0 1 1.0 5 0.0 17
 10011401 1026.1 1 1026.1 2 1014.6 3 984.91 4 939.53 5
 10011402 879.51 6 846.61 7 816.79 8 789.52 9 764.61 10
 10011403 750.73 11 737.34 12 724.23 13 711.39 14 696.80 15
 10011404 656.45 16 674.34 17 662.44 18
 10011501 0 0 0 0 0. 11
 10011601 018010000 0 1 0 0.22097 1
 10011602 019010000 0 1 0 0.18429 2
 10011603 020010000 0 1 0 0.18416 3
 10011604 021010000 0 1 0 0.18399 4
 10011605 221010000 0 1 0 0.23078 5
 10011606 222010000 0 1 0 0.13750 6
 10011607 023010000 0 1 0 0.18416 7
 10011608 024010000 0 1 0 0.18416 8
 10011609 025010000 0 1 0 0.25779 9
 10011610 026010000 0 1 0 0.29461 10
 10011611 027010000 0 1 0 0.36832 11
 10011701 100 0.00966 0. 0. 1
 10011702 100 0.01257 0. 0. 2
 10011703 100 0.01617 0. 0. 3
 10011704 100 0.01859 0. 0. 4
 10011705 100 0.02481 0. 0. 5
 10011706 100 0.01478 0. 0. 6
 10011707 100 0.01859 0. 0. 7
 10011708 100 0.01617 0. 0. 8
 10011709 100 0.01760 0. 0. 9
 10011710 100 0.01185 0. 0. 10
 10011711 100 0.00499 0. 0. 11
 10011801 0. 0. 0. 0. 11
 10011901 0 0.0465 0.0465 0.500 1
 10011902 0 0.0465 0.0465 0.417 2
 10011903 0 0.0465 0.0465 0.4165 4
 10011904 0 0.0465 0.0465 0.522 5
 10011905 0 0.0465 0.0465 0.311 6
 10011906 0 0.0465 0.0465 0.417 8
 10011907 0 0.0465 0.0465 0.533 9
 10011908 0 0.0465 0.0465 0.677 10
 10011909 0 0.0465 0.0465 0.833 11

*
***** CRIME (AVERAGE CHANNEL) *****

10021000 11 18 2 1 0.0 1 1 8
10021100 0 1
10021101 1 0.002917 4 0.010084 4 0.014334 8 0.017584
10021201 1 1 3 5 1 9 2 17
10021301 0.0 1 1.0 5 0.0 17
10021401 1026.1 1 1026.1 2 1124.6 3 984.91 4 939.53 5
10021402 879.51 6 846.61 7 816.79 8 789.52 9 764.61 10
10021403 750.73 11 737.34 12 724.23 13 711.39 14 698.80 15
10021404 686.45 16 674.34 17 662.44 18
10021501 0 0 0 0 0. 11
10021601 008010000 0 1 0 1.7684782 1
10021602 009010000 0 1 0 1.4737318 2
10021603 010010000 0 1 0 1.4726050 3
10021604 011010000 0 1 0 1.4726050 4
10021605 121010000 0 1 0 1.8463593 5
10021606 122010000 0 1 0 1.1000340 6
10021607 013010000 0 1 0 1.7319567 7
10021608 014010000 0 1 0 1.4731958 8
10021609 015010000 0 1 0 2.0624742 9
10021610 016010000 0 1 0 2.3571156 10
10021611 017010000 0 1 0 2.9463545 11
10021701 100 0.044937 0. 0. 1
10021702 100 0.063580 0. 0. 2
10021703 100 0.081803 0. 0. 3
10021704 100 0.094019 0. 0. 4
10021705 100 0.125489 0. 0. 5
10021706 100 0.074765 0. 0. 6
10021707 100 0.094019 0. 0. 7
10021708 100 0.081803 0. 0. 8
10021709 100 0.089013 0. 0. 9
10021710 100 0.059916 0. 0. 10
10021711 100 0.025232 0. 0. 11
10021801 0 0. 0. 0. 11
10021901 0 0.0352 0.0523 0.500 1
10021902 0 0.0352 0.0523 0.417 2
10021903 0 0.0352 0.0523 0.4165 4
10021904 0 0.0352 0.0523 0.522 5
10021905 0 0.0352 0.0523 0.311 6
10021906 0 0.0352 0.0523 0.417 8
10021907 0 0.0352 0.0523 0.583 9
10021908 0 0.0352 0.0523 0.477 10
10021909 0 0.0352 0.0523 0.833 11

*
***** UPPER PLENUM I *****

10031000 4 18 2 1 0.
10031100 0 1
10031101 1 0.002917 4 0.010084 4 0.014334 8 0.017584
10031201 1 1 3 5 1 9 2 17
10 1301 0.0 1 1.0 5 0.0 17
10031401 597.0 18
10031501 0 0 0 0 0. 4
10031601 028010000 010000 1 0 1.0211 3
10031602 029010000 0 1 0 1.2023 4
10031701 0 0. 0. 0. 4

10284000	4	5	2	1	0.2856	
10284100	0	1				
10284101	2	0.2956	1	0.29977	1	0.35987
10284201	4	2	6	3	5	4
10284301	0.0	4				
10284401	500.0	5				
10284501	028010000	010000	1	0	4.16104	3
10284502	029010000		0	1	0	4.88195
10284601		0	0	0	0	5.24558
10284602		0	0	0	0	6.15321
10284701	0	0.0	0.0	0.0	0	4
10284801	0	1.4387	0.0	0.0	0	4
10284901	0	0.0	0.0	0.0	0	4
*						
***** PIPELINE HEAT SLAPS *****						
10185000	12	6	2	1	0.1094	
10185100	0	1				
10185101	5	0.1458				
10185201	2	5				
10185301	0.0	5				
10185401	570.0	6				
10185501	214010000		1	0	1.220	1
10185502	151010000	0	1	0	4.482	2
10185503	102010000	0	1	0	5.088	3
10185504	109010000	0	1	0	6.590	4
10185505	112010000	0	1	0	5.440	5
10185506	201010000	0	1	0	1.700	6
10185507	202010000	0	1	0	5.895	7
10185508	203010000	0	1	0	6.625	8
10185509	204010000	0	1	0	1.170	9
10185510	206010000	0	1	0	1.200	10
*10185511	207010000	0	1	0	1.420	11
10185511	212010000	0	1	0	1.250	11
10185512	213010000	0	1	0	1.821	12
10185601	0	0	0	0	1.62592	1
10185602	0	0	0	0	5.97327	2
10185603	0	0	0	0	4.11545	3
10185604	0	0	0	0	8.78265	4
10185605	0	0	0	0	7.25002	5
10185606	0	0	0	0	2.26563	6
10185607	0	0	0	0	7.85641	7
10185608	0	0	0	0	8.82230	8
10185609	0	0	0	0	1.55929	9
10185610	0	0	0	0	1.59927	10
*10185611	0	0	0	0	1.89247	11
10185611	0	0	0	0	1.66590	11
10185612	0	0	0	0	2.42689	12
10185701	0	0.	0.	0.		12
10185801	0	0.05	0.	0.		1
10185802	0	0.6436	0.	0.		2
10185803	0	0.6436	0.	0.		3
10185804	0	0.556	0.	0.		4
10185805	0	0.463	0.	0.		5
10185806	0	0.144	0.	0.		6
10185807	0	0.5015	0.	0.		7
10185808	0	0.5625	0.	0.		8
10185809	0	0.100	0.	0.		9
10185810	0	0.100	0.	0.		10
*10185811	0	0.012	0.	0.		11

10175811	0	0.0776	0.	0.		11
10175812	0	0.0776	0.	0.		12
10175901	0	0.	0.	0.		12
e						
***** DCH HEAT SLABS : C)RE PARFEL SIDE *****						
***** ***** ***** ***** ***** ***** ***** *****						
e						
10046000	3	6	2	1	0.20313	
10046100	0	1				
10046101	2	0.22576	1	0.23293	2	0.24293
10046201	7	2	6	3	4	5
10046301	0.0	5				
10046401	564.0	6				
10046501	0	0		0	0	0.4037 3
10046601	004010000	010000		1	0	0.4 26 3
10046701	0	0.	0.	0.	0.	3
10046801	0	0.	0.	0.	0.	3
10046901	0	0.71	0.	0.	0.	3
e						
***** LOWER - PLENUM - SLABS *****						
***** ***** ***** ***** ***** ***** *****						
e						
10057000	2	11	2	1	0.25167	
10057100	0	1				
10057101	2	0.29167	1	0.29584	3	0.35604
10057201	4	2	6	3	2	10
10057301	0.0	10				
10057401	560.0	11				
10057501	006010000	0	1	0	1.2977	1
10057502	005010000	0	1	0	2.9638	2
10057601	0	0	0	0	2.031944	1
10057602	0	0	0	0	4.640730	2
10057701	0	0.	0.	0.	0.	2
10057801	0	0.2738	0.	0.	0.	1
10057802	0	0.6253	0.	0.	0.	2
10057901	0	0.568	0.	0.	0.	2
e						
***** INLET ANN SLABS : VESSEL SIDE *****						
***** ***** ***** ***** ***** ***** *****						
e						
10018000	3	7	2	1	0.32604	
10018100	0	1				
10018101	2	0.34771	4	0.43271		
10018201	2	2	5	6		
10018301	0.0	6				
10018401	563.0	7				
10018501	001010000	0	1	0	0.55924	1
10018502	002010000	0	1	0	0.67512	2
10018503	003010000	0	1	0	1.91423	3
10018601	0	0	0	0	0.795292	1
10018602	0	0	0	0	0.895998	2
10018603	0	0	0	0	2.540506	3
10018701	0	0.	0.	0.	0.	3
10018801	0	0.39437	0.	0.	0.	3
10018901	0	0.16	0.	0.	0.	3
e						
***** INLET ANN HEAT SLABS *****						
***** ***** ***** ***** ***** ***** *****						

10016000	3	6	2	1	0.20313	
1001616	0	1				
10016101	2	0.22676	1	0.23293	2	0.24293
10016201	7	2	6	3	4	5
10016301	0.0	5				
10016401	564	0	6			
10016501	0	0	0	0	0.378022	1
10016502	0.	0	0	0	0.424597	2
10016503	0	0	0	0	1.203930	3
10016601	001010000	0	1	0	0.45209	1
10016602	002010000	0	1	0	0.50779	2
10016603	003010000	0	1	0	1.43982	3
10016701	0	0.	0.	0.	3	
10016801	0	0.	0.	0.	3	
10016901	0	0.016	0.	0.	3	

STRUCTURE **STRUCTURE** **STRUCTURE**

20100100	TPL/FCTN	1	1					
*20100101	500.	4.611-3	1000.	4.417-3	1500.	4.25-3	2000.	4.083-3
*20100102	2500.	3.917-3	3000.	3.75-3	3500.	3.556-3		
20100101	32.0	0.00255	200.0	0.00241	500.0	0.00216	1000.	0.00174
20100102	1500.	0.00133	2000.	9.09-4	2500.	4.91-4	3000.	7.40-5
20100103	4000.	7.40-5						
20100151	32.	37.5	400.	37.5	800.	48.3	1200.	54.6
20100152	1400.	58.3	2000.	60.5	2400.	61.4	3400.	62.5

316 LSS

20100200	TBL/FCTN	1	1						
20100201	100.	2.153-3	800.	3.056-3	1600.	3.972-3	4000.0	3.972-3	
20100251	32.0	61.3	400.	61.3	600.	64.6	800.	67.1	
20100252	2200	82.3							

CONSTANTAN

20100300	TRL/FCTN	1	1					
20100301	0.	3.889-3	3000.	3.889-3				
20100351	212.	56.	572.	61.	932.	67.	1472.	73.
20100352	212.	78.	2552.	84.	3000.	90.		

304 55

20100400	TRL/FCTN	1	1					
20100401	100.	2.444-3	400.	2.8056-3	600.	3.0278-3		
20100402	1000.	3.5-3	1200.	3.75-3				
20100451	100.	45.01	400.	45.01	600.	46.09	1000.	49.35

20210035	13.0434	1.23910507201E+01
20210036	13.7390	1.23496507300E+01
20210037	14.4347	1.23393127400E+01
20210038	14.7825	1.22824035500E+01
20210039	15.1303	1.16460357700E+01
20210040	15.4781	1.03577804600E+01
20210041	15.8260	9.16782531700E+02
20210042	16.1738	8.58319397000E+02
20210043	16.5216	8.47454681400E+02
20210044	16.8694	8.67114868200E+02
20210045	17.2173	1.17753784200E+01
20210046	17.5651	1.53297210700E+01
20210047	17.9129	1.59143493700E+01
20210048	18.2607	1.60592132600E+01
20210049	18.9564	1.60489678000E+01
20210050	19.3042	1.56297973600E+01
20210051	19.6520	1.12890472400E+01
20210052	19.9999	6.36367034900E+02
20210053	20.3477	5.52035522500E+02
20210054	20.6955	5.47379150400E+02
20210055	21.0433	5.47379129400E+02
20210056	21.3912	5.44274972600E+02
20210057	21.7390	5.40135955800E+02
20210058	22.0868	5.41170730600E+02
20210059	22.4346	5.40135955800E+02
20210060	22.7825	5.39101181000E+02
20210061	23.1303	5.38583331800E+02
20210062	23.4781	5.42722854600E+02
20210063	24.8694	5.40135955800E+02
20210064	25.2172	5.38066406800E+02
20210065	25.5651	5.37031784100E+02
20210066	25.9129	5.42205505400E+02
20210067	26.2607	5.30823288000E+02
20210068	26.6085	4.25279464700E+02
20210069	26.9564	2.80932807900E+02
20210070	27.3042	2.38508300200E+02
20210071	27.6520	2.34693161000E+02
20210072	28.3477	2.33334617600E+02
20210073	30.0868	2.25921478300E+02
20210074	30.4346	2.32299881000E+02
20210075	30.7824	2.31724936000E+02
20210076	31.4781	2.35404090900E+02
20210077	34.6085	2.36956176800E+02
20210078	34.9563	2.39025688200E+02
20210079	35.3042	2.44199409500E+02
20210080	35.6520	2.59203224200E+02
20210081	35.9998	2.73689575200E+02
20210082	36.3476	2.92314049000E+02
20210083	36.6955	3.07835074800E+02
20210084	37.0433	3.27496185300E+02
20210085	37.3911	3.44569473300E+02
20210086	38.0868	3.78715972900E+02
20210087	38.4346	3.96306636400E+02
20210088	38.7824	4.14932022100E+02
20210089	39.1302	4.31487960800E+02
20210090	39.4781	4.56321716300E+02
20210091	39.8259	4.71325531000E+02
20210092	42.9563	4.78568801900E+02
20210093	43.9998	4.75464477500E+02
20210094	45.7389	4.74429702800E+02
20210095	46.0867	4.72360305800E+02
20210096	46.7824	4.69773407000E+02

1102300	2	5							
1102301	0.000	-0.630	0.200	-0.510	0.400	-0.390	0.600	-0.600	
1102302	0.800	-0.200	0.900	-0.160	1.000	-0.130			
1102400	2	6							
1102401	0.000	0.360	0.200	0.320	0.400	0.270	0.600	0.180	
1102402	0.800	0.050	1.000	-0.130					
1102500	2	7							
1102501	-1.000	-1.440	-0.800	-1.250	-0.600	-1.080	-0.400	-0.920	
1102502	-0.200	-0.770	0.000	-0.630					
1102600	2	8							
1102601	-1.000	-1.440	-0.800	-1.120	-0.600	-0.790	-0.400	-0.520	
1102602	-0.200	-0.310	0.000	-0.150					
e									
*****	*****	*****	*****	*****	*****	*****	*****	*****	
*****	TWO-PHASE MULTIPLIER TABLES *****	*****	*****	*****	*****	*****	*****	*****	
*****	*****	*****	*****	*****	*****	*****	*****	*****	
9									
1103000	0								
1103001	0.000	0.000	0.100	0.000	0.150	0.050	0.240	0.500	
1103002	0.300	0.960	0.400	0.980	0.600	0.970	0.800	0.900	
1103003	0.900	0.800	0.960	0.500	1.000	0.000			
1103100	0								
1103101	0.000	-0.170	0.001	-0.170	0.006	0.000	0.100	0.000	
1103102	0.150	0.050	0.240	0.570	0.500	0.560	0.460	0.450	
1103103	1.000	0.000							
b									
*****	*****	*****	*****	*****	*****	*****	*****	*****	
*****	TWO-PHASE DIFFERENCE TABLES *****	*****	*****	*****	*****	*****	*****	*****	
*****	*****	*****	*****	*****	*****	*****	*****	*****	
b									
1104100	1	1							
1104101	0.000	0.000	0.100	0.830	0.200	1.090	0.500	1.020	
1104102	0.700	1.010	0.900	0.940	1.000	1.000			
1104200	1	2							
1104201	0.000	0.000	0.100	-0.040	0.200	0.000	0.300	0.100	
1104202	0.400	0.210	0.800	0.670	0.900	0.800	1.000	1.000	
1104300	1	3							
1104301	-1.000	-1.160	-0.900	-1.240	-0.800	-1.170	-0.700	-2.360	
1104302	-0.600	-2.790	-0.500	-2.910	-0.400	-2.670	-0.250	-1.690	
1104303	-0.100	-0.500	0.000	0.000					
1104400	1	4							
1104401	-1.000	-1.160	-0.900	-0.780	-0.800	-0.500	-0.700	-0.310	
1104402	-0.600	-0.170	-0.500	-0.080	-0.350	0.000	-0.200	0.050	
1104403	-0.100	0.080	0.000	0.110					
1104500	1	5							
1104501	0.000	0.000	0.200	-0.034	0.400	-0.650	0.600	-0.930	
1104502	0.800	-1.190	1.000	-1.470					
1104600	1	6							
1104601	0.000	0.110	0.100	0.130	0.250	0.140	0.400	0.130	
1104602	0.500	0.070	0.600	-0.040	0.700	-0.230	0.800	-0.510	
1104603	0.900	-0.910	1.000	-1.470					
1104700	1	7							
1104701	-1.000	0.000	0.000	0.000					
1104800	1	8							
1104801	-1.000	0.000	0.000	0.000					
1104900	2	1							
1104901	0.000	0.540	0.200	0.590	0.400	0.650	0.600	0.770	
1104902	0.800	0.950	0.900	0.980	0.950	0.960	1.000	0.870	
1105000	2	2							
1105001	0.000	-0.150	0.200	0.020	0.400	0.220	0.600	0.460	
1105002	0.800	0.710	0.900	0.810	0.950	0.850	1.000	0.870	
1105100	2	3							

BIBLIOGRAPHIC DATA SHEET

See instructions - Form reverse.

REPORT NUMBER
Assigned by NRC Add Vol. Subj. Rev.
and Addendum Numbers, if any

NUREG/IA-0046

1. TITLE AND SUBTITLE
Assessment of RELAP5/MOD2 Using Semiscale Large Break Loss-of-Coolant Experiment S-06-3

3. DATE REPORT FILED, APPROVED
04/09/92

April 1992

4. FIN OR GRANT NUMBER
A4682

5. AUTHORISI

Kuo-Shing Liang, Lainsu-Kao, Jeng-Lang Chiou, Lih-Yih Liao,
Song-Feng Wang, Yi-Bin Chen

6. TYPE OF REPORT
Technical

7. PERIOD COVERED

8. PERFORMING ORGANIZATION - NAME AND ADDRESS (If NRC provide Division, Office or Region, U.S. Nuclear Regulatory Commission, and mailing address; if contractor, provide name and mailing address.)

Institute of Nuclear Energy Research
P.O. Box 3, Lung-Tan 32500
Taiwan, Republic of China

9. SPONSORING ORGANIZATION - NAME AND ADDRESS (If NRC type "Same as above"; if contractor, provide NRC Division, Office or Region, U.S. Nuclear Regulatory Commission and mailing address.)

Office of Nuclear Regulatory Research
U. S. Nuclear Regulatory Commission
Washington, DC 20555

10. SUPPLEMENTARY NOTES

11. ABSTRACT (200 words or less)

This report presents the results of the RELAP5/MOD2 post-test assessment utilizing a semiscale large break loss-of-coolant experiment numbered S-06-3. Emphasis was placed on the capability of the code to calculate break flow rates during system blowdown stage, emergency core cooling system (ECCS) injection bypass during refill stage, quenching during reflood stage, and peak cladding temperature behavior throughout the whole experiment.

12. KEY WORDS/DESCRIPTORS (List words or phrases that will assist researchers in locating the report.)

ICAP Program, RELAP5/MOD2, Semiscale S-06-3

13. AVAILABILITY STATEMENT

Unlimited

14. SECURITY CLASSIFICATION

(This Report)

Unclassified

(This Report)

Unclassified

15. NUMBER OF PAGES

16. PRICE

THIS DOCUMENT WAS PRINTED USING RECYCLED PAPER

UNITED STATES
NUCLEAR REGULATORY COMMISSION
WASHINGTON, D.C. 20555

OFFICIAL BUSINESS
PENALTY FOR PRIVATE USE, \$300

SPECIAL FOURTH-CLASS RATE
POSTAGE AND FEES PAID
USNRC
PERMIT NO. G-67

120555139531 1 1ANICI
US NRC-OADM
DIV FOIA & PUBLICATIONS SVCS
TPS-PDR-HUREG
P-211 DC 20555
WASHINGTON